UNIVERSITY OF OKLAHOMA

GRADUATE COLLEGE

BIOCHEMISTRY OF HEMIN UPTAKE IN LISTERIA MONOCYTOGENES AND THE FUCTION OF TONB IN ESCHERICHIA COLI

A DISSERTATION

SUBMITTED TO THE GRADUATE FACULTY

in partial fulfillment of the requirements for the

Degree of

DOCTOR OF PHILOSOPHY

By

XIAOXU JIANG
Norman, Oklahoma
2009

THE BIOCHEMISTRY OF HEMIN UPTAKE IN LISTERIA MONOCYTOGENES AND THE FUCTION OF TONB IN ESCHERICHIA COLI

A DISSERTATION APPROVED FOR THE
DEPARTMENT OF CHEMISTRY AND BIOCHEMISTRY

BY

_____
Dr. Phillip E. Klebba

_____
Dr. Elena I. Zgurskaya

_____
Dr. Valentin V. Rybenkov

_____
Dr. Michael T. Ashby

_____
Dr. Roger G. Harrison

I dedicate this dissertation to my parents.

Acknowledgements

First, I want to thank my major professor, Dr. Phillip E. Klebba, who introduced me to the magical world of biochemistry and taught me biological techniques starting from inoculating *E. coli* in LB broth. I would also like to thank Dr. Salete M.C. Newton, who guided me to do my first PCR reaction and my first plasmid clone. I thank them for their great guidance, infinite patience and continuous support. From them, I learned the way to be a good scientist and delight in science.

I also want to thank all my graduate committee members, Dr. Elena I. Zgurskaya, Dr. Valentin V. Rybenkov, Dr. Michael T. Ashby, and Dr. Roger G. Harrison, for their advices and helps throughout my graduate study.

Confucius said: When I walk along with two others, they may serve me as my teachers. I feel lucky to know and work with all lab members during my study. I thank them for their help and friendship. These people are: Li Ma, Qiaobin Xiao, Bo Jin, Yi Shao, Wallace Kaserer, Daniel Schuerch, Raj Annamalai, Chuck Smallwood, John Best, Amparo Gala Marco, Vy Trinh, Jenny Bauer and Lynn Mercer.

I also must thank my wife, Qiong Lei, and my parents. They always love me, understand me, support me and help me going through all the hard times.

I also want to thank my loving grandparents, who are always proud of me.

Last, but not least, I want to thank my uncle, Sixiang Jiang, who is my first teacher of science.

Table of contents

List of Tables

List of Figures

Abstract

Iron is an essential metal element for the metabolism pathway of most microorganisms. For pathogens, iron is also an important factor for virulence. But in the host body, the availability of free iron is very low. Iron mainly associates with heme in hemoglobin or is tightly bound to iron-associated proteins like transferrin, lactoferrin and ferritin. Both Gram-negative and Gram-positive pathogens have iron transporters in their cell envelopes to acquire iron from the environment, and one of the target iron compound for these transport systems is heme in the red blood cells.

Listeria monocytogenes is a Gram-positive pathogen, which can infect human and animals and causes listeriosis. *L. monocytogenes* can utilize multiple iron sources including siderophores, transferrin, lactoferrin, heme and hemoglobin. In the genome of *L. monocytogenes* EGD-e, the *hup* operon encodes an ABC transporter for the uptake of heme. Site-directed deletion of *hupC* and *hupG* impaired the uptake of heme and hemoglobin in *L. monocytogenes* EGD-e. The function of these two genes can be complemented via a *Listeria* phage integration vector.

[^{59}Fe]-heme was used to measure the thermodynamic and kinetic parameters of heme transport by *L. monocytohenes*. The [^{59}Fe]-heme binding experiments showed that EGD-e wild type bound heme with an affinity about 4.7nM. The

deletion of genes in *hup* operon did not change the binding affinity very much, and also the deletions did not completely eliminate the uptake of heme in the [^{59}Fe]-heme transport experiments. This data indicates there are other transporters available in *L. monocytogenes* to transport heme other than the Hup transporter.

Binding experiments revealed that the sortase B-dependent surface protein (formerly called “SvpA”) encoded by *lmo2185*, has a role in heme binding. Deletion of these proteins resulted in the increase of K_D and decrease of capacity. Deletion of *lmo2185* also reduced the uptake of hemoglobin in nutrition tests.

The second part of this study is about the function of TonB in *E. coli*. TonB is an inner-membrane-associated protein in Gram-negative species. In the outer membrane of Gram-negative bacteria, there are ligand-gated receptors for the active transport of nutrients, such as siderophores and vitamins. These receptors are TonB-dependent, probably because TonB facilities the transport by transducing the proton motive force energy from the inner membrane to the outer membrane.

The C-terminus of TonB contains LysM motifs, whose main function is binding to bacterial peptidoglycan. The TonB C-terminus has affinity for peptidoglycan. Site-directed mutagenesis and fluorescence quenching methods were used in this study to investigate the binding. Peptidoglycan quenched the fluorescence of FM labeled cysteine mutants of a MalE-TonB69C fusion protein. After changing two residues, E205 and D189, which may be part of the binding

site, to alanine, the affinity of the C-terminus of TonB for peptidoglycan still remains.

Chapter 1 Introduction

1.1 Iron uptake is important for the growth and virulence of bacteria

Iron is an essential metal element for almost all organisms, including bacteria (113). In bacterial cells, iron is needed in many metabolic pathways such as electron transport, the TCA cycle, formation of heme, peroxide reduction, and nucleotide biosynthesis. To sustain growth, bacteria must get sufficient iron from the environment (23, 24, 136).

Extensive research indicated that iron acquisition is also strongly related to bacterial virulence (22). In the mammalian body, free iron is tightly bound to eukaryotic proteins such as transferrin, lactoferrin, hemoglobin, myoglobin and ferritin, which maintain a low level of available iron to guard against invading pathogens. For most bacterial pathogens, whether they can achieve rapid growth and cause disease depends on their ability to acquire a sufficient amount of iron from their host during the infection. The relationship between iron acquisition and Gram-negative bacterial pathogen virulence has been well investigated (13, 32, 99, 167). For Gram-positive pathogens, not as much research has been done as Gram-negative, but it is obvious that iron acquisition ability is still important

for their pathogenesis (25, 84, 109).

1.2 Bacteria have developed sophisticated strategies for iron-uptake

Iron is one of the most abundant metal elements on our planet. However, in aerobic aqueous conditions, the availability of free iron is very limited. In such conditions, iron is mainly present in ferric form (Fe^{3+}), which is ready to react with the hydroxide group in aqueous solution and forms insoluble oxy-hydroxide polymers. When bacteria grow in aerobic environments, the free iron concentration is as low as 10^{-18} M, which is far below the minimal iron concentration acquirement for their growth (~10^{-8} M) (24, 114, 185). For pathogenic bacteria, the situation is similar during infection: free iron in their host body is bound to iron-carrier proteins like transferrin, lactoferrin, and ferritin or incorporated to the protoporphyrin ring to make heme and hemoproteins. The sequestration of iron is so strict that there is almost no free iron in the body of living organisms.

In order to overcome this iron shortage, bacteria have developed several sophisticated mechanisms to collect iron from environments.

Many bacteria can secret “siderophores” to chelate iron from their surroundings. Siderophores are low molecular weight iron chelators which

specifically bind to ferric iron with exceptionally high affinity and thermodynamic stability. Based on different functional groups, that are used to chelate iron, siderophores can be divided into two major groups: hydroxamate type (e.g. ferrichrome), and catechol type (e.g. ferric enterobactin)(114) (Figure 1).

Gram-negative bacteria have two membranes, an outer membrane and a cytoplasmic membrane. The transport of siderophores include three stages: (I) crossing the outer membrane, (II) going through periplasmic space and (III) crossing the cytoplasmic membrane (34). Siderophores usually are too big to diffuse through general porins on the cell envelope. They are recognized and bind to their outer memberane receptor proteins (eg. FepA, FhuA, CirA). These receptor proteins have a C-terminal transmembrane β-barrel domain with several external surface loops and an N-terminal globular plug domain inside the barrel (26, 55, 56). When FepA, the receptor of ferric enterobactin, binds the metal complex in its surface loops, it causes a conformational change in the N-terminal plug domain, and then the plug domain likely comes out from the barrel and a channel is made to let ferric enterobactin go through. This transport process needs energy and it is TonB-dependent (4, 102, 117). When enterobactin enters the periplasmic space, it binds to FepB, a periplasmic binding protein, which delivers it to the FepGDC complex, an ABC transporter in the inner membrane that transports ferric enterobactin into the cytoplasm using the energy from ATP hydrolysis. Once inside the cytoplasm, enterbactin is degraded, iron is reduced,

and ferrous iron is released.

Gram-positive bacteria also transport ferric siderophores and some Gram-positive bacteria also can secrete siderophores by themselves, such as the members in *Bacillus cereus* group, which produces two siderophores, corynebactin and petrobactin (90, 191). Different from Gram-negative bacteria, Gram-positive bacteria do not have an outer membrane; therefore there is no periplasmic space either. The whole mechanism of siderophore transport in Gram-positive bacteria is still unclear. In some species, ABC transporters of ferric siderophores were found. The genes of the *fhu* operon in *B. subtilis* encode a ferrichrome transport system: *fhuD* encodes a binding lipoprotein anchored in the cell surface by a covalent lipid linkage. *fhuB* and *fhuG* are predicted to encode transmembrane proteins, and *fhuC* encodes a predicted ATPase (150). Recently it was found that *B. cereus* has at least five binding lipoproteins for bacillibactin and xenosiderophores (110, 121) and some siderophore binding proteins in *B. cereus* were characterized (194). Ferric hydroxamate transport systems were also found in *Listeria monocytogenes*. *L. monocytogenes* can utilize ferrichrome, ferrichrome A and ferric enterobactin with a lower affinity and slower rate compared with Gram-negetive bacteria, such as *E.coli*. The deletion of *fhuD* and *fhuC* genes strongly reduced the uptake of ferrichrome (84).

As a response to the siderophore-dependent iron acquisition by bacteria during infection, the mammalian immune system contains proteins, that can bind

to ferric siderophore complexes (such as FeEnt) to prevent the iron transport. Recently, one such mammalian protein, lipocalin, has been crystallized, and its interaction with FeEnt was studied (1, 77).

Another mechanism to get iron, especially for pathogenic bacteria, is stealing it from iron-carrier proteins, such as transferrin (Tf) and lactoferrin (Lf) in the host body. In order to prevent the toxicity against free iron radicals and promote

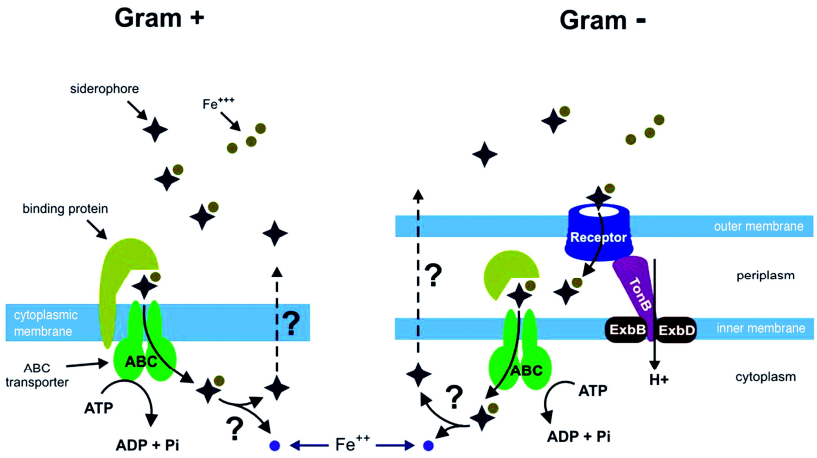

Figure 1 Siderophore transport systems in the cell envelope of Gram-positive and Gram-negative bacteria

(185)

iron transport into cells, most iron in plasma is bound to transferrin (128). Lactoferrin, found in lymph, is a protective iron chelator that plays an important role during homeostasis (186). Tf and Lf exhibit high affinity for Fe^{3+} (K_a~10^{20} M^{-1}). Many bacteria have Tf and Lf transport systems. In the pathogenic *Neisseria* species, two transferrin transport involved proteins, TbpA and TbpB are known. TbpA is an outer membrane Tf receptor and TbpB is a binding lipoprotein (87). However, the mechanism by which bacteria exctract iron from

these proteins is still unknown. Recently, a new technique, SUPREX (**S**tability of **U**npurified **P**roteins from **R**ates of H/D **E**xchange) has been used to investigate the Tf iron transport system in *N. gonorrhoeae*. The direct interaction between TbpA and FbpA (periplasmic ferric binding protein) was reported and the SUPREX data also showed that TbpA can discriminate between apo-FbpA and holo-FbpA, TbpA has a higher affinity for apo-FbpA (156).

1.3 *Listeria monocytogenes*

1.3.1 *L. monocytogenes* is a Gram-positive pathogen and causes listeriosis

Listeria monocytogenes is a Gram-positive, intracellular pathogen. It expresses listeriolysin O, which can destory red blood cells. It grows between -0.4℃ to 50℃ and is wide spread in soil, sewage and food products (53). *L. monocytogenes* is a typical food-borne pathogen. Once a human gets infected, it may suffer “listeriosis”, a serious disease which mainly targets pregnant women, newborns and individuals with immune deficiency. The fatality rate of listeriosis is about 25%~30%.

1.3.2 The life cycle of *L. monocytogenes* in the host cell

The entry of *L. monocytogenes* into host cells starts with the interaction of its two virulence factors, internalin A and internalin B with the surface of host cells. Once inside host cell, bacteria reside in a vacuole (also called phagosome). The secreted pore-forming protein listeriolysin O, another virulence determinant for *L. monocytogenes*, is essential for bacteria to escape from vacuole. The function of LLO is pH dependent (63, 151, 173). After escaping from vacuole, *L. monocytogenes* grows rapidly and assembles an F-actin tail, which propels the bacterium to move toward the cell membrane (41, 162). This actin polymerization needs a surface protein, ActA, that promotes the actin nucleating activity (160). When *L. monocytogenes* reaches the cell membrane, it continues to infect neighboring cells (70, 173) (Figure 2).

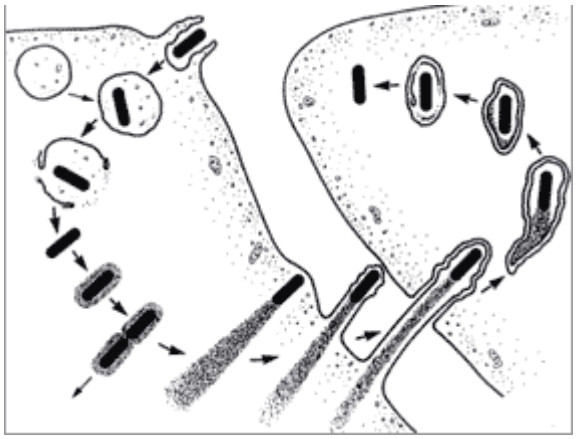

Figure 2 The life cycle of *L. monocytogenes* in the host cell

(173)

1.3.3 Iron and the pathogenesis of *L. monocytogenes*

In the chromosome of *L. monocytogenes*, a gene cluster exists that called the *Listeria* Pathogenicity Island 1. It consists of six genes: *prfA*, *plcA*, *hly*, *mpl*, *actA* and *plcB*. The products of these six genes are crucial virulence determinants in the intracellular life cycle of *Listeria* (129, 182). The transcription of these listeria virulence factors is regulated by *prfA* (85).

Iron is an essential element for bacteria to grow and more and more evidence showed that the availability of iron is also a key determinant of *Listerial* virulence during infection. High levels of iron stimulate the entry of *L. monocytogenes* into host cells by modifying the surface hydrophobicity of *Listeria* (39), and adding iron to the medium also strongly increases the activity of listeriolysin O (57). When the environmental iron concentration is low, such as in a vacuole, the *prfA* gene will be activated and regulates the expression of other virulence factor genes, resulting in the acceleration of the spreading of *listeria* from cell to cell (40, 64).

Like some other Gram-positive bacteria, *L. monocytogenes* cannot synthesize siderophores. Sequencing of the whole genome showed that such kind of genes are absent in this bacterium (67), which means that *L. monocytogenes* relies more on the uptake of iron from the iron-binding proteins in its host cell. It is known that *L. monocytogenes* utilizes transferrin, lactoferrin and hemoglobin as iron source (84). Since heme in hemoglobin is the most abundant source of iron

in mammalian cells, we can presume that heme uptake plays an important role during listerial infection.

1.4 Heme and hemoglobin are important iron sources for pathogenic bacteria

Heme is a complex, in which ferrous iron (Fe^{2+}) is incorporated in protoporphyrin IX or its derivatives. When ferric iron (Fe^{3+}) bonds to protoporphyrin IX, it is known as “hemin”. However, both “heme” and “hemin” are commonly called heme. Figure 3 shows three different types of heme. They are different in structure by the substitution side chains on the porphyrin ring. Heme *b* is the heme which is bound to hemoglobin. Heme *a* is found in cytochrome-*a*, a_1 and a_3 in the chlorophyll of green plants. Heme *c* is in cytochrome-c and it is covalently linked to protein by -Cys-S- bond. Among these three different heme molecules, heme *b* is the carrier of oxygen in blood.

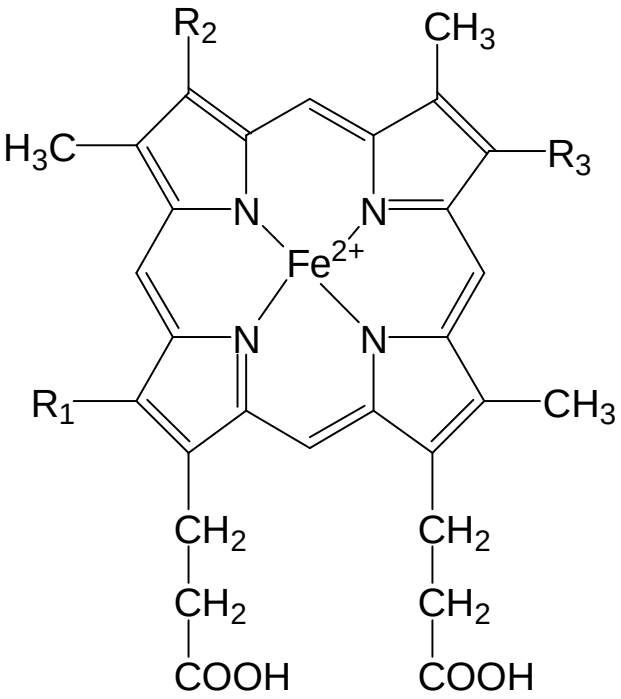

Figure 3 Structure of heme *a*, *b* and *c*

for heme *b*, R_1=—CH_3, R_2, R_3= —$CH{=}CH_2$;

for heme a, R_1= —C(=O)—H, R_2= —CH(OH)—CH_2—(CH_2—CH=C(CH_3)—CH_2)$_3$—H, R_3= —$CH{=}CH_2$; for heme c, R_1= —CH_3, R_2, R_3= —CH(SH)—CH_3)

About 70% of the intercellular iron pool is heme, which is bound to hemoglobin and myoglobin. In mammals, hemoglobin transports oxygen from lungs to the cells of the body. Each hemoglobin molecule has four globular subunits: two α-chains and two β-chains. Each of these subunits has a strong heme-binding pocket that tightly binds a single heme molecule.

Heme can go into a lipid bilayer and disturbs membrane structure. Heme also

catalyzes the formation of radicals, so the accumulation of free heme in the cells could badly damage them; therefore, free heme is not tolerated (82, 143, 183). Once heme is released after the degrading of heme-proteins in the cell, it is quickly bound by hemopexin and serum albumin. Free hemoglobin is also deleterious, hemoglobin dimers are bound by haptoglobin. All these heme and hemoglobin binding proteins have high affinity for ligands, therefore, even though heme is abundant in human and animal bodies, free heme concentration is very low (65, 176, 189, 196).

1.5 Regulations of heme uptake in bacteria

Free heme overload in cytoplasm is toxic. The amount of heme in the cell is strictly controlled to avoid heme toxicity. The expression of heme (iron) uptake proteins is regulated by Fur (**F**erric **U**ptake **R**egulator) as a response to the heme (iron) level in the cell environment (73).

The Fur protein has two domains. The N-terminal domain is in charge of the binding of DNA. The C-terminal domain contains metal binding sites and help Fur to form a homodimmer in *vivo* (3, 81).

Under iron rich conditions, Fe^{2+} binds to Fur dimer, which can bind the DNA strand at a specific site, which is called the “Fur box”. In *E. coli*, the ‘Fur box’ is a 19 bp consensus DNA sequence (10, 50). The sequence of “Fur box” varies in

different species. The binding of holo-Fur to DNA blocks RNA polymerase; therefore the downstream genes cannot be transcribed. When the iron level is low in the cell, Fe^{2+} leaves Fur and apo-Fur releases from DNA, then RNA polymerase regains its accessibility to the promoter region and the transcription starts (Figure 4). In *E. coli*, about 60 Fur-regulated genes are known, including iron receptor genes, iron permease genes, siderophores biosynthesis genes, heme uptake genes and other iron metabolism genes. Fur is also found in many bacterial pathogens, such as *Y. pestis*, *P. aeruginosa*, *V. cholerae* and *L. monocytogenes* (118-120, 171).

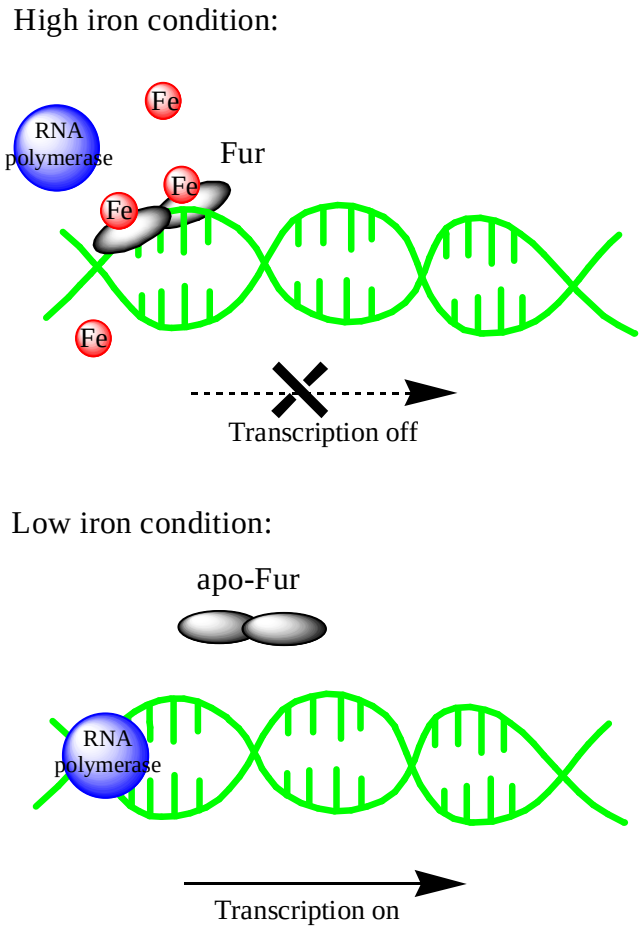

Figure 4 Fur regulated gene expression

Some Gram-negative bacteria produce another iron uptake repressor, DtxR, which shares structural similarities with Fur. DtxR also has two domains in each monomer. The N-domain is in charge of DNA binding; C-domain contains the binding sites for Fe^{2+} in *vivo* (127).

Some bacteria have regulation factors other than Fur and DtxR. For example, the Has system in *S. marcescens* is regulated by extracytoplasmic function sigma factors (65).

1.6 Heme uptake in Gram-negative bacteria

1.6.1 Direct heme uptake system

So far, two major heme acquisition systems have been indentified in Gram-negative bacteria. These two systems have most of their protein components in common, the major difference between them is whether they need “hemophore”, a small heme scavenging protein, to “steal” heme from hemoproteins or not.

One of the heme uptake systems can be called a “direct heme uptake system”. It includes an outer membrane receptor, which binds heme or hemoproteins on the bacterial cell surface. After crossing the outer membrane, heme is transported into the cell though ATP-binding cassette (ABC) transporters. This category of heme uptake system includes the *hem*RSTUV system in *Yersinia enterocolitica* (165), the *hmu*RSTUV systerm in *Yersinia pestis* (171), and the *shu*ASTUV system in *Shigella dysenteriae* (28).

The uptake of heme starts with the release of heme from hemoglobin (the mechanism of this process is still unknown). Once released from hemoglobin, heme is recognized by the receptor proteins in these systems. These receptor proteins have the similar structural topology with siderophore receptors, like FepA, FhuA and FecA, including the β-barrel domain and the globular plug

domain. Some studies showed that the heme binding sites in these receptors are conserved (21). These receptors also need energy to make heme go though outer membranes, and the energy provider is proposed to be the TonB-ExbB-ExbD complex. In the periplasmic space, heme adsorbs to the periplasmic binding proteins, which transfer heme to the ABC transporter in cytoplasmic membrane (75, 177). Several kinds of periplasmic heme binding proteins have been indentified, such as HemT in *Y. enterocolitica*, ShuT in *S. dysenteriae*, and ChuT in *E. coli*. The crystal structure of ShuT was recently solved, it is a 28.5 kD monomer and each ShuT binds one molecule of heme (49, 76).

The ABC transporter in the cytoplasmic membrane consists of a periplasmic binding protein, a transmembrane protein and an ATPase protein. The gene clusters of these systems may also encode a protein called “heme oxygenase”. Once heme is transferred into the cytoplasm, the heme oxygenase opens the porphyrin ring and breaks the coordation between iron and nitrogen atoms, thus releasing iron, and the two degradation products of protoporphyrin IX are biliverdin and CO.

1.6.2 Hemophore-dependent heme uptake system

Hemophores are small extracellular heme-binding proteins that are secreted by several Gram-negative bacteria. The function of hemophore is to bind heme outside the cell envelope and bring it to outer membrane heme receptors (185).

One type of hemophore is HxuA from *Haemophilus influenzae*. It binds to hemopexin (72). The other hemophore, HasA, which is the most studied hemophore up to date, was found in several Gram-negative bacteria, including *Yersinia enterocolitica*, *Yersinia pestis*, *Pseudomonas fluorescens* and *Serratia marcescens* (185).

The structure of *Serratia marcescens* HasA has been solved. HasA (**H**eme **A**cquisition **S**ystem) is a 19 kD globular protein with 4 α-helixes and 7 β-sheets (6). HasA has high affinity for heme ($K_d=10^{-11}$ M) and it can capture heme from a broad spectrum of heme-containing molecules, including hemoglobin, myoglobin and hemopexin (94, 95). The mechanism of extracting heme from hemoglobin by HasA is still unknown. After capturing heme, HasA transfers heme to HasR, the outer membrane receptor. The binding between HasA and HasR is energy, temperature and TonB-ExbB-ExbD complex independent (80, 95).

1.7 Heme uptake in Gram-positive bacteria

1.7.1 The structure of Gram-positive bacteria cell wall

Compared with Gram-negative bacteria, less is known about the heme uptake pathways in Gram-positive bacteria kingdom. Unlike Gram-negative bacteria,

the Gram-positive bacterial cell envelope doesn’t have an outer membrane. Outside the cytoplasmic membrane, there is a thick cell wall around the cell. The different cell envelope structure of Gram-positive bacteria raises a number of interesting questions, such as: How do cells recognize heme/hemoglobin on the cell surface? Where are the heme transport proteins located? What is the pathway for heme to pass through the cell wall? Where does the energy come from? Finding answers for these questions is important because many Gram-positive bacteria are human or animal pathogens and they depend on heme as the major iron source during the infection.

The cell wall of Gram-positive bacteria is a multiple layered peptidoglycan network around the cytoplasmic membrane. There are many cell surface molecules attached to it, such as teichoic acids, lipoteichoic acids, surface molecules attached to it (111).

Peptidoglygan consists of repeating N-acetylglucosamine (NAG)-(β1, 4)-N-acetylmuramic acid (NAM) strands. For most Gram-positive bacteria, the D-lactyl group of each NAM is linked to a short peptide, and the short peptide is linked to an adjacent peptide that attached to a neighbor glycan strand via a cross-linked peptide. The crosslinking between each glygan strand generates the cell wall network surrounding the cell (66, 111, 168, 174) (Figure 5)

In the *Listeria monocytogenes* cell wall, the linkage between each NAM from different glycan strands is different from other species. Instead of a cross-linked peptide, two short peptides are joined together via an amide bond between the two short peptide (146).

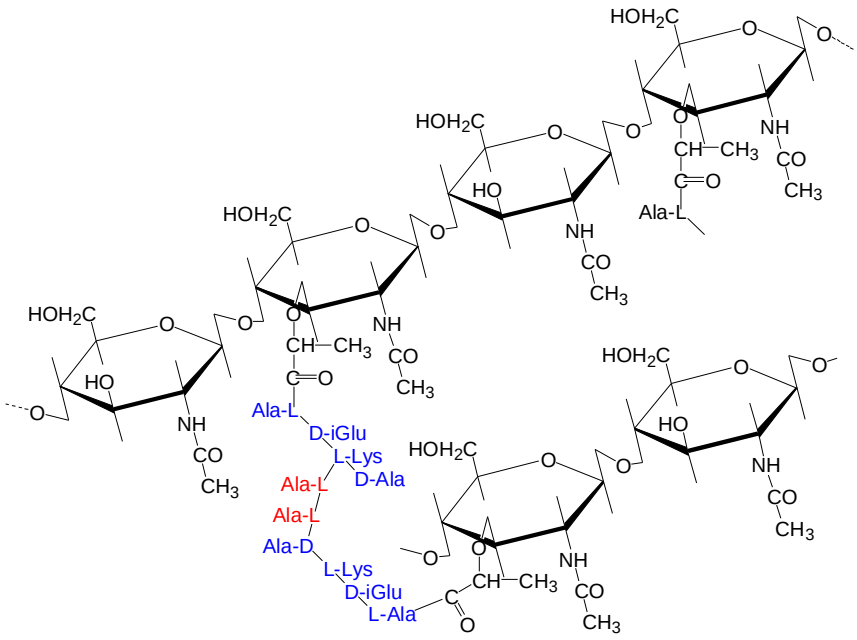

Figure 5 Structure of peptidoglycan from S.pyogenes

Different colors show short peptide (blue) and cross linkage (red).

1.7.2 Protein sorting in the Gram-positive bacteria cell wall

The main function of the cell wall is to protect cells from their enviroment. It also provides a surface scaffold for Gram-positive pathogens' surface proteins to interact with the excellular environment in host tissue. To accomplish their

biological functions, these proteins must be properly attached to the cell wall.

Such surface proteins are covalently anchored to petidoglygan by sortases, a class of membrane-anchored transpeptidases, that were indentified in all known Gram-positive bacteria genome (9, 38, 104, 122). In most cases, the precursor of Gram-positive surface proteins has a signal peptide on both the N-terminus and C-terminus. The N-terminal signal leads surface proteins to be translocated across cytoplasmic membrane (9). The C-terminal signal is also called a “sorting signal”, it includes a highly conserved motif, that is recognized by sortase (148).

The first sortase found in *S. aureus* was SrtA. It recognizes the surface protein precursor by the LPXTG motif in its sorting signal and cleaves the peptide bond between T and G (175). After cleaving, the free carboxy terminus of threonine is covalently linked to the amino group at the end of the glycine cross-bridge peptide of “lipid II” (the biosynthesis precursor of peptidoglycan). Later “lipid II” is cross linked to the growing network of peptidoglygan and the surface protein is been anchored on the cell wall at the same time (111, 124, 141).

Another sortase, SrtB, anchors surface proteins that have an NPQTN sorting signal (107). SrtB cleaves the sorting signal between T and N, and the rest of the sorting mechanism is similar to that of SrtA (105). In *S. aureus*, SrtB is a part of the *isd* operon and it anchors IsdC, a surface heme binding protein to the cell wall.

SrtA and SrtB are both found in *L. monocytogenes* (16, 17). In *L. monocytogenes*, SrtB anchors two proteins on the cell surface: The protein

encoded by *lmo2185*, which is formerly called “SvpA” and the protein encoded by *lmo2186*, which is the homologous of IsdC in *S. aureus* (118).

1.7.3 Heme uptake in *L. monocytogenes* and other Gram-positive bacteria

Several heme and hemoglobin binding proteins were identified in some Gram-positive species. According to the locations of heme transport proteins in the Gram-positive cell envelope, these mechanisms can be divided into two categories: One heme uptake mechanism is sortase-dependent. It relies on the cell wall anchored proteins to bind heme or hemoglobin. The second heme uptake mechanism is sortase-independent. It only has an ABC transporter in the cytoplasmic membrane, which usually includes a heme-binding lipoprotein, a trans-membrane permease protein and an ATPase. One Gram-positive bacteria cell can have both systems at same time, which has been shown with several Gram-positive bacteria, such as *Streptococcus aureus*.

In *S. aureus*, the *isd* (**I**ron-regulated **S**urface **D**eterminants) gene cluster encodes a heme/hemoglobin uptake system to acquire heme iron during the infection (Figure 6) (106, 137). After the releasing of hemoglobin from host red blood cells, hemoglobin is proposed to bind to surface receptors IsdB and IsdH. IsdA, another cell wall protein removes heme molecules from globins and transfers heme to IsdC. Heme then passes across the cytoplasmic membrane via IsdDEF. The crystal structures of the heme-IsdC complex and the soluble portion

of heme-IsdE complex were sloved recently (69, 154). Once in side cyroplasm, IsdI and IsdG, two heme degrading enzymes, degrade heme and release iron (93, 192).

In the *isd* system, IsdA, IsdB and IsdC are all covalently anchored to the cell wall by sortases. The first two proteins are anchored by SrtA with a LPXTG sorting signal, and the last one is anchored by SrtB with a NPQTN sequence.

isd homologous systems are also found in several other Gram-positive bacteria. *Bacillus anthracis*, the anthrax pathogen, is capable of scavenging heme as iron source during infection. The *isd* locus in *B. anthracis* encodes IsdC, and the deletion of IsdC and SrtB defects heme uptake in *B. anthrascis*. In *vitro*, IsdC binds heme with a K_d about 3.1 uM. More results about the heme and hemoglobin binding fuction of IsdC and IsdK were reported recently (62, 103).

Besides the *isd* locus, *S. aureus* has another heme uptake complex, HtsABC, which appears to be sortase-independent (159). HtsABC is a heme ABC transporter and it turns out that Hts is the primary heme transport system in *Streptococci* rather than *isd* system. Spectroscopic data showed that the lipoprotein HtsA binds heme (98, 135, 142).

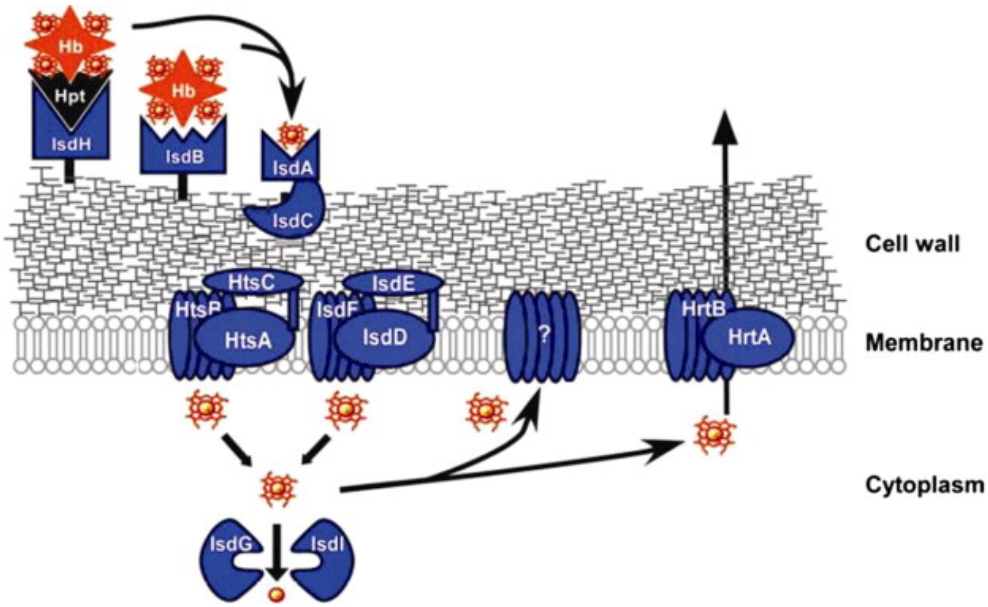

Figure 6 Heme acquisition systems in *S. aureus*

(137)

The iron acquisition systems in *L .monocytogenes* were left unknown until 2006, when a ferric hydroxamate uptake system and a heme/hemoglobin uptake system were indentified for the first time (84). Nutrition tests and growth assay showed that *L. monocytogenes* can use multiple types of iron complex, including: hydroxamate siderophores, such as ferrichrome, ferrichrome A and ferrioxamine B; catecholate siderophore, such as ferric enterobactin, ferric corynebactin; and iron-binding proteins, such as lactoferrin, transferring and feritin and hemoglobin.

[^{59}Fe]-siderophore uptake experiments showed the K_m for ferric siderophores is about 1~10 nM, which is 10~100 fold lower than Gram-negative bacteria, such as *E. coli*. The transport rate (V_{max}) for ferric enterobactin and ferric

corynebactin are also 400 fold lower than that of *E.coli*. For ferrichrome, the transport rate is about the same.

In the genome of *L. monocytogenes*, the Fur regulated *fhu* region encodes a transporter system for hydroxamate siderophores, and deletions of *fhuD* (*lmo1959*) or f*huC* (*lmo1960*) severely reduced the transport of ferrichrome. The *hup* region, including *hupD* (*lmo2431*), *hupG* (*lmo2430*) and *hupC* (*lmo2429*), which is also Fur regulated, encodes an ABC transporter. Nutrition tests showed the deletion of *hupC* didn't hurt the uptake of hydroxamates or catecholates, but impaired the uptake of both heme and hemoglobin, which indicated that HupDGC is a heme/hemoglobin ABC transporter.

In the genome of *L. monocytogenes* (EGD-e strain), the homolog of the *isd* locus was also found (118). The *svpA-srtB* locus contains seven genes. A fur box sequence in the promoter indicates that this operon is iron regulated. The first gene, *lmo2186*, encodes a protein with 33% identity to IsdC. The second gene, *svpA* (*lmo2185*) encodes a protein that shows similarities to both IsdC and the protein encoded by *lmo2186*. Similar to *S. aureus* IsdC and *B. anthracis* IsdC, co-chromatography experiment showed that SvpA also binds heme in solution. Both lmo2186 and svpA contain the sortase B sorting motif at the end of the gene and it seems like they are the only two proteins that are anchored on the cell wall by sortase B (16). The three genes downstream from SvpA (*lmo2184*, *lmo2183* and *lmo2182*) together encode an ABC transporter whose substrate is still unknown. *srtB* (*lmo2181*) is the penultimate gene in the locus and the last

gene, *lmo2180*, encodes a small protein with 153 residues, whose function is unknown. Although the *svpA-srtB* locus in *L.monocytogenes* is similar to the *isd* cluster in *S. aureus* and *B.anthracis*, the deletions of *srtA, srtB, svpA* or *lmo2186* didn't affect the acquisitions of heme or hemoglobin in nutrition tests. Also, these mutants have no impact on the virulence of *L. monocytogenes* in the mouse model system.

These data raise interesting questions about whether the heme/hemoglobin uptake system (e.g. Hup transporter) is sortase dependent or not. Perhaps, like the Isd and Hts systems in *S. aureus*, more than one heme transport systems coexists in *L. monocytogenes*, and not all of them depend on the sortase-anchored surface proteins to transport heme.

Organism	Transporter	Reference
Gram-negative bacteria		
N. meningitidis	HmbR	(166)
Y. enterocolitica	HemRSTUV	(165)
Y. pestis	HmuRSTUV	(171)
S. dysenteriae	ShuASTUV	(28)
V. cholerae	HutABCD	(74)
P. aeruginosa	PhuRSTUVW	(177)
E. coli	ChuATUVS	(169)

Gram-positive bacteria		
S. pyogenes	SiaABC	(12)
S. aureus	IsdHABCDEF	(106)
	HtsABC	(159)
C. diphtheriae	HmuTUV	(147)
B. anthracis	IsdCEE2F	(103)
L. monocytogenes	HupDGC	(84)

Table 1 Heme/hemoglobin transport systems in Gram-negative and Gram-positive bacteria

1.8 ATP-binding cassette (ABC) transporters

1.8.1 The general structure of an ABC transporter

ABC transporters are a family of membrane-intergrated proteins that transport different kinds of substrates across lipid bilayers, either inside the cell or outside the cell. ABC transporters are represented in both prokaryote cells and eukaryote cells. In prokaryote cells, ABC importers are in charge of the uptake of essential nutrients, such as sugars, amino acids, metals and vitamins. The importers are further divided into two subtype groups (type I and type II) based on their

topologies (78). ABC exporters release toxic substance or drugs, therefore they contribute to the antibiotic and drug resistance in bacterial pathogens (43, 195).

The detailed structure of ABC transporters is diverse, but they have the same basic organization: two transmembrane domains (TMDs) to make a pathway for the substrate and two nucleotide-binding domains (NBDs) in cytoplasm bind and hydrolyze ATP. In bacterial ABC importers, a substrate-binding protein is also required to deliver the substrates to the TMDs from exterior (Figure 7).

The energy of the transport is from ATP hydrolysis by the NBDs. Several sequence motifs are highly conserved in NBDs, that are either used to bind nucleotides or to help assemble of the whole transporter (43, 149).

Unlike the NBDs, the primary amino acid sequences of TMDs are quite different from each other due to the different substrates they carry. The main secondary structure of the TMD is transmembrane α-helix (44).

The binding proteins have a high specific affinity for their substrates. In Gram-negative bacteria, they are periplasmic proteins. In Gram-positive bacteria, since the outer membrane does not exist, the binding proteins are lipoproteins that are covalently anchored on the outside lipid of the cytoplasmic membrane.

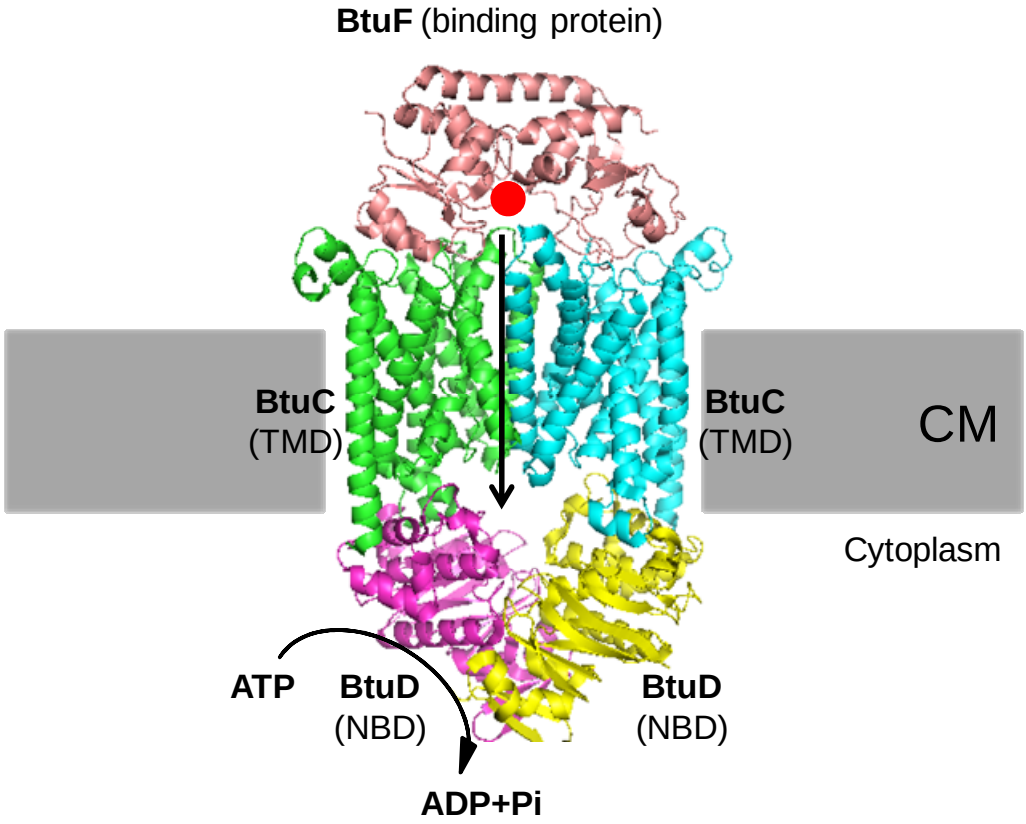

Figure 7 Structure of Gram-negative bacterial ABC transporters

Crystal structure of BtuCDF (PDB 2QI9), the ABC transporter of vitamin B_{12} in *E.coli* is used here as a model. BtuC (green and light blue) is the transmembrane domain (TMD) inserted in the cytoplasmic membrane (CM). BtuD (purple and yellow) is the nucleotide-binding domin (NBD), which is in charge of the binding and hydrolysis of ATP. BtuF (magenta) is the periplasmic binding protein for the substrate.

1.8.2 The transport mechanism of ABC transporter in bacteria

The crystal structures of several ABC transporters are known (45, 46, 79, 100, 126). These structures give people a great insight about the coorperation

between each domain during transport, and they suggest that the binding of ATP to the NBDs can cause conformational changes and make two NBDs closer to each other. This conformational change signal is transferred to TMDs, then TMDs are proposed to convert their inward-facing conformation to an outward-facing one and get ready to internalize the substrate, that they get from the external binding protein. After ADP and phosphates are released from NBDs, the conformation of both NBDs and TMDs are reset and the transporter is ready to start a new transport cycle (44). It is still debatable whether all ABC transporters follow this general mechanism. The question maybe answered when more 3-D biochemistry is completed.

1.8.3 Heme ABC transporter

Heme ABC transporters have been indentified in many bacteria, such as HemTUV in *Y. enterocolitica*, PhuUVW in *P. aeruginosa*, ShuTUV in *S. dysenteriae*, IsdDEF and HtsABC in *S. aureus* and HupDGC in *L. monocytogenes*. These transporters all consist of a binding protein, a membrane permease and an ATP-binding protein. The crystal structures of several heme-binding proteins (periplasmic binding protein in Gram-negative bacteria and cell wall anchored heme binding proteins in Gram-positive bacteria) were recently solved and the heme binding pockets in these proteins were investigated (76, 154).

Although there are no crystal structures available for the whole transporters yet, some experimental data in *vitro* already showed that in such kinds of ABC transporters, the three components work together and ATP hydrolysis promotes the transport of heme from the binding protein to the periplamic side of the permease. Recently the ShuTUV complex in *S. dysenteriae* was reconstituted into proteoliposomes and the transfer of heme from the periplasmic binding protein ShuT, through ShuUV, to the cytoplasmic binding protein ShuS was observed when ATP was applied (29). The translocation of heme is coupled to increased levels of ATP hydrolysis. In the same paper, by using site-directed mutagenesis, the anthors found that two histidine residues in ShuA, His 252 and His 262, are important for forming a high affinity heme binding site.

On the Gram-positive side, not much work has been done to characterize the heme ABC transporter in the cytoplasmic membrane. Current data mainly focuses on heme binding lipoproteins. In *S. aureus*, the crystal structure of heme-IsdE (soluble portion) complex has been solved (69). In *S. pyogenes*, the coordination chemistry of heme with the SiaA has been studied by Raman resonance, magnetic circular dichroism and NMR (164). However, the interaction between the binding protein and the TMD domain of the heme ABC transporter in Gram-positive bacteria is still unclear, as well as the forming and closing of the transmembrane channel for heme.

1.9 TonB protein

1.9.1 The structure of TonB in *E.coli*

The Gram-negative bacterial cell envelope has two membranes. The inner membrane (IM) is a phospholipid bilayer. Between the inner membrane and the outer membrane (OM) is periplasmic space with a thin multiple layer of peptidoglycan. The structure of the outer membrane is asymmetrical. The inner side of the outer membrane is phospholipids and the outer side is negatively charged lipopolysaccharide. Outer membrane protects the cell from environmental hazards, but on the other hand, it interferes with the uptake of many important nutrient molecules, such as vitamin B_{12} and siderophore-iron complexes, that are too big (>600 Dalton) to diffuse through general porins. Gram-negative bacteria use ligand-gated active transport to uptake these substances, a process that needs energy that is not found in the outer membrane. To accomplish this mission, an inner membrane integrated TonB-ExbB-ExbD protein complex is thought to transduce the potential proton motive force from IM to these transporters in OM and the TonB protein appears to be the bridge that links these two membranes together (131).

E.coli TonB contains three distinct domains with 239 amino residues total. The N-terminal domain (residues 1-65) anchors TonB in the cytoplasmic

membrane and contacts the ExbB-ExbD complex (130). The C-terminus (residues 103-239) interacts with the outer membrane. Between the N-terminal domain and the C-terminal domain a proline-rich spacer domain (residues 66-102) exists, that links the N-terminus and C-terminus together (51). The function of TonB as an energy transducer is still not completely clear.

Numerous studies on TonB have drawn a rough picture of how TonB does its job: The N-terminal domain combined with ExbB and ExbD is the energy motor for the whole protein which uses the proton motive force across IM as energy source. The energy is transduced through the spacer domain and energizes the C-terminal domin. Then the energetic C-terminal domain interacts with the OM substrate receptors by a mean which is still unknown and provides energy to these receptors to make the active transport happen.

It is important to study the fuction of TonB since TonB is crucial for the active transports of many different kinds of substrates across the OM in Gram-negative bacteria (145). Except siderophores and vitamin B_{12}, these substrates also include heme, hemoproteins, hemophores (33), maltodextrins (115), nickel (144), sucrose (20), cobalt (138), thiamin (139) and copper (92).

The crystal structure of TonB C-terminus was solved as a homo-dimer in 2001 (36) (Figure 8). For each monomer, the C-terminal of TonB folds into three antiparallel β-sheets and one short α-helix. More TonB C-terminal structure models, either as a dimer or monomer, became available later by X-ray cryptography or NMR methods (89, 153). The TonB C-terminus as a monomer

was co-crystallized with BtuB and FhuA recently and this structure data suggested that the C-terminal β-sheet interacts with the 'TonB box' motif in these receptor proteins (123, 155).

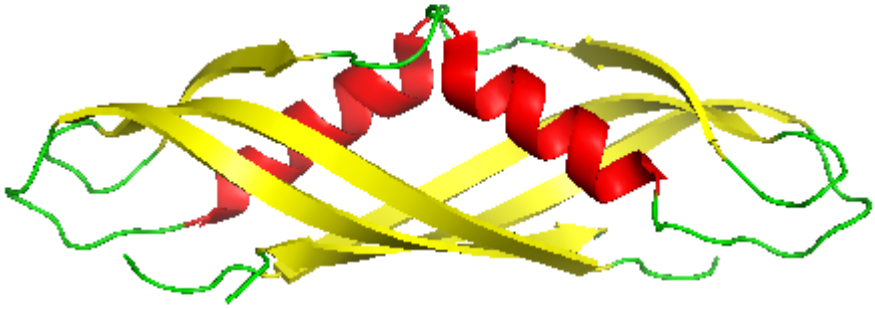

Figure 8 Crystal structure of the dimeric TonB C-terminus

1.9.2 Two models for the function of TonB

Intensive research has been done to investigate the mechanism of TonB function. Two models are proposed.

In the shuttling model (131), the TonB-dependent energy transduction cycle begins with the energizing of TonB by ExbB-ExbD complex. TonB stores the energy of the proton gradient via a conformational change and leaves IM to OM, where TonB transfers stored energy to the ligand-gated transporters to internalize ligand to the periplasmic space. After that, TonB goes back to IM for the next

transduction cycle. Our experiment data disputed this model: TonB N-terminus remains in the inner membrane rather than shuttling to the outer membrane during siderophore transport (86).

In the second model, the rotation model (36), TonB dimer does not leave IM during the energy transduction. The N-terminus of TonB inserts in the ExbB-ExbD complex and after TonB get energized, it starts to rotate and the proline-rich spacer domain sends the rotating C-terminus to the OM transporter and delivers energy.

1.10 Significance

Hemin and hemoglobin are important iron sources for bacterial pathogens, including *L. monocytogenes*. Until now, it was not clear how capable Gram-positive bacteria utilized hemin, what kind of protein systems were involved in the transport, and where they were located. Furthermore, the kinetics and thermodynamics of hemin transport in Gram-positive bacteria have not been elucidated. The answers of these questions will be valuble for us to understand the mechanisms of listerial iron acquisition and the relation between hemin uptake and virulence.

On the Gram-negative side, the inner membrane protein TonB is essential for the function of many outer membrane receptors that transport different nutrients, including iron. The knowledge of TonB can lead to new methods of preventing

Gram-negative bacterial infections in humans. The C-terminus of TonB interacts with OM receptors, which is the most importance part of the TonB-dependent mechanism that transports nutrients across the outer membrane in Gram-negative bacteria.

1.11 Research focus

This study focused on the hemin uptake in *L. monocytogenes* and the affinity of TonB C-terminus for peptidoglycan. By using molecular biology techniques and radioisotope labeled hemin, the aim of this study is to answer these questions: What is the function of the genes in the Hup system? Are there other hemin uptake systems in *L. monocytogenes* other than Hup? Are sortases and sortase-dependent surface proteins involved in hemin uptake or not? What is the hemin binding and uptake parameters of *L. monocytogenes*? For the TonB study, my research mainly focused on the measurement of the affinity of the TonB C-terminus for peptidoglycan by fluorescence quenching and exploring the binding site on the TonB C-terminus using alanine mutants.

Chapter 2 Materials and Methods

2.1 Bacteria strains and plasmids

For the *E. coli* strains used in this study, BN1071 was the wild type in control experiments. AN102 was used for the purification of enterobactin. BL21 and C43 were used for the overexpression of his-tagged proteins. XL1-blue and DH5α were hosts for plasmids. SM10 is a conjugation donor strain. OKN3 is a Δ*fepA* strain derived from BN1071.

Strain or plasmid	Genotype and characterization	Source or reference
E.coli		
BN1071	*F⁻ thi entA pro trp rpsL*	(88)
AN102	*thi trp fep proC leu tonA*	(193)
BL21	*F⁻ dcm ompT hsdS*(r_B^- m_B^-) *gal*	Stratagene cloning systerm
C43(DE3)	*F⁻ompT gal hsdSB* ($r_B^-m_B^-$) *dcm lon* λDE3 and two uncharacterised mutations described in the reference	(108)
XL1-blue	*recA1 endA1 gyrA96 thi-1 hsdR17 supE44 relA1 lac*	Stratagene cloning systerm
DH5α	*supE44 ΔlacU169(Φ80lacZ ΔM15) hsdR17 recA1 endA1 gyra96 thi-1 relA1*	(71)

SM10	*F⁻ thi-1 thr-1 leuB6 recA tonA21 lacY1 supE44* (Mu_C^+) λ^- Km^r Tra^+	(91)
OKN3	BN1071 *ΔfepA*	(102)
L. monocytogenes		
EGD-e	wild type	(16)
Plasmids		
pKSV7	*E.coli - L.monocytogenes* shuttle vector	(163)
pPL2	site-specific shuttle integration vectors	(91)
pET28a(+)	His-tag cloning vector	Novagen cloning system
pET21a(+)	His-tag cloning vector	Novagen cloning system
pMalp2	MalE fusion protein cloning vector	New England Biolabs Inc.
pSTON	pMalp2 *malE::tonB* 170-239	(86)
pUC18	High copy number cloning vector	

Table 2 Strains and plasmids used in this study

2.2 Growth media

In this study, Luria-Bertani broth (LB) was used as the iron-rich media for *E.coli*. T-media was used to grow AN102 for the purification of enterobactin. MOPS media was the iron-deficient media for *E.coli*. BHI was the iron-rich media for *L. monocytogenes*. RPMI1640, KRM and Rich MOPS media were

iron-deficient media for the growth of *L. monocytogenes* (Table 3)

Media	**Reference**
Luria-Bertani Broth (LB)	Miller. 1972. Experiments in molecular genetics (Cold Spring Harbor Laboratory, Cold Spring Harbor, NY)
T-media	(88)
MOPS media	(112)
Rich MOPS media	In this study
RPMI1640	Sigma
KRM	(118)
Brain Heart Infusion (BHI)	Difco
Grimm-Allen medium	(60)

Table 3 Media used in this study

2.3 Oligonucleotides

All primers (25 nmole, desalted) used in this study were purchased from Invitrogen Corporation (Table 4). Plasmid purification kits, reactions (PCR, ligation and digestion) clean kits were from QIAGEN. Zymoclean^{TM} DNA recovery kit was used for the recovery of ligation products from agrose gel. All restriction enzymes, ligase and Taq polymerase were from New England Biolabs. All site-directed single residue mutants were constructed by using

QuikChange™ site-directed mutagenesis kit from Stratagene.

Primer name	Sequence (5'-3')
Primers for the chromosomal deletion of *lmo2430*	
2430 BamHI	GTTTTGACC**GGATCC**AACTCAATT
2430 XhoI-up	GGGGGG**CTCGAG**AGTTGTCATTAGTTATCCACCTTA
2430 XhoI-down	GGGGGG**CTCGAG**AAAGAGGGAGGGTTGCTTC
2430 PstI	GCCGCCCA**CTGCAG**CTTATCATAGTCGAAAAA
Primers for pKSV7/*lmo2430* integration checking	
Inter-checkup	CGAGATTGCTAATGTCTATACCGGCCCG
Inter-checkdown	AATAAATACTAGAATCGTCCCAAGGTCC
2430-check-up	CTACCGTCCTCATTAAGTGGAAAT
2430-check-down	CTCGTCCTCCTCTTGCAAAGTG
Primers for 6Histag clone of HupC (*lmo2429*) in pET28-a(+)	
2429hisBamHI	CCCCCC**GGATCC**ATGAAATCAGCATTAGAACTA
2429hisXhoI	CCCCCC**CTCGAG**TTAATATTCAAAACGAGTCGA
Primers for the complementation of *lmo2429* in pKSV7	
PropKSVBglII	CCCCCC**AGATCT**TTTTCATCGCCTCCTTAAGTTAATTATA
PropKSVBamHI:	CCCCCC**GGATCC**AATTCCCCTCCACAACACTGTCCTTTT
2429pKSVBamHI	CCCCCC**GGATCC**ATGAAATCAGCATTAGAACTAAAAAATGTT
2429pKSVPstI	CCCCCC**CTGCAG**TTAATATTCAAAACGAGTCGAAGCAAG

Primers for the sequencing of promoter-*lmo2429* ligated in pKSV7

SeqPro2429pKSV (promoter)	GAGCCAGCTTCGGTGCGGCAAACG
SeqPro2429pKSV (stop codon)	GGCTCGCCTAGAGAAGTTTTCACG
2429pKSVup	CCCCAGTTGGATTTGTTTTAAGTGGTTTT
2429pKSVdown	TTTCCTATTCCATAAAGATAGTATGCCC

Primers for the site-directed Cys mutants on HupG (*lmo2430*) in pUC18

pUC182430PstI	CCCCCC**CTGCAG**ATGACAACTGTGAAGGCG
pUC182430EcoRI	CCCCCC**GAATCC**TCATGAAGCAACCCTCCC
A45C.for	GTAAAAGTTACATATAGCGAC**TGT**TGGCAAACTTTGACTGG
A45C.rev	CCAGTCAAAGTTTGCCA**ACA**GTCGCTATATGTAACTTTTAC
S54C.for	GGCGGCGGG**TGT**GACCTTGCTAACC
S54C.rev	GGTTAGCAAGGTC**ACA**CCCGCCGCC
A119C.for	GACATTAGCATTTCCT**TGT**TTAGCTTCCTTTGTGCC
A119C.rev	GGCACAAAGGAAGCTAA**ACA**AGGAAATGCTAATGTC
S194C.for	GGACACTTTCCGGAAAAT**TGT**TGGTATCATTTGGATATG
S194C.rev	CATATCCAAATGATACCA**ACA**TTTTCCGGAAAGTGTCC
S308.for	GAAGTTGGTTCGGA**TGC**ATCGAGCTTCCAG
S308.rev	CTGGAAGCTCGAT**GCA**TCCGAACCAACTTC

Primers for the complementation of *lmo2429* in pPL2

pPL2ProBamHI	CCCCCC**GGATCC**TTTTCATCGCCTCCTTAAGTTAAT
pPL2ProPstI	CCCCCC**CTGCAG**AATTCCCCTCCACAACACTGTCCT

pPL22429PstI	CCCCCC**CTGCAG**ATGAAATCAGCATTAGAACTAAAA
pPL22429KpnI	CCCCCC**GGTACC**TTAATATTCAAAACGAGTCGAAGC

Primers for checking the integration of pPL2/Pro/2429 into EGD-e chromosome*

PL95	ACATAATCAGTCCAAAGTAGATGC
NC16	GTCAAAACATACGCTCTTATC

Primers for the complementation of *lmo2430* (Cys mutants) in pPL2

(primers for promoter and the 5' (PstI) end of lmo2430, see above)

pPL22430KpnI	CCCCCC**GGTACC**TCATGAAGCAACCCTCCC

For the sequencing of *lmo2430* (Cys mutant) in pPL2/Pro/2430(C)

(three primers are designed in different positions of lmo2430 to make sure the whole gene was covered)

Seq2430pPL2-1	ACATATAGCGACGCTTGGCAA
Seq2430pPL2-2	TTACTAGCATGGGATCGCGGC
Seq2430pPL2-3	TTTTTCATTATTATGTTGGCG

Primers for 6Histag clone of *lmo2430* (cutting first 38 aa signal sequence) in pET28a(+)

HisEcoRI(Δ38)	CCCCCC**GAATCC**AAAGTTACATATAGCGAC
HisXhoI(Δ38)	CCCCCC**CTCGAG**TCATGAAGCAACCCTCCC

Primers for 6Histag clone of *lmo2430* in pET28a(+) with 6-his in both ends

24302HisEcoRI	CCCCCC**GAATTC**ACAACTGTGAAGGCG
24302HisXhoI	CCCCCC**CTCGAG**TGAAGCAACCCTCCC

Primers for 6Histag clone of TonB69C in pET21a(+)	
TonB69HisNdeI	CCCCCC**CATATG**TTGCGCATTGAAGGGCAG
TonB69HisXhoI	CCCCCC**CTCGAG**CTGAATTTCGGTGGTGCC
TonB69noHisBamHI	CCCCCC**GGATCC**TTACTGAATTTCGGTGGT
Primers for site-directed Cys mutants of MalE-TonB69 fusion in pMALp2	
S222C.for	CCGGGTAAGCCAGGC**TGT**GGGATTGTGGTG
S222C.rev	GGCCCATTCGGTCCG**ACA**CCCTAACACCAC
N227C.for	GGCAGTGGGATTGTGGTG**TGT**ATCCTGTTTAAAATTAACGGC
N227C.rev	CCGTCACCCTAACACCAC**ACA**TAGGACAAATTTTAATTGCCG
S195C.for	GATAACGTACAAATCCTC**TGT**GCCAAGCCTGCGAACATG
S195C.rev	CTATTGCATGTTTAGGAG**ACA**CGGTTCGGACGCTTGTAC
Primers for site-directed Ala mutants of MalE-TonB69 fusion in pMALp2	
E205A.for	CATGTTTGA**GCG**TGCGGTGAAAAATGCGATGCGC
E205A.rev	GTACAAACT**CGC**ACGCCACTTTTTACGCTACGCG
D189A.for	CCGGATGGTCGCGTG**GCG**AACGTACAAATCC
D189A.rev	GGCCTACCAGCGCAC**CGC**TTGCATGTTTAGG

Table 4 Primers used in this study

All primers are purchased from Invitrogen.
* Primers from reference (91)

2.4 Purification of *L. monocytogenes* EGD-e chromosomal DNA

L. monocytogenes EGD-e strain was grown overnight in 25 mL BHI. Cells were spun down at 8000 rpm for 12 minutes and the cell pellet was kept on ice. Cell pellet was resuspended in 1 mL ice cold water and then broken by Fast Prep bead-beater at intensity 6.5 for 30 seconds, 3 repeats. Unbroken cells were pelleted by microcentrifuge for 2 minutes and the supernatant was transferred to an eppendorf tube. NaCl was added to a final concentration of 100 mM and the supernatant was subjected to two extractions with buffered-phenol (1:1, V: V). After two more extractions with chloroform/isoamyl-alchol, the supernatant was transferred to a fresh tube. DNA was precipitated with 2 volumes of ethanol and centrifuged in refrigerated microcentrifuge at 13000 rpm for 30 minutes. The DNA pellet was washed with 70% ethanol and resuspended in 100 uL TE buffer.

2.5 Preparation of *E.coli* and *Listeria* competent cells

2.5.1 Preparation of *E. coli* competent cells

E. coli strain for making competent cell was inoculated in 5 mL LB overnight, then subcultured (1:100) to 500 mL LB. The culture was harvested at OD_{600}=0.5 (DU®640 spectrophotometer, Beckman) and placed on ice for 5 min then spun for 15 mins at 8000 rpm, 4°C. The cell pellet was resuspended in 250 mL of ice cold water and centrifuged again. After two washes with cold water, the cell pellet was resuspended in 50 mL ice chilled water with 10% glycerol and spun down again. Finally, the pellet was resuspended in 1 mL water with 10% glycerol and 40 uL-aliquots were stored at -80°C.

2.5.2 Preparation of *L. monocytogenes* competent cells

L. monocytogenes strain were inoculated in 5 mL BHI at 37°C overnight and subcultured (1%) to 100 mL BHI and grown at 37°C with agitation. When the OD_{600} reached 0.3, penicillin G was added to a final concentration of 0.12 ug/mL and the cells were shaken for 2 more hours (OD_{600} between 0.8 and 0.9), then spun down at 4°C. The cell pellet was washed 5 times with cold electroporation buffer (1mM HEPES+500mM sucrose); (1×100 mL, 1×66 mL

and 3×50 mL). After washing, the cell suspension was resuspended in 300 uL electroporation buffer with 15% glycerol and 100 uL-aliquotswere stored at -80°C.

2.6 Site-directed chromosomal gene deletion of *hupG* (*lmo2430*)

The method used here was for the in-frame precise deletion of *hupG* gene (*lmo*2430), which encodes a membrane permease protein in the the *hup* operon. Chromosomal deletions of structural genes in *L. monocytogenes* were constructed by allelic replacement (15, 16, 48, 118, 132). Two DNA fragments, P1, upstream (0.54 kb, BamHI and XhoI) and P2, downstream (1.18 kb, XhoI and PstI) of *lmo*2430 were amplified by PCR with appropriate restriction enzyme sites on both ends of each fragment. P1 and P2 were ligated into the thermo-sensitive shuttle vector, pKSV7, and transformed to DH5α by electroporation. DH5α cells carrying pKSV7/P1P2 were streaked on LB+Ap (100 ug/mL) plates and incubated overnight at 37°C. Single colonies were picked and verified by colony PCR. The pKSV7/P1P2 was purified again from DH5α and transformed to EGD-e wild type competent cells and plated on BHI+Cm (5 ug/mL) plates, incubated overnight at 30°C. After verification by colony PCR, EGD/pKSV7/P1P2 was grown in 5 mL BHI+ Cm at 37°C overnight. In this step, pKSV7/P1P2 integrated into the EGD chromosome by

homologous recombination. The integrants cells were grown in 5 mL BHI without Cm at 37°C and subcultured twice a day for at least 8 passages. Without Cm in BHI at 37°C, a second recombination event ocurred and pKSV7 was lost from the chromosome. After 8 time passages, cells well diluted in 10^4 or 10^5 fold and plated on both BHI+Cm and BHI plates for the Cm sensitivity assay, at least 250 colonies were tested. The Cm-sensitive colonies were screened and the deletion of *hupG* was verified by colony PCR and DNA sequencing.

2.7 Complementation of Δ*hupC* (Δ*lmo*2429) andΔ *hupG* (Δ*lmo*2430)

Spontaneous streptomycin-resistant mutants of *L. monocytogenes* recipient strains (ΔHupC and ΔHupG) were selected from BHI plates with streptomycin (100 ug/mL). Cells were grown in 5 ml BHI overnight, then subcultured (1:100, V: V) to 100 ml BHI and grown until OD_{600}=1.0. Cells were spun down at 5000 rpm for 15 mins and the pellet was resuspended in 1 ml dH2O. For each plate, 100 uL was plated and incubated at 37°C.

The natural promoter of the *hup* operon was amplified by PCR with BamHI and PstI restriction sites at the extrimities. The wild type gene *lmo*2429 and *lmo*2430 was similarly amplified from EGD-e chromosome (PstI and KpnI). The PCR products of promoter and wild type gene were ligated together and inserted

into pPL2 (Figure 10). Then the vector was transformed into *E. coli* XL-1 blue. Purified plasmids from XL-1 blue were transformed to the *E. coli* SM10 donor strain by electroporation.

For mating, The *E. coli* SM10 donor, carring pPL2, was grown in LB broth containing 20 ug/mL chloramphenicol at 30°C. The *Listeria monocytogenes* recipient was grown in BHI containing 100 ug/mL streptomycin at the same temperature. Cells were both grown to mid-log phase (OD_{600}=0.5). A 0.45 um filter was washed with LB. A mixture of 2.5 mL donor culture and 1.5 mL recipient culture was filtered, and the filter was washed with 10 mL BHI. Then the filter was placed on a fresh BHI plate at 30°C for 2 hours. The cells were gently resuspended for 5 mins in 2.5ml BHI and aliquots (25 ul, 50 ul and 100 ul) were plated in LB soft agar on BHI plate containing 100 ug/ml streptomycin and 5 ug/mL chloramphenicol. The plates were incubated at 30°C overnight and shifted to 37°C. The doule-resistant colonies were picked and verified by PCR and sequencing.

2.8 Synthesis of [^{59}Fe]-hemin

The synthesis of [^{59}Fe]-hemin followed the procedure of M. Babusiak, et al. (8); (Figure 9). Protoporhyrin IX (Sigma-Aldrich) was dissolved in pyridine (Sigma-Aldrich) to make a stock solution (6 mg/ml). 50 uL of this solution was

added to 450 uL of glacial acetic acid in a 10 mL double-neck flask at 60°C, under nitrogen atmosphere. ^{59}Fe ($^{59}FeCl_3$ in 0.5 M HCl, PerkinElmer) was mixed with $^{56}FeCl_3$ (also dissolved in 0.5 M HCl) in a microtube and the total amount of iron in the tube was 30 ug. 0.25 ul thioglyolic acid (sigma-Aldrich) was added to the microtube and the mixer was injected into the protoporhyrin IX solution immediately. After 30 mins heating at 60°C, the reaction mixer was kept at room temperature for another 1.5 hours. The mixer was transferred to 20 mL ether and extracted by 30 mL 1M HCl for at least 6 times. The organic phase was transferred to another round bottom flask and the ether was dried overnight under a flow of nitrogen. The dried [^{59}Fe]-hemin was dissolved in dimethyl sulfoxide (DMSO) and stored in cold room.

The purity of [^{59}Fe]-hemin was verified by TLC. [^{59}Fe]-hemin was dissolved in DMSO and spotted a silica gel plate (60 F_{254}, Merck). The solvent was dried and the plate was developed by a mixture solution of 2, 6-lutidine and water (5:3.5 v/v). After developing, the plate was dried and examined under UV light (52).

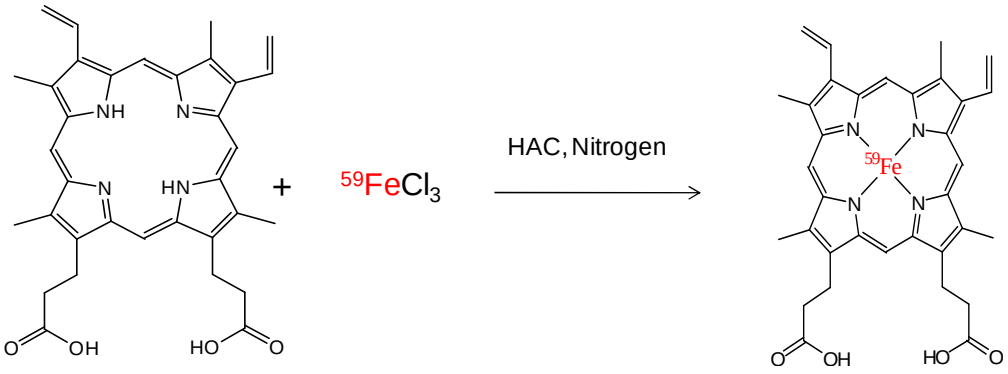

Figure 9 Synthesis of [^{59}Fe]-hemin

2.9 Nutrition tests of *L. monocytogenes*

Cells were grown in 5 mL BHI medium containing antibiotics at 37°C overnight. The culture was subcultured to 20 mL BHI medium with 2.5×10^7 cells. When OD_{600} was between 0.1 and 0.2, bypirydil was added to 1 mM final concentration. Cells were grown for another 3.5 hours.

For each plate, 8 mL of molten BHI top agar was mixed with 200 ul cells and 20 uL bypirydil (from 0.1M stock solution) and allowed to solidify. Paper discs (6 mm diameter, Becton Dickinson and Company, Sparks, MD) were placed on the top of the agar and 10 ul appropriate dilutions of iron compounds solutions were applied on the discs. The plates were incubated at 37°C overnight and the diameters of growth halos around the paper discs were measured (84, 117, 118, 188).

2.10 [^{59}Fe]-hemin binding in *L. monocytogenes*

2.10.1 Growth of cells

Cells were grown in 250 mL flask with 20 ml BHI containing streptomycin (100 ug/mL) at 37°C, 150 rpm, overnight. Cultures were subcultured (1: 100 v/v) in polystyrene tissue culture flasks (50 ml, Falcon) containing 10 mL Rich-MOPS medium, a medium modified from *E.coli* MOPS medium for the better growth of *L. monocytogenes* based on (133, 180). When OD_{600} was between 0.8~1.0, the cells were subcultured (1:50 v/v) to 50 ml Rich-MOPS again in 250 mL tissue culture flasks at 37°C, 130 rpm. Cultures were used for the hemin-binding assay when OD_{600} was between 0.6~0.8.

2.10.2 Prepartion of [^{59}Fe]-hemin solutions

The concentration of [^{59}Fe]-hemin stock solution was determined by UV-VIS spectroscopy (158). The [^{59}Fe]-hemin in DMSO was diluted about 250 fold in 40% (v/v) DMSO and scanned from 300 nm to 700 nm. Its concentration was calculated using a millimolar extinction coefficient of 180 $mM^{-1}cm^{-1}$ at 400 nm.

The [^{59}Fe]-hemin stock solution was diluted with DMSO to make [^{59}Fe]-hemin in different concentrations. For the high-concentration hemin solutions (>500nM), [^{59}Fe]-hemin was mixed with nonradioactive hemin in DMSO at calculated ratios.

2.10.3 [^{59}Fe]-hemin binding assay

All the media and buffers used in the binding assay were cooled on ice. Cells were also chilled on ice for 10 mins before starting the experiment and kept on ice all the way through. 250 uL of chilled cell culture was added to a 50 ml glass tube. 25 ml of MOPS (L) was added to another 50 mL glass tube on ice, then 250 uL [^{59}Fe]-hemin solution was added (hemin solution must be added to the tube after MOPS (L), otherwise, DMSO will freeze in the bottom of the tube), the tube was shaken slightly to help the mixing of DMSO. The binding assay was begun by transferring the mixture of hemin and MOPS (L) to the tube containing 250 uL of cells. The mixture was allowed to rest on ice for 1 min and then filtered through a 0.45 um Daropore filter (Millipore) under vacuum. The filter was immediately washed with 25 mL ice-cold wash buffer (50 mM Tris, 0.05% Tween-20, pH 9.0) immediately and placed into a 15 mL plastic tube that was counted in a Packard gamma counter. The experiment was done in triplicate for each concentration of hemin and the radioactivity of each sample counted by a Packard Cobra gamma counter. For each concentration, the counts (cpm) were

averaged and converted to cpm/10^9cells. The binding affinity (K_d) and Capacity were determined by GraFit 5.0 (Erithacus Software) by using the “1 site (with background)” method.

2.11 [^{59}Fe]-hemin uptake in *L. monocytogenes*

Cells were grown in the same conditions as for the binding assay. MOPS (L) medium was pre-warmed at 37°C in a water bath. The wash buffer was cooled on ice. 50 mL glass tubes were also waemed in 37°C water bath. 250 uL of [^{59}Fe]-hemin solution was added to a tube before the addition of 25 ml MOPS (L). The mixture of hemin and MOPS (L) was transferred to another tube containg 250 uL of cells. Each concentration was done in triplicate and incubated at 37°C for 1 min and 30 mins (for the 30 mins incubation, tubes were incubated at 37°C with shaking at 180 rpm). After incubation, the mixture was filtered through 0.45 um Durpore filters and washed with 25 mL cold wash buffer (the same as the buffer in binding assay). Samples were collected and counted in Packard Cobra gamma counter. For each concentration, the counts (cpm) were averaged and converted to cpm/10^9cells/min. The K_m and V_{max} were determined by GraFit 5.0 (Erithacus Software) by using the “Enzyme Kinetics” method.

2.12 Cloning and purification of 6His-tagged HupC and HupG

2. 12.1 Cloning of 6His-tagged protein

The DNA sequence of *lmo*2429 (without stop codon) was amplified from EGD-e chromosome by PCR with appropriate restriction enzyme sites on both sides (BamHI and XhoI) and ligated into pET28a (+). Then the plasmid was transformed into DH5α for amplification. Single colonies were picked from LB plates containing kanamycin (20 ug/mL), and the correct inserts were verified by colony PCR. Then the vector carrying *hupC* was transformed into BL21 for expression. For *hupG*, a putative transmembrane protein, we also used pET28a (+), either with or without the first 38 aa of its signal peptide. Instead of BL21, C43 was also used for the expression of HupG since C43 tolerates better the over expression of membrane proteins.

2.12.2 Purification of 6His-tagged protein

E. coli BL21 carrying pET28 (+) with the wild type gene was grown in 10mL LB broth containing 20 ug/mL kanamycin overnight at 37°C and then subcultured to 1L LB containing 20 ug/mL kanamycin. When OD_{600} reached 0.5, IPTG was added to the culture to a final concentration of 1 mM. The culture was

grown for another 3-4 hours and harvested by centrifugation at 5500 rpm for 20 min. The cell pellet was resuspended in 50 mL lysis buffer (50 mM NaH_2PO_4, 300 mM NaCl, 10 mM imidazole, pH 8.0) and broken by French press. The cell lysate was centrifuged again at 10,000 rpm, 4°C for 1 hour to separate the cytoplasm and cell membranes. If the over-expressed 6H-protein was located in the cytoplasmic portion, then the cytoplasm fraction was passed through a Ni-NTA column (Qiagen). The column was washed by 5-10 volume lysis buffer until OD_{280} was stable and followed by 5-10 volume wash with 50 mM NaH_2PO_4, 300 mM NaCl, 20 mM imidazole, pH 8.0. After washing, the 6His-tagged protein was eluted with 50 mM NaH_2PO_4, 300 mM NaCl, 250 mM imidazole, pH 8.0. In some experiments, the desired proteins were eluted by a step-gradient of imidazole to achieve better column resolution. If the 6His-tagged protein was in the membrane fraction, then the membrane pellet was resuspended and solubilized in lysis buffer containing 0.01% Triton X-100. The wash buffer and elution buffer also contained the same concentration of Triton X-100.

If desired, the purified 6His-tagged protein was dialyzed against PBS, (but not 6His-HupC, which precipitates in PBS) or lysis buffer without imidazole and stored at -20°C. The concentration of the purified protein was determined by Lowry protein assay (101).

2.13 Preparation of polyclonal α-HupC

After dialysis against PBS, about 90% of purified 6H-HupC precipitated from the solution. The precipitated protein was spun down at 10,000 rpm for 1 hour and resuspended in 1 mL PBS, and then SDS solution was added to a final concentration of 1% (V/V). The mixture was boiled for 5 min and the denatured 6H-HupC was precipitated again from the solution by cold acetone.

Mice were immunized with purified 6His-HupC (a mixture of denatured protein and protein in PBS buffer, 25 to 100 μg)six times over a 6-week period, with Freund's complete adjuvant in the first injection and with Freund's incomplete adjuvant and alum in subsequent injections. Mice were bled by cutting the tail vein.

2.14 Gram-positive bacterical cell envelope fractionation

Cells were grown in 10 mL BHI at 37°C overnight, subcultured in 100 mL BHI until OD_{600} reached 1.0. The culture was spun at 5000×g, for 20 min at 4°C and the pellet and supernatant were both kept on ice. The cell pellet was suspended in distilled water to a final volume in which the cell density was 10^{10}cells/0.25 mL. Cells were lysed by Fast Prep bead-beater for 3 times (intensity 6, 30 sec.) and the lysate was spun down in a micro centrifuge at

14000 rpm, 4°C for 1 hour to separate cytoplasm and inner membrane.

The inner membrane pellet was suspended in 0.5% sarkosyl in TBS buffer and incubated at 37°C for 30 mins. After incubation, the membrane suspension was spun at 14000 rpm, 4°C for 1 hour and the supernatant containing solublized cytoplasmic membrane proteins was stored at -20°C. The pellet was suspended in TBS. 20 uL bacteriophage amidase was added to the suspension and incubated at 37°C for 2 hours to release the peptidoglycan –associated proteins. After 2 hours incubation, the suspension was spun down at 14000 rpm, 4°C for 1 hour and the supernatant containing PG-associated proteins was saved at -20°C.

6 M TCA solution was added to the culture supernatant that was saved at very beginning, for the precipitation of secreted proteins. The solution was spun at 5000×g, 4°C for 25 mins. The protein pellet was resuspended in 10 mL 70% acetone and spun down again at 8800 rpm for 25 mins to wash out TCA. The pellet of precipitated secreted proteins was suspended in 200 uL TBS and stored at -20°C.

2.15 Immunoblots

In this study, all immunoblots were performed by using a semi-dry blotting unit (FB-SDB-2020, Fisher Scientific). Generally, the protein samples on the SDS-PAGE were transferred to nitrocellulose transfer membrane (0.45 um, PROTRAN, Whatman) at 100 mA for 2 hours (transfer buffer: 2.4 g/L Tris,

11.25 g/L glycine). When the transfer was complete, the membrane was blocked by 1% gelatin in TBS for 30 mins and incubated with primary antibody at room temperature for 3 hours or overnight at 4°C. The unbound first antibody was washed off by 0.05% Tween-20 in TBS and the membrane was incubated with an alkaline phosphatase conjugated secondary antibody at room temperature for 2 hours or overnight at 4°C. After washing with 0.05% Tween-20 in TBS, the membrane was developed by a solution of 33 mg nitro blue tetrazolium (NBT) (in 0.5 mL DMF) and 17 mg bromochloroindolyl phosphate (BCIP) (in 1 mL water) in 100 mL substrate buffer. The reaction was stopped by addition of water (19, 178).

2.16 Growth curve measurements

Cells were grown in BHI at 37°C overnight, then either subcultured (1: 100, V:V) into BHI containing 1 mM bypirydil, or subcultured twice in modified MOPS medium. OD_{600} of cells was monitored using spectrophotometer.

2.17 Constructions of site-directed cysteine substitution mutants in HupG

The gene encoding HupG (*lmo2430*) was amplified from the *L. monocytogenes* chromosome and cloned into pUC18 using PstI and EcoRI as the restriction sites on the 5' and 3' ends respectively. pUC18/*hupG* was transformed to DH5α and the cells were spreaded on LB plates containing ampicillin (100 ug/mL), IPTG and X-gal. After incubating at 37°C, white colonies were picked from the plate and the correct clones were confirmed by colony PCR.

Five single cysteine mutants, A45C, A119C, S54C, S194C and S308C, were constructed in pUC18hupG by using the QuikChange® site-directed mutagenesis kit (Stratagene, La Jolla, CA) (Figure 11).

After changing the targeting amino acid to cysteine, the *hupG* mutations were amplified from pUC18/*hupG* and ligated into pPL2/Pro (pPL2 carrying the promoter region of *hup* operon) with PstI and EcoRI restriction sites, then pPL2 plasmid carrying each *hupG* cysteine mutant was transformed into *E. coli* SM10 and the mutated *hupG* was used to complement the chromosomal deletion mutant Δ*hupG* (Sm^r) by mating. The phenotype of each complementation was tested by nutrition tests.

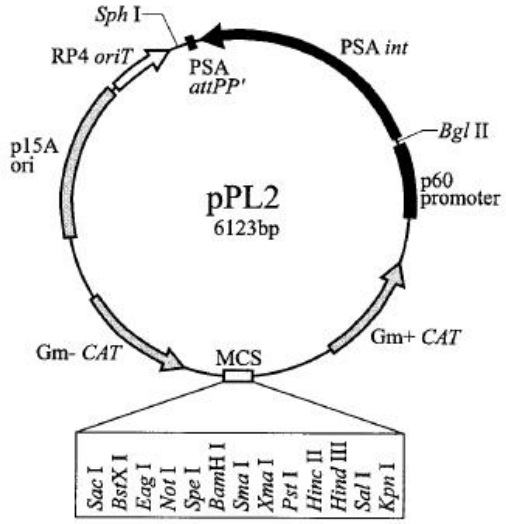

Figure 10 Plasmid map of pPL2 integration vector

(91)

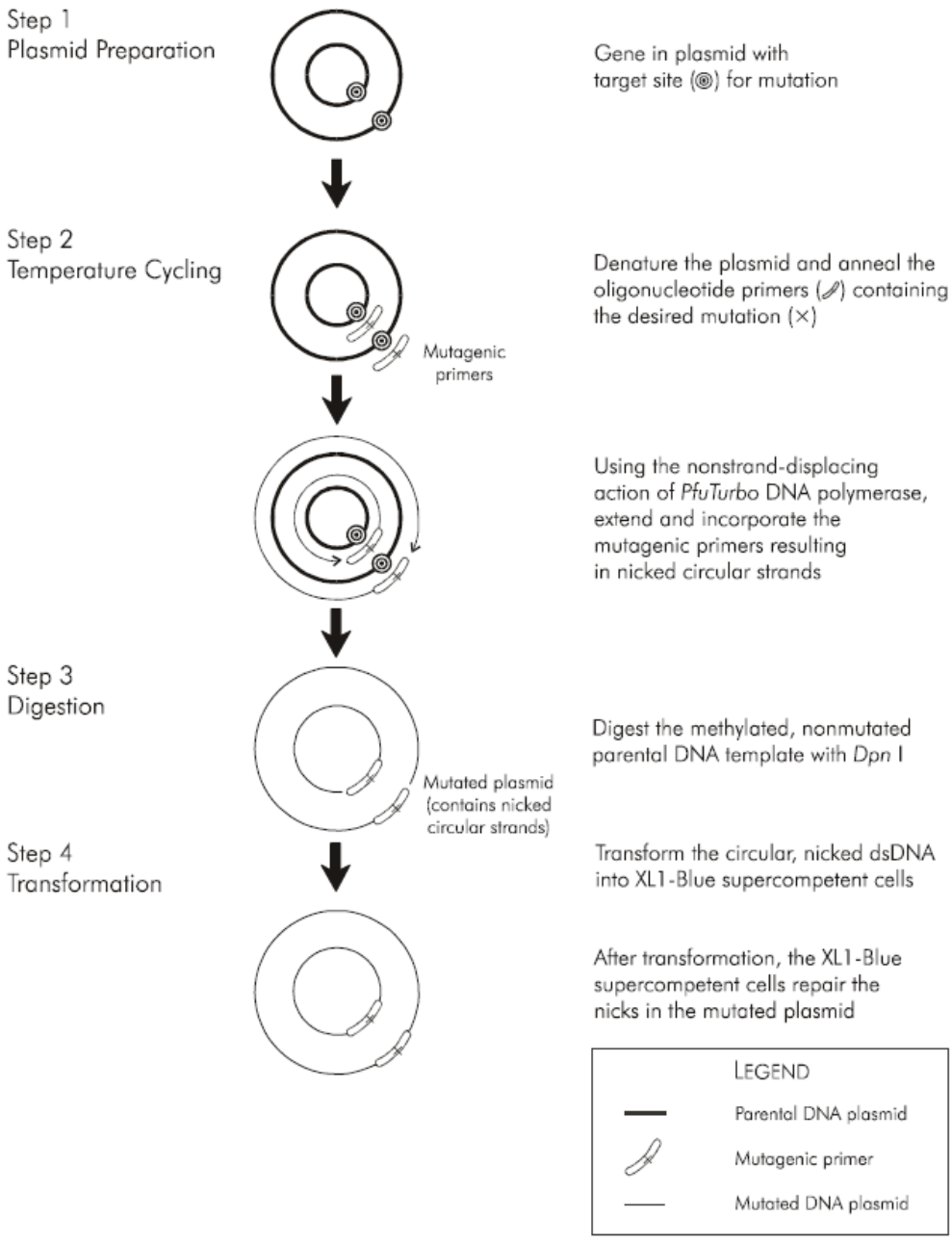

Figure 11 Steps for QuikChange site-directed mutagenesis

Picture from Manual: QuikChange **Site-Directed** Mutagenesis Kit (http://www.stratagene.com/manuals/200518.pdf)

2.18 Fluorescein -5- maleimide labeling of HupG cysteine mutants in *vivo*

Listeria cells were grown in 10 mL BHI at 37°C, overnight and subcultured (1:100) to 50 mL BHI. Bypyridyl was added to a final concentration of 1 mM when OD_{600} reached 0.1. After 3 hours incubation, 4×10^9 cells were transferred into 2.0 ml micro centrifuge tubes and spun down at 4500 rpm for 15 mins. Cells were washed in 1 mL labeling buffer (50 mM NaH2PO4, 0.2% glucose, 137 mM NaCl, pH 7.0) and resuspended in 0.5 mL labeling buffer.

A pipet tip of fluorescein-5-maleimide (FM) was dissolved in 100 uL DMF. To determine the concentration of fluorescein-5-maleimide, the DMF solution was diluted in 10 mM Tris buffer, pH 8.0 (1/500, V/V). The millimolar extinction coefficient is 81.5 $mM^{-1}cm^{-1}$ at 492 nm.

All buffers used in the labeling reactions were ice cold and cells were also kept on ice. Fluorescein-5-maleimide solution was added to the cell suspension to a final concentration of 1 uM. The labeling reactions were performed under low light condition at 37°C for 15 mins, pH 7.0. The labeling reactions were then quenched by adding cysteine to a final concentration of 100 uM. Cells were washed three times with 0.5 mL labeling buffer and finally suspended in 0.4 mL labeling buffer.

Cells were broken by bead beater (intensity 6.0, 30 s each cycle). 50 uL cell lysate was mixed with 25 uL SDS sample buffer and boiled for 5 min. 30 uL

samples were loaded to SDS-PAGE and the gel was run in dark. When the electrophoresis was completed, the gel was washed with water and transferred to Storm scanner to detect fluorescent bands.

2.19 Purification of Siderophores

2.19.1 Purification of enterobactin

E. coli strain AN102 was grown in 5 mL LB (100 ug/mL streptomycin) overnight and subcultured in 150 mL LB for another 8-10 hours. Then, the cells in 150 mL LB were subcultured again (1%) in 15 L T-media and grown until OD_{600} they logged out. The cells were spun down at 4000 rpm for 40 min. Each liter of the supernatant was extracted with ethyl acetate 3 times (1×150 mL, 2×100 mL), the organic phase was combined and any remaining aqueous phase was removed. The volume of combined organic phase was reduced to 100 mL by rotary evaporation and washed with 10 mL 100 mM citrate (pH 5.5), followed by washing with 10 mL water. Then the extract was dried overnight with anhydrous $MgSO_4$. After drying, $MgSO_4$ was filtered and the volume of the extract was reduced to 10 mL. Hexane was slowly added to the extract until crystals formed. The enterobactin crystals were collected by centrifugation, dried and stored at room temperature.

2.19.2 Purification of ferrichrome

U. sphaerogena was grown in Grimm-Allen medium for one day. Then, 1 mL of the culture was subcultured to 1L of the same medium and incubated at 30°C on a rotary shaker. After 7-10 days, when the culture was ready, it was spun for 20 mins at 7000 rpm. Ferrous sulfate was added to the supernatant until OD_{425} stablized and the pH of the supernatant was dropped to 2.5 by addition of HCl. Ammonium sulfate was added to saturate the solution and pH was kept at 2.5. Each 250 mL supernatant was extracted with 10 mL benzyl alcohol three times. The combined benzyl alcohol extracts were centrifuged for 20 mins at 3000 rpm. After centrifugation, the organic solution was kept at room temperature for 15 mins. Three volumes of diethyl ether were added followed by back extraction with 1/10 volume of dH_2O, until the color of the solution became clear. Ferrichrome was found in aqueous layer. The water extracts were combined and washed two times with ethyl ether to remove the remaining benzyl alcohol.

2.20 ^{59}FeEnt binding and uptake in *E. coli*

E. coli strains were grown in 20 mL LB broth at 37°C overnight and subcultured (1%) into MOPS for another 5 hours to get an OD_{600} about 0.8.

Cells were put on ice for 30 mins then 100 uL cell culture was mixed with aliquots of ^{59}FeEnt in 10 mL ice-cold MOPS on ice. For each concentration of ^{59}FeEnt, samples were collected in triplicate and incubated on ice for 5 seconds and 1 min. After incubation, the mixed solutions were filtered and washed with 10 mL 0.9% ice-cold LiCl. The radioactivity of each sample was counted by a Packard Cobra gamma counter. Binding affinity (K_d) and capacity were determined by GraFit 5.0 (Erithacus Software) by using the "Bound vs. Total" method.

Uptake experiments were performed at 37°C. For each concentration of ^{59}FeEnt, samples were collected in triplicate and incubated in 37°C water bath for 5 seconds and 25 seconds. When the incubation finished, 100-fold concentrated cold FeEnt was added to the mixtures immediately to quench the uptake of ^{59}FeEnt. After quenching, solutions were filtered and also washed by 10 mL of ice-cold 0.9% LiCl. Samples were collected and counted in a Packard Cobra gamma counter. The uptake K_m and V_{max} were determined by GraFit 5.0 (Erithacus Software) by using the "Enzyme Kinetics" method.

2.21 Inhibition of ^{59}FeTrn uptake

For ^{59}FeTrn uptake, *E.coli* BN1071 was grown in LB broth containing 100 ug/mL streptomycin overnight, then cells were subcultured into MOPS (1: 100,

V:V) and grown until OD_{600} reached 0.8. The uptake of 100 nM ^{59}FeTrn by 100 uL cells in 10 mL MOPS was measured after 1 min and 6 min incubation at 37°C. After incubation, cells were filtered and washed by 0.9% LiCl. Filters were collected and counted. The initial uptake in 1 min period was subtracted from the uptake of 6 min period to obtain the net uptake in 5 min. V_{max} and K_m were calculated using GraFit 5.0.

In the inhibition experiments, appropriate amount of FeEnt (from 0.05 nM to 500 nM) were also added to 6 min reactions and the V_{max} of ^{59}FeTrn uptake at each concentration of FeEnt was calculated. The IC_{50} of the inhibition was obtained using GraFit 5.0.

2.22 Preparation of polyclonal α-TonB

2.22.1 Generation of rabbit α-TonB serum

A rabbit was intramuscularly immunized with purified 6His-TonB (50 to 100 μg) six times over two months; Freund's complete adjuvant was used in the first injection and Freund's incomplete adjuvant or alum was used in the following injections. The rabbits were bled by cardiac puncture to obtain the serum.

2.22.2 Adsorption of rabbit serum

Due to the presence of small amount of contaminating proteins in the 6His-tagged TonB protein sample injected into the rabbit, there were several bands other then TonB that reacted with the antibody in the *E. coli* BN1071 cell lysate.

The polyclonal antisera contained α-OmpA activity. To remove these these antibodies, the rabbit serum was passed over OmpA-Sepharose, that was prepared by coupling of purified OmpA to CNBr-activated Sepharose 6B. The activation protocol was modified from Axen et al (7): in a small beaker, 5 mL of cyanogen bromide in water (50 mg/mL) was stirred and the pH was adjusted to 11.5 by adding 2M NaOH. 1 g of Sepharose 6B cellulose was added and stirred for 8 mins. The mixture was washed with 10 mL of cold water and 10 mL of cold 0.1M $NaHCO_3$ on a glass filter under vacuum. The agarose was transferred to a small beaker and 5 mL of OmpA solution (50 mg/mL) was added to the beaker. The mixture was slowly stirred at 4°C for 24 hours. The coupled product was packed in a small column and sequentially washed by 0.1 M $NaHCO_3$, 0.001 M HCl, 0.5 M NaCl and water respectively. 1 mL of rabbit serum was loaded on the column and eluted by TBS buffer at 4°C. α-OmpA bound to the immobilized OmpA when the serum passed through the column (data not shown).

The rabbit serum was further purified by adsorption. *E. coli* OKN1($TonB^-$)

was grown in 50 mL LB broth at 37°C, overnight. In the next morning, 0.25 mL formaldehyde solution (37%, v/v) was added to the culture and the culture was grown for another 6 hours. Culture was spun down at 7500 rpm for 15 mins and the pellet was resuspended in 10 mL PBS buffer and separated into 10 micro centrifuge tubes (1 mL for each tube). 0.5 mL rabbit serum containing α-TonB was added to the first tube and resuspended completely. After 10 min, the mixture was spun down at 14,000 rpm for 3 mins. The adsorption was repeated four times. The rabbit serum was stored frozen and for experiments, it was diluted in TBS with 1% gelatin.

2.23 Purification of MalE-TonB fusion proteins

The purification was based on the instruction manual of pMAL^{TM} protein fusion and purification system (New England Biolabs) by using one-step amylose resin columns (47, 54, 170). ER2507/pSTonB69C (86) was grown in 20 mL LB (with 100 ug/mL ampicillin) at 37°C, overnight and re-inoculated (1:100, v/v) in 1 L LB with ampicillin. When OD_{600} reached 0.5, IPTG was added to the culture to a final concentration of 0.3 mM. Cells were incubated at 37°C for 2 more hours and spun down at 4000×g for 20 mins. The cell pellet was suspended in 50 mL of column buffer (20 mM Tris-HCl, pH 7.4, 200 mM NaCl, 1 mM EDTA) and cells were broken by French press. The cell lysate was centrifuged at

9000×g for 30 mins; the supernatant was diluted 1:5 with column buffer and loaded on an amylose resin column (2.5×10 cm). The column was washed with 12 volumes of column buffer and the fusion protein was eluted by the same buffer containing 10 mM maltose. The purity of the purified fusion protein was evalutated by SDS-PAGE. Protein concentration was determined by using a molar extinction of 0.8887 $(mg/mL)^{-1}cm^{-1}$ at 280 nm (calculated by Protein Calculator v3.3, The Scripps Research Institute).

2.24 Cloning and Purification of 6His-tagged TonB69C

DNA encoding TonB69C (amino acids 170-239) was cloned into pET21a(+) in two forms, with or without a 6His-tag. For the clone with 6His-tag, the DNA sequence of TonB69C was amplified by PCR without a stop codon. An NdeI and an XhoI restriction site were engineered on the 5' and 3' ends of the sequence, respectively. For the clone without 6His-tag, the DNA sequence of TonB69C was amplified witht stop codon. An NdeI and a BamHI restriction site were engineered on the 5' and 3' of the sequence respectively.

pET21a(+) carrying TonB69C was transformed to *E.coli* DH5α, then the purified plasmid was transformed to BL21 for expression. 6His-tagged TonB69C was induced by 1 mM IPTG and purified by Ni-NTA affinity chromatography at 4°C. The purity of 6His-tagged TonB69C was checked by

SDS-PAGE (17% acrylamide). The concentration of purified protein was determined by using a molar extinction of 6970 $M^{-1}cm^{-1}$ at 280 nm (calculated by Protein Calculator v3.3, The Scripps Research Institute).

2.25 Site-directed mutagenesis of MalE-TonB69C

The site-directed mutagenesis of MalE-TonB69C fusion protein followed the QuikChange® site-directed mutagenesis protocol (Stratagene, La Jolla, CA). Starting from the pSTon plasmid (86), three residues in the TonB C-terminal, S222, N227, and S195 were changed to cysteine. Two residues, E205 and D189 were changed to alanine. Each mutant fusion protein was induced by IPTG and purified by amylose resin column at 4°C.

2.26 Fluorescein-5-maleimide labeling of MalE-TonB69C cysteine mutants

Purified MalE-TonB69C (S222C) was dialyzed with column buffer to remove maltose. 10 mL purified MalE-TonB69C (S222C) (about 2 uM) in column buffer (20 mM Tris-HCl, pH 7.4, 200 mM NaCl, 1 mM EDTA) was transferred into a 15 ml centrifuge tube, and the pH of the protein solution was adjusted to 6.5.

Fluorescein-5-maleimide (in DMF) was added to the solution to a final concentration of 10 uM. The mixture was vortexed and incubated on ice for 15 mins in dark. After incubation, the solution was loaded to an amylase resin column in the cold room. The column was washed with 12 volumes of column buffer and the FM-labeled fusion protein was eluted by column buffer containing 10 mM maltose. The collected fractions were analyzed by SDS-PAGE and the gel was also scanned by Storm scanner to check the fluorescent labeling efficiency. The labeled protein was store at -20°C in dark.

2.27 Purification of *E.coli* peptidoglycan

The murein sacculus (peptidoglycan) from *E. coli* was prepared by lysing cells with SDS solution (68, 96, 181). *E. coli* BN1071 was grown in 500 mL LB at 37°C with aeration. When OD_{600} reached 0.7~0.9, the cells were rapidly chilled on an ice-salt-bath, then spun down at 4°C and resuspended in ice-cold water. The cell suspension was added dropwise to 10 mL of boiling 4% sodium dodecyl sulfate (SDS) solution over a period of about 10 mins. After boiling for 30 mins, crude sacculi were collected by centrifugation at 100,000×g, 25°C for 1.5 hours. SDS was washed out by repeated resuspension in 15 mL water and centrifugation for 4 times.

To digest high molecular weight glycogen, α-amylase (100 ug/mL) in 10 mM

Tris-HCl buffer (pH 7.0) was added and incubated at 37°C for 2 hours. Then pronase (200 ug/mL) (pre-incubated at 60°C to inactive any lysozyme contaminations) was added and incubated at 37°C for 2 hours to digest bound lipoprotein and other protein contaminations. After addition of SDS to 1%, the sacculi sample was boiled for 15 mins, and SDS was removed by repeated centrifugation-resuspension in water for 4 times. The purified sacculi were stored in water with 0.05% NaN_3 at 4°C at a concentration of about 1 mg/mL.

2.28 Peptidoglycan binding of TonB C-terminus

2.28.1 Fluorescence quenching

2 mL of FM-labeled MalE-TonB69C (S222C) (0.992 uM) in column buffer (20 mM Tris, 200 mM NaCl, pH 7.4) was added into a sample cuvette. *E. coli* peptidoglycan suspension (in the same buffer, at 2 mg/mL) was added to the cuvette in 5 uL increments. Each time when peptidoglycan was added, the mixture was stirred at 25°C for 30 seconds, then the fluorescence intensity of the labeled protein was measured by an SLM-AMINCO 8000 fluorimeter (Rochester, NY) upgraded to 8100 functionality, from 510 nm to 535 nm. The

background fluorescence and volume changes were accounted and the data was analyzed with the bound (1-F/F_0) *versus* total function of GraFit 5.0.

2.28.2 Co-sedimentation of MalE-TonB69C and peptidoglycan

Different amounts of purified *E. coli* peptidoglycan (from 2 to 20 uL, 2 mg/mL in TBS) were mixed with 50 uL purified MalE-TonB69C fusion proteins in 20 mM Tris-Cl containing 100 mM NaCl, 1 mM EDTA and 0.01% Tween-20, pH 8 (final volume of 100 µL) on ice for 30 mins. The mixtures were centrifuged at 40,000 rpm for 30 mins at 4°C in a Beckman Optima TL ultracentrifuge. The supernatants and the pellets were separated. After adding SDS-PAGE sample buffer and boiling for 5 mins, both supernatant and pellet samples were subjected to SDS-PAGE and the gels were stained with Coomassie blue.

Chapter 3 Sequence Analysis and Mutagenesis of Genes in *hup* Operon

3.1 Sequence analysis of the *hup* Operon

The *hup* operon in the chromosome of *L. monocytogenes* encodes three structural genes: *hupD* (lmo2431, from 2,500,179 bp to 2,501,150 bp), *hupG* (lmo2430, from 2,499,169 bp to 2,500,179 bp) and *hupC* (lmo2429, from 2,498,381 bp to 2,499,172 bp). 155 base pairs exist between *hupD*, the first gene of *hup* operon, and its upstream neighboring gene, lmo2432. A conserved “fur box” sequence (TGAAAATAATTCTCA) is located in this upstream region (-89) obefore the start codon of *hupD* (Figure 12). The existence of a “fur box” in the promoter region of *hup* operon suggests that this gene cluster is Fur-regulated and that the protein products of these three genes may be involved in the iron acquisition by *L. monocytogenes*.

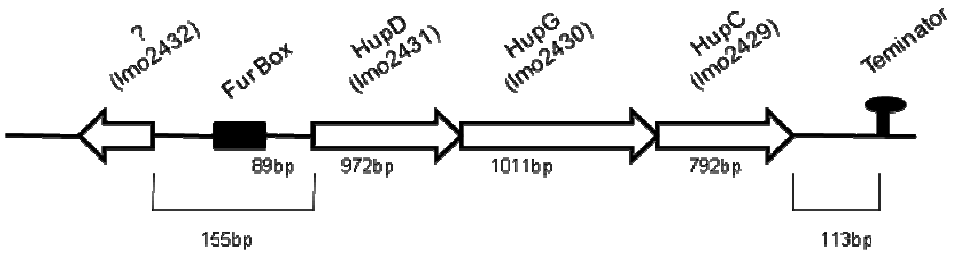

Figure 12 Schematic representation of *hup* operon of *L. monocytogenes*

I obtained the protein amino acid sequences of HupC, HupG and HupD from the ListiList web server (http://genolist.pasteur.fr/ListiList/) and compared these sequences with the protein library by using BLASTP (http://blast.ncbi.nlm.nih.gov).

The results showed that HupG likely belongs to the superfamily of "transmembrane subunit of Periplasmic Binding Protein (PBP)-dependent ABC transporters". HupC, which has Walker A and Walker B motifs for nucleotide-phosphate binding, is likely a member of the "P-loop NTPase superfamily". HupD is probably a member of the "helical backbone metal receptor (TroA-like domain) superfamily". The members of these three superfamilies were usually encoded by ABC-type operons and formed ABC

transporters for the uptake of siderophores, heme, vitamin B12 and other metal ions, like Mg^{2+} and Zn^{2+}. Some members in these three superfamilies are listed in Table 3.1. Multiple sequence alignments of these three proteins with their homologus proteins in different microorganisms were made by ClustalW (http://www.ebi.ac.uk/Tools/clustalw2/index.html) and Jalview (187) (Figure 13).

Superfamily	**Protein**	**Identity*** (%)
P-loop NTPase	**HupC_*Listeria monocytogenes***	
	FhuC_*Bacillus subtilis*	51
	FecE_*Escherichia coli*	47
	FepC_*Escherichia coli*	42
	HmuV_*Escherichia coli*	38
	FhuC_*Escherichia coli*	40
Transmembrane subunit I of (PBP)-dependent ABC transporters	**HupG_*Listeria monocytogenes***	
	HmuU_*Yersinia pestis*	39
	FhuG_*Bacillus subtilis*	33
	FecD_*Escherichia coli*	42
	IsdF_*Staphylococcus aureus*	31
	BtuC_*Escherichia coli*	37
Helical backbone metal receptor (TroA-like domain)	**HupD_*Listeria monocytogenes***	
	IsdE_*Staphylococcus aureus*	30
	BtuF_*Escherichia coli*	28
	FhuD_*Bacillus subtilis*	24
	FeuA_*Bacillus subtilis*	26
	FatB_*Listonella anguillarum*	22

Table 5 Identity of HupC, HupG and HupD to their homologs

* Numbers from BLASTP (NCBI).

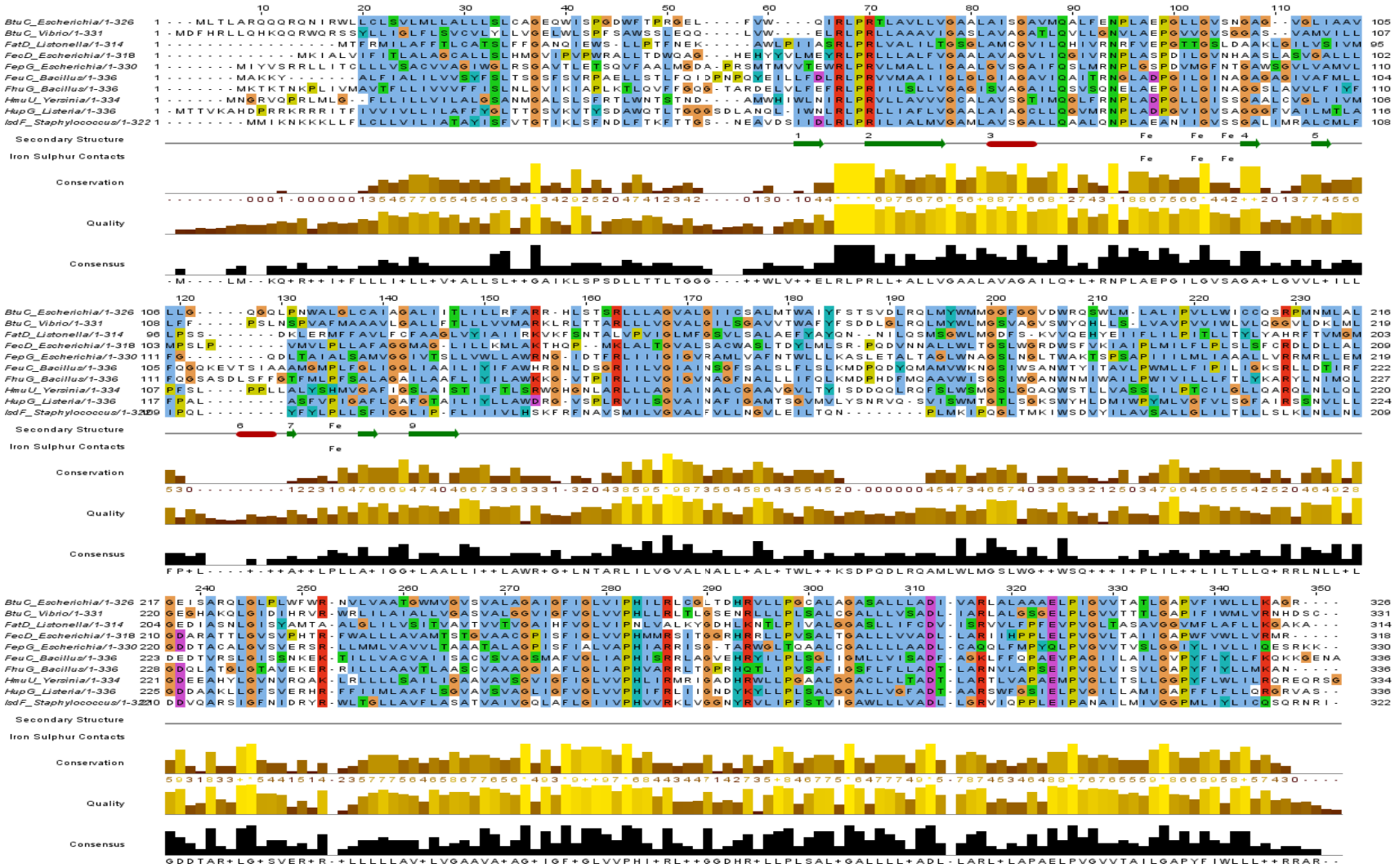
BtuC_Escherichia/1-326
BtuC_Vibrio/1-331
FatD_Listonella/1-314
FecD_Escherichia/1-318
FepG_Escherichia/1-330
FeuC_Bacillus/1-336
FhuG_Bacillus/1-336
HmuU_Yersinia/1-334
HupG_Listeria/1-336
IsdF_Staphylococcus/1-322
Secondary Structure
Iron Sulphur Contacts
Conservation
Quality
Consensus

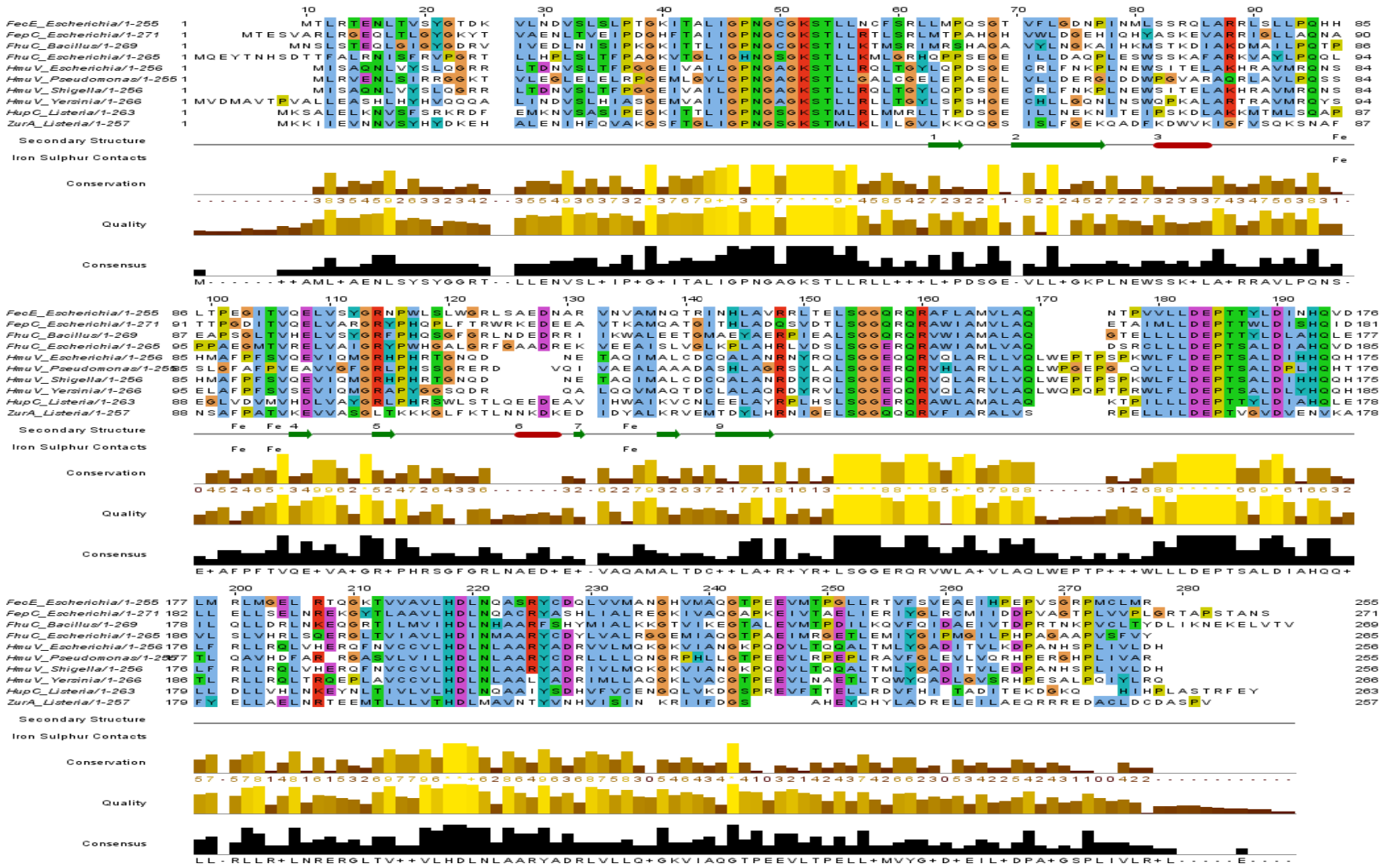
FecE_Escherichia/1-255
FepC_Escherichia/1-271
FhuC_Bacillus/1-269
FhuC_Escherichia/1-265
HmuV_Escherichia/1-256
HmuV_Pseudomonas/1-255
HmuV_Shigella/1-256
HmuV_Yersinia/1-266
HupC_Listeria/1-263
ZurA_Listeria/1-257
Secondary Structure
Iron Sulphur Contacts
Conservation
Quality
Consensus

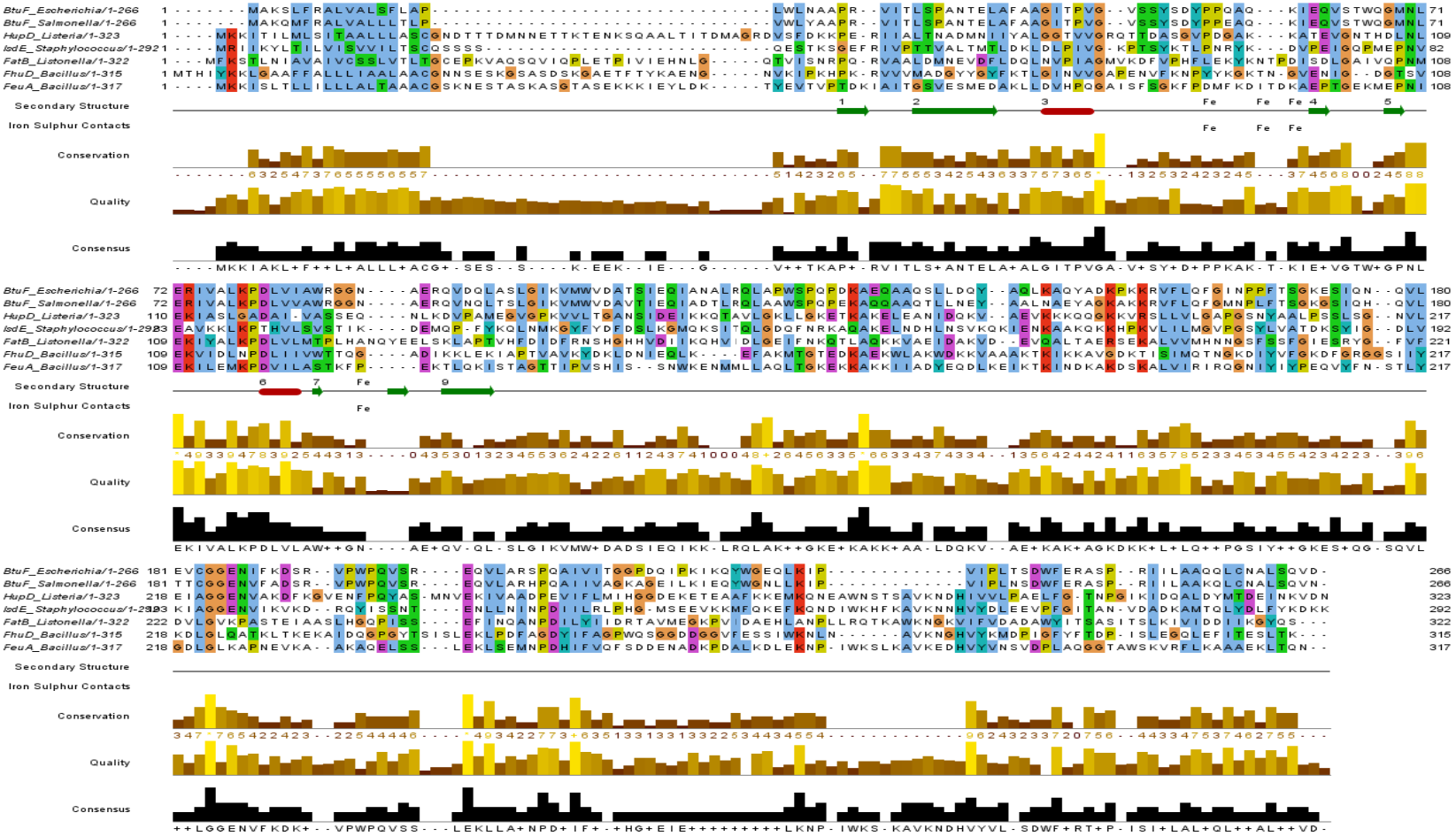

Figure 13 Multiple sequence alignments of HupC, HupG and HupD with their homologs in other microorganisms

3.2 Chromosomal deletion of *hupG*

3.2.1 Allelic replacement strategy

Site-directed deletion mutagenesis is a powerful experimental approach to study the function of a particular region in the genome of *L. monocytogenes*. A popular strategy for disrupting a chromosomal gene is the insertion of a transposon-mediated extraneous DNA or antibiotic resistant cassette in to the target gene (30, 179). However, this method has several disadvantages and sometimes unexpected problems happen after the insertion, for instance, polar effect on downstream structural genes. Furthermore, in some cases, the function of the target gene is not fully eliminated (42).

Another way to inactivate a target gene in *L. monocytogenes* is insertional plasmid mutagenesis: inserting a plasmid into the target position in the chromosome just by a single cross-over (35). Like transposon mutagenesis, it is a straightforward and fast method, but the major shortcoming is still the polar effect on the downstream genes (18).

When studying the function of iron-uptake genes in *L. monocytogenes*, we want precise, in-frame chromosomal genes deletion mutants. So we chose the allelic replacement method (84, 118). Compared with other strategies, in-frame allelic replacement maybe a little bit time consuming but it offers stable and

nonpolar mutants, and the inactivation of the structural gene is guaranteed.

Allelic replacement deletion begins with the amplification of two PCR fragments flanking the target gene. These PCR fragment are ligated to a suitable thermosensitive shuttle vector and transformed into *Listeria* cells. Cells are allowed to grow at a permissive temperature in the presence of antibiotic pressure, allowing intergration of the plasmid into the chromosome by homologous recombination (first cross-over), which happens in one of the two homologous flanking fragments. After integration, the culture is switched to the restrictive temperature and cells are grown without antibiotic. After a number of life cycles at this condition, the integrated vector sequence is spontaneously removed from the genome by a second homologous recombination (the second cross-over). Depending on which side of the plasmid the cross-over take place, the wild type or the deletion derivative will remain in the chromosome (Figure 14).

Picking a good thermosensitive shuttle vector is key for allelic replacement method. Several candidate vectors are known, such as pAUL-A (35), pCON1 (14), pKSV7 (163) and pMAD (5). We chose vector pKSV7 in our experiments because it is relatively small, highly thermosensitive, and shows high frequency of chromosomal integration.

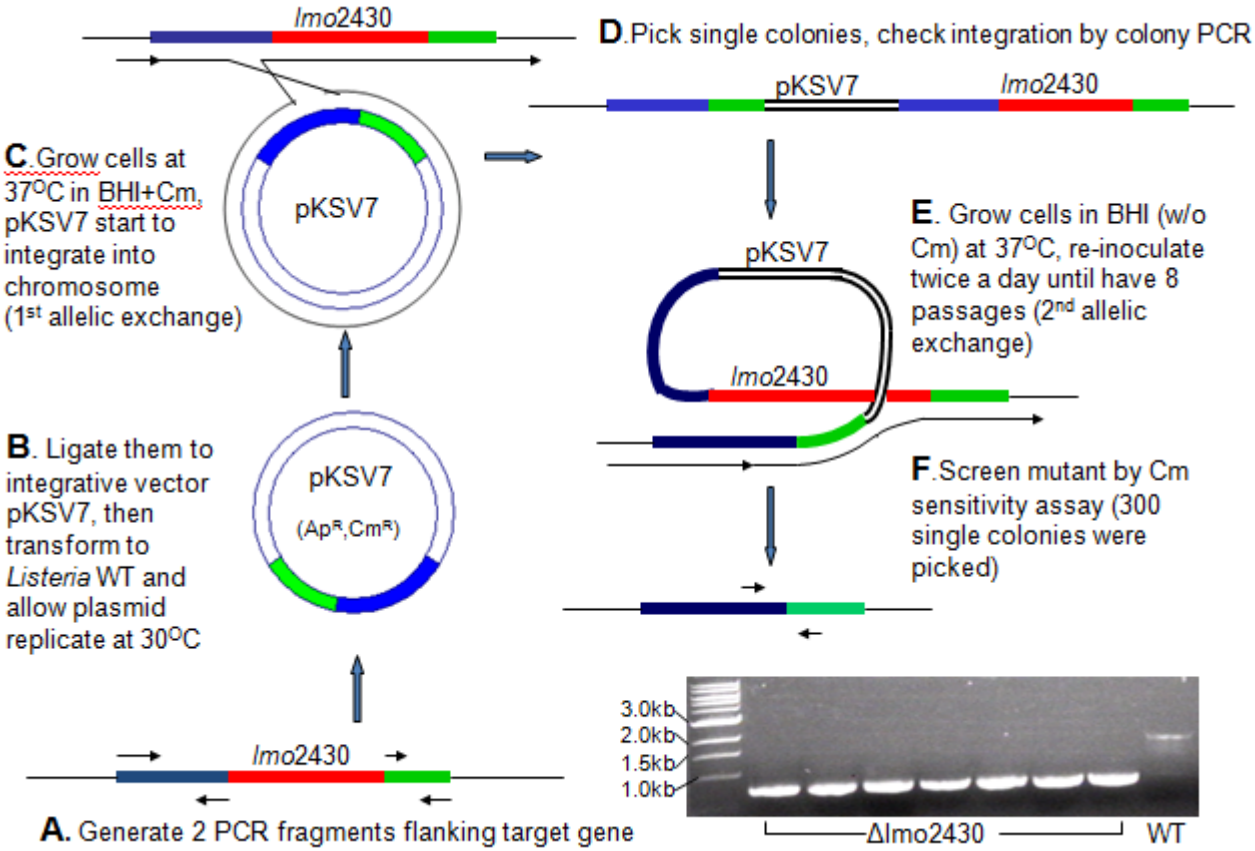

The agarose gel (bottom right) showed the deletion of lmo2430. Colony PCR with the primers designed as the picture indicated: EGD-e wild type gave a product about 1.7kb; the deletion mutants gave a product about 0.7kb.

3.2.2 Deletion of *hupG*

I designed primers and amplified two PCR fragments flanking the gene *lmo2430*. First I tried “double ligation”, joining both fragments together *in vitro*. The band of the ligation product was cut from agrose gel and the DNA recovered as described in Chapter 2. I inserted the product into pKSV7 and transformed it in DH5α competent cell. Based on the result of colony PCR, I only got one colony and the size of the insertion was not right. Then I did a “triple ligation”, I digested the vector and two PCR products individually and ligated them together. After ligation, aliquots of the reaction were transformed into DH5α. It turned out that the “triple ligation” was much more efficient then the double ligation. After two allelic replacements and Cm-sensitive screening, I got 8 mutant colonies out of 20 Cm sensitive clones (Figure 15).

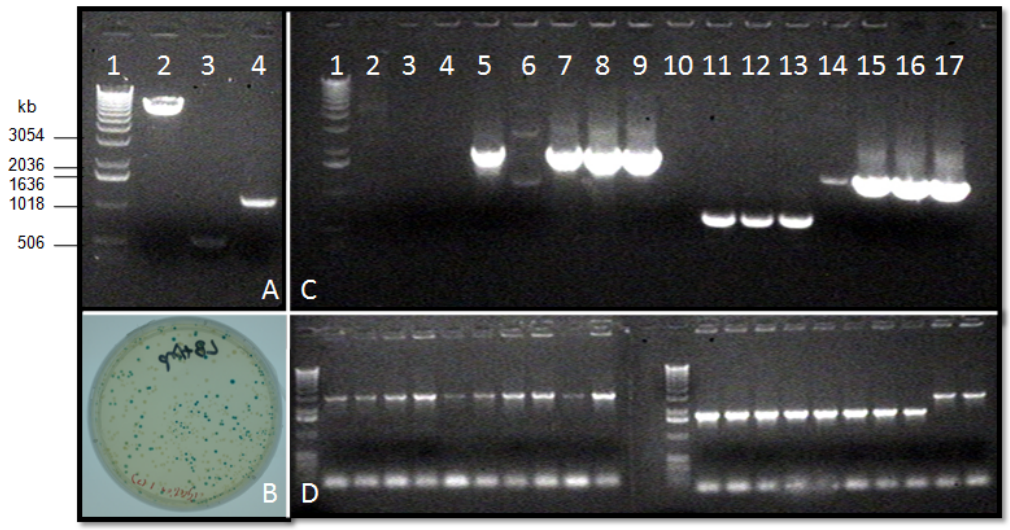

Figure 15 Deletion of hupG

(A) lane 1, mini-prep of pKSV7; lane 2 and 3, upstream and downstream fragments (0.54kb and 1.18kb). (B) LB plate (with IPTG and X-gal) of DH5α carrying pKSV7 and two PCR fragments. White colonies are colonies containing pKSV7 with DNA insertion. (C) Colony PCR to test the insertion of two fragments in pKSV7 hosted by DH5 α. Lane 1, 1 kb DNA ladder. Primers used in the experiment were: lane 2, 3, 4, 5, M13 primers; lane 6, 7, 8, 9, 5' primer of the upstream fragment and 3' primer of the downstream fragment; lane 10, 11, 12, 13, primers of upstream fragment; lane 14, 14, 16, 17, primers of downstream fragment. In each primer group, the order of the DNA templates (from left to right) was pKSV7 and three picked DH5α colonies. The last colony showed correct bands with all primer pairs. (D) Colony PCR to test 20 Cm sensitive *Listeria* colonies. Colonies showing bigger band on the gel were wild type EGD-e, others showing smaller band were Δ*hupG* mutants.

3.2.3 Complementation of Δ*hupC* and Δ*hupG*

In our lab, we had already constructed the deletion mutant of Δ*hupC* (84) when I made Δ*hupG*. We wanted to complement these two mutations by introducing the wild type genes to confirm the role of *hupC* and *hupG* in heme and hemoglobin uptake.

First, we thought it could be possible to complement these genes by cloning the promoter region of *hup* operon and the structural genes into pKSV7. I amplified the whole 155bp region between *lmo2432* and *lmo2431* by PCR and ligated it to pKSV7, *lmo2429* was also amplified and inserted into pKSV7 following the promoter region. The insertion of the promoter region and *lmo2429* was confirmed by colony PCR (Figure 16) and DNA sequencing. Finally the vector was transformed into Δ*hupC* competent cells, but the heme and hemoglobin nutrition tests showed that the phenotype was not complemented. Apparently, the cloned genes in pKSV7 do not lead to proper expression of HupC in *L. monocytogenes* EGD-e Δ*hupC*.

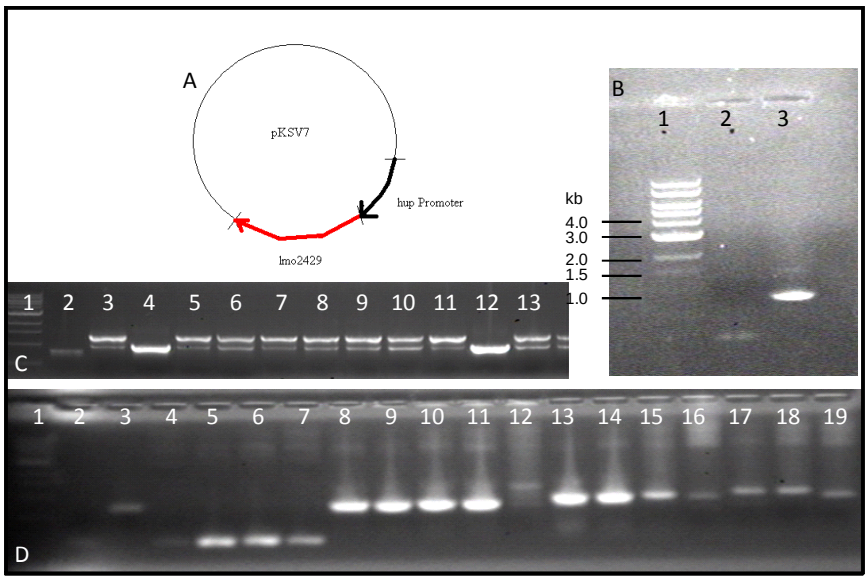

Figure 16 Complementation of *hupC* in pKSV7

(A) Experimental design. (B) agarose gel of *hup* promoter region (lane 2) and *hupC* (lane 3). (C) Colony PCR to test pKSV7 carrying promoter-*hupC* in DH5α using 5' promoter primer and 3' *hupC* primer. Lane 4 and lane 12 showed colonies with right insertion. (D) Colony PCR to test the insertion of promoter-*hupC* in pKSV7 hosted by DH5α with different primers. Lane 2, promoter region; lane 3, *hupC*; lane 4-7, four picked colonies tested by promoter primers; lane 8-11, same colonies tested by *hupC* primers; lane 12-15, 5' promoter primer and 3' *hupC* primer; lane 16-19, M13 primers. The two colonies in the middle showed correct bands with all primers (5 and 6, 9 and 10, 13 and 14, 17 and 18).

Because *lmo2429* was not be complemented by using pKSV7, we chose another plasmid, pPL2 to try again. Plasmid pPL2 is a site-specific integration shuttle vector. It has a listeriophage PSA integration site (91). It can be transformed into *E.coli* and transferred to listerial cells by conjugation (Figure 17). Once integrated into the listerial chromosome, pPL2 remains as a single copy.

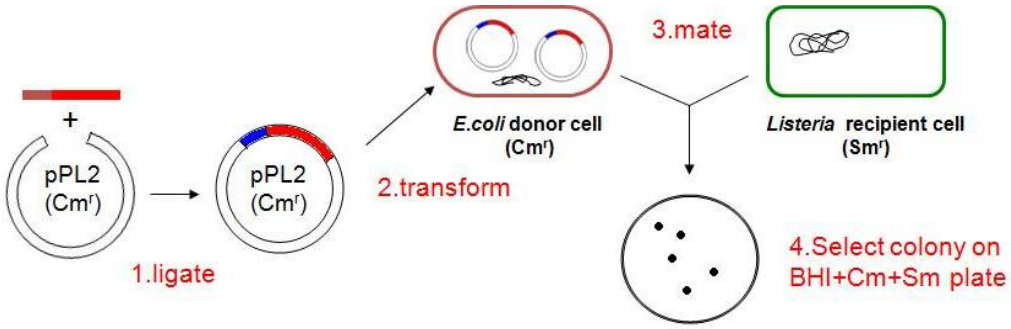

Figure 17 Complementation of *hupC* and *hupG*

Promoter (blue bar) and coding regions (red bar) were ligated into pPL2 and transformed into the donor cells (SM10). After conjugation between *E.coli* donor cells (Cm^r) and *Listeria* recipient cells (Sm^r), the integrants were selected from plates containing both antibiotics.

I amplified the promoter-*hupC* fragment from pKSV7 by PCR and inserted it into pPL2, introducing the construct into *E.coli* SM10 (Cm^r). After conjugation between SM10 (Cm^r) and Δ*hupC* (Sm^r), pPL2 carrying the promoter region and *hupC* integrated into the chromosome, as confirmed by colony PCR (Figure 18) and DNA sequencing. The complementation of *hupG* (5 single-Cys mutants of *hupG*, see Chapter 5) followed the same procedure as that of *hupC*, except that the promoter and the coding region were inserted into pPL2 separately (Figure 19).

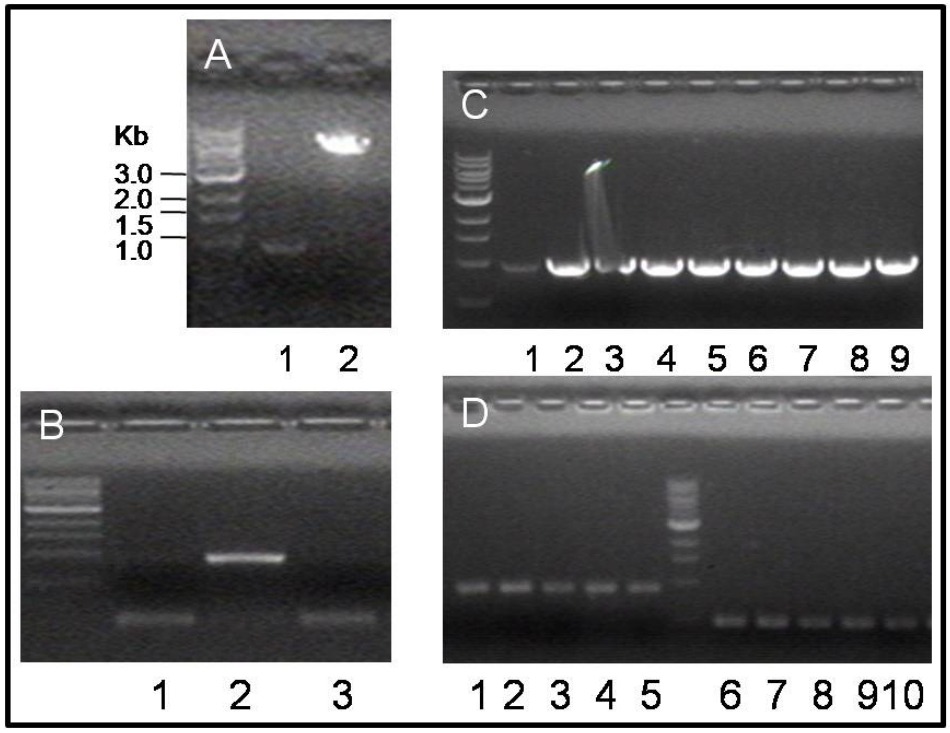

Figure 18 Complementation of *hupC* with pPL2

(A) Agarose gel of promoter-*hupC* (lane 1) and plasmid pPL2 (lane 2). (B) Colony PCR to test the insertion of promoter-*hupC* in pPL2 (hosted by XL-1) with 5' promoter primer and 3' *hupC* primer, lane 2 showed the colony with the correct insertion. (C) Colony PCR to test pPL2/pro-*hupC* in *E.coli* SM10 with the same primers that were used in (B), all colonies showed the correct bands. (D) Colony PCR to test the integration of pPL2 into the chromosome of Δ*hupC* (Sm^r). Five colonies were tested by LLO primers (lane 1-5) and NC16 and PL95 primers (lane 6-10), to verify the recipients as *L. monocytogenes*.

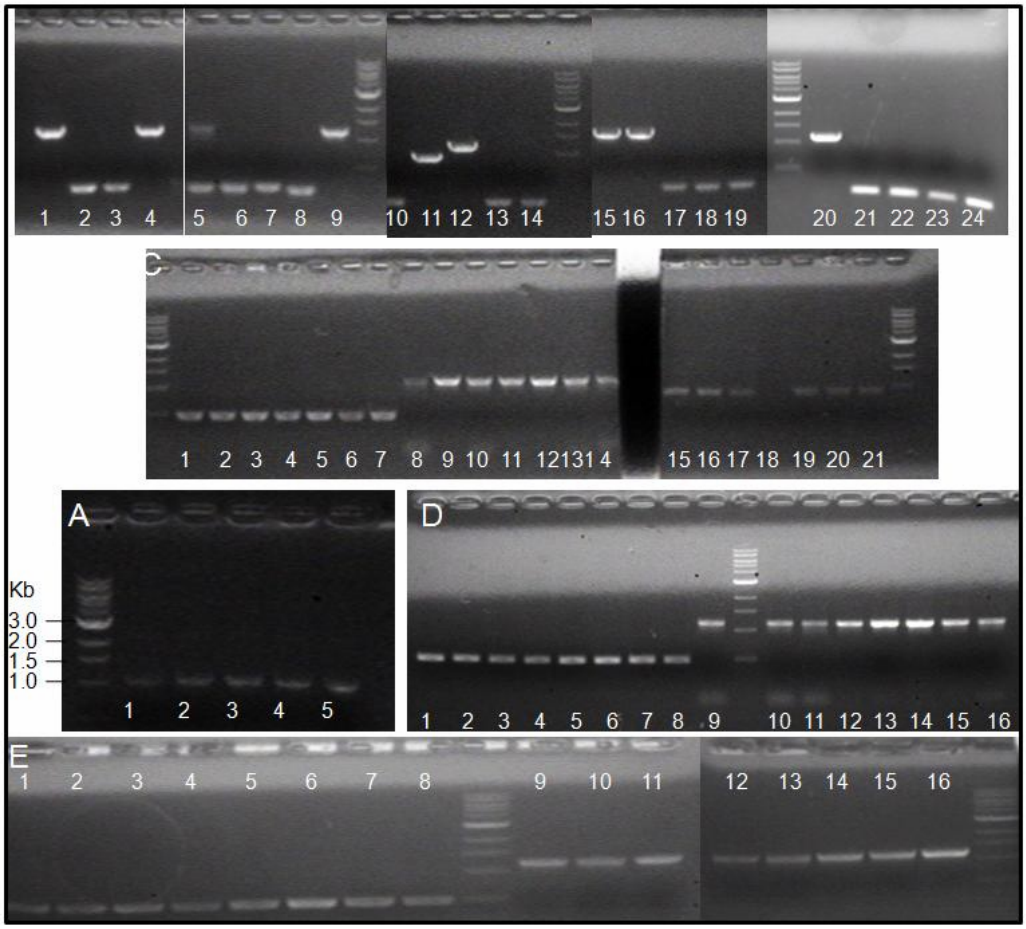

Figure 19 Complementation of Δ*hupG* with single-cys hupG gene in pPL2

(A) PCR amplified 5 *hupG* single-Cys mutants from pUC18. From lane 1 to lane 5: A45C, A119C, S54C, S194C and S308C. The mutations were also sequenced (data not shown) (B) Colony PCR to test the insertion of promoter-*hupG* in pPL2 with 5' promoter primer and 3' *hupG* primer. Lane 1 and 4, two correct insertions for A45C; lane 9, S54C; lane 11 and 12, A119C; lane 15 and 16, S308C; lane 20, S194C. (C) Colony PCR to test integration in Δ*hupG* (Sm^r). Lane 1-7, NC16 and PL95 primers; lane 8-14, 5' promoter and 3' *hupG* primers; lane 15-21, LLO primers. In each group, from left to right: four colonies of A45C, two colonies of A119C and 1 colony of S54C. (D) Colony PCR to test 8 S308 integrated colonies. Lane 1-8, NC16 and PL95 primers; lane 9-16, 5' promoter and 3' *hupG* primers. (E) colony PCR to test 8 S194 colonies. Lane 1-8, NC16 and PL95 primers; lane 9-16, 5' promoter and 3' *hupG* primers.

3.3 Conclusions

1. In the genome of *L. monocytogenes*, the three genes in the *hup* operon encode an ABC transporter for metal uptake. Each of the three protein components shares significant homology to that of other metal ABC transporters in different species.
2. Allelic replacement via shuttle vector pKSV7 is a feasible way to make in-frame gene deletion mutant in *L. monocytogenes*.
3. Two site-directed precise deletion mutants, Δ*hupC* and Δ*hupG* were complemented by using the pPL2 system.

Chapter 4 Hemin Uptake in *Listeria monocytogenes*

4.1 Polymerization of hemin in different solvent

Hemin is the key compound in both qualitative and quantitative experiments in this study. Due to the big, aromatic, planar ring structure with a ferric iron atom coordinated in the center, the chemical properties of hemin in solution are special and unlike many other iron chelating organic compounds, such as siderophores. For my experiments, it would be ideal if hemin could be dissolved in an aqueous solution, which is safe and convenient for biological studies *in vivo*.

Hemin is solubilized by aqueous alkalies, such as NaOH. However, this hemin basic solution is unstable due to the quick formation of a μ-oxo-dimer (Figure 20) at pH higher than 7 (157). When the hemin concentration is high, further aggregation may occur that eventually precipitates hemin from the solution. Therefore, an alkali solution of hemin is not optimal for biological assays or for long term storage. Clearly, when aqueous NaOH is used as the solvent, the hemin solution must be used immediately after preparation.

When I used 0.1 M NaOH as the solvent for my [^{59}Fe]-hemin to do binding and uptake experiments freshly made solution led to very consistent results, but

the variation in the data increased more and more with storage. Avoiding light and storing at low temperature did not help to inhibit the aggregation of hemin.

I also tried some common organic solvents such as $CH_2Cl_2$and CH_3OH, but they both dissolve hemin very poorly. After searching the literature, I changed the hemin solvent from aqueous NaOH to dimethyl sulfoxide (DMSO). DMSO is a polar aprotic solvent, which is miscible with water. It solubilizes a wide range of organic compounds, including hemin. The solutions of hemin in DMSO/H_2O system had been studied by Grant Collier, et al (37). They found that hemin will stay as a monomer in the DMSO/H_2O mixture containing from 40% to 100% DMSO and that a homogeneous hemin solution could still be obtained after diluting it from 100% DMSO to 0.01% DMSO in water. DMSO/H_2O was a good solvent system for my experiments. Although DMSO may potentially affect membrane permeability, growth curves assay showed that *Listeria* cells grew normally with 1% (V:V) DMSO in the media. For nutrition assays, cells grew normally even if 40% DMSO was applied on the paper disc.

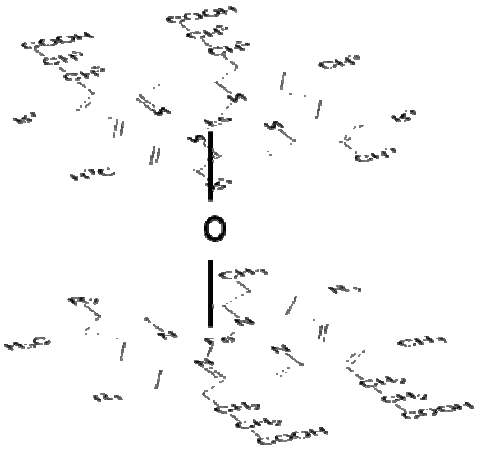

Figure 20 Hemin stays as a μ-oxo-dimer in alkali solution

4.2 Expression of HupC in iron-deficient media

4.2.1 Iron-deficient media for *L. monocytogenes*

The existence of a Fur box upstream of the *hup* operon indicates that the expression of this gene cluster is iron regulated, thus we wanted to use an iron deficient medium, in which the encoded proteins would be expressed at a high level and the culture of *Listeria* will reach high cell density. In our lab, we have used RPMI 1640 based minimal medium, KRM (84). But in my experiments, sometimes the growth of *L. moncytogenes* in KRM was not reproducible, especially when cells were subcultured twice in KRM. For *E. coli*, the iron-deficient medium we used in our lab is MOPS (112). MOPS media is a chemical defined synthetic minimal media for enterobacteria. The components

in MOPS medium are much simpler than RPMI1640 and its buffering ability is stronger. I tried to use MOPS medium to grow *L. monocytogenes* but the bacterium grew very poorly in it, with a long doubling time and low final optical density. The reason is that some key nutrition factors for *L. monocytogenes* are missing in MOPS medium, as a result of metabolic differences between *L. monocytogenes* and *E.coli*. It seemed like the MOPS medium must be adjusted to promote the growth of *L. monocytogenes*.

Studies on a chemical defined minimal medium for *Listeria* started as early as 1960s (59, 190). Research gradually revealed essential nutritents for *Listeria* including carbon sources, amino acids, and vitamins. Several minimal media were developed based on these studies and among them, Welshimer medium was widely used (190). But these media, including Welshimer medium, could not support good growth of all *Listeria* strains in sequential subcultures. In 1991, R. Premaratne，et al developed a new minimal medium, which was called MWB medium for *L. monocytogenes* (133). This medium supported better growth for more strains and adding iron compounds, including hemin and ferric citrate stimulated the growth. In 2003, another minimal medium, HTM was developed by H. Tsai, et al and they claimed HTM was the simplest synthetic minimal medium for *Listeria* and it also supported the growth of EGD-e strain (180). It was also mentioned in that paper that cysteine was essential for EGD-e strain since it lacks the *trans*-sulfuration pathway.

After comparing all these four different media, KRM, MOPS, MWB and

HTM, I modified MOPS as following: the basic MOPS medium and all its inorganic components were kept unchanged. In addition, a solution of supplements from KRM medium (Gold supplements) was added (1:100, V: V), that contains four vitamins needed by *L. monocytogenes*. Glucose was still the carbon sources in the new medium but the concentration was increased from 0.4% to 1%. Cysteine and glutamine were also added to the medium. Although there are conflicting reports in the literature concerning the need for micronutrients (40, 59, 180), I still added MOPS micronutrients to the medium and the final pH was adjusted to 7.4. All glassware used in the experiments was prewashed by 0.1 M HCl. All components in the modified MOPS medium are listed in Table 6.

L. monocytogenes grew much better in modified MOPS, which I called MOPS (L). When subcultured from overnight BHI (1:100, V: V), EGD-e wild type grew much faster in MOPS (L) than MOPS and HTM (Figure 21 A). HTM didn't support the growth of EGD-e well in my experiments. Adding hemin (fresh made in 0.1 M NaOH) into the 1st subculture of MOPS (L) did not affect growth; but when cells were subcultured again into MOPS (L) (1:50, V: V), the stimulation of the growth by adding 0.2 uM hemin was obvious (Figure 21 B). When 0.2 uM hemin was added, it took EGD-e about 15 hours to reach an OD of 0.6, but it took more than 24 hours to reach the same OD without hemin. This data indicated that in the 2nd subculture of MOPS (L), cells were iron starving and ready to uptake hemin as iron source.

Component	Concentration in medium				
	KRM[a]	MWB[b]	HTM[c]	MOPS[d]	MOPS(listerial)
MOPS			100 mM	40 mM	40 mM
K_2HPO_4		48.2 mM	4.82 mM	1.32 mM	1.32 mM
NH_4Cl				9.52 mM	9.52 mM
$MgCl_2$				0.523 mM	0.523 mM
K_2SO_4				0.276 mM	0.276 mM
$CaCl_2$				5×10^{-4}mM	5×10^{-4}mM
NaCl				50 mM	50 mM
Na_2HPO_4		115.5 mM	11.55 mM		
$MgSO_4$		1.70 mM	1.70 mM		
KH_2PO_4					
$(NH4)_2SO_4$			0.6 mg/ml		
$NaHCO_3$	0.2%				
Ferric Citrate		360 uM			
Glucose	0.4%	0.99%	0.99%	0.4%	1.0%
RPMI1640	1.04%				
Thiamine	1.0 ug/ml	2.96 uM	2.96 uM		1.0 ug/ml
Riboflavin	0.5 ug/ml	1.33 uM	1.33 uM		0.5 ug/ml
Biotin	1.0 ug/ml	2.05 uM	2.05 uM		1.0 ug/ml
Lipoic acid	5×10^{-3}ug/ml	24.0 pM	24.0 pM		5×10^{-3}ug/ml
Histidine		0.1 mg/ml			
Tryptophan	0.05 mg/ml	0.1 mg/ml			0.05 mg/ml
Leucine		0.1 mg/ml			
Isoleucine		0.1 mg/ml			
Valine		0.1 mg/ml			
Arginine		0.1 mg/ml			
Cysteine		0.1 mg/ml	0.1 mg/ml		0.1 mg/ml
Methionine		0.1 mg/ml	0.1 mg/ml		
Glutamine		0.6 mg/ml			0.6 mg/ml
Casamino acids	0.1%				0.1%
Micronutrients	+			+	+

a. data from reference (118);

b. data from reference (133);

c. data from reference (180);

d. data from reference (112).

* Components in micronutrients are: $(NH4)_6Mo_7O_{24}\cdot4H_2O$ (3×10^{-7} M), $CoCl_2\cdot6H_2O$ (3×10^{-6} M), HBO_3 (4×10^{-5} M), $CuSO_4\cdot5H_2O$ (10^{-6} M), $MnCl_2$ (8×10^{-6} M), $ZnCl_2$ (10^{-6} M).

Table 6 *L. monocytogenes* minimal media

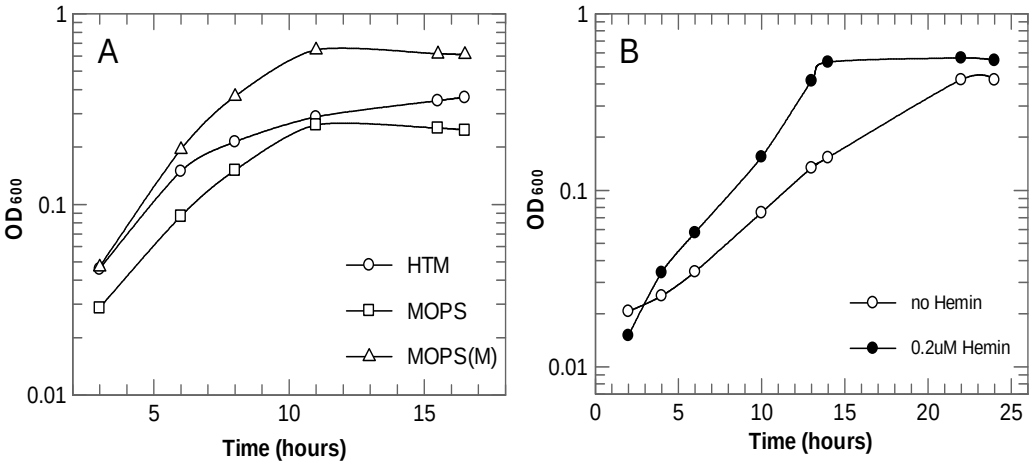

Figure 21 Growth of *L. monocytogenes* EGD-e in minimal medium

(A) EGD-e wild type was grow in BHI overnight and subcultured (1%) into MOPS, MOPS (L) and HTM. (B) EGD-e wild type was grown in BHI overnight and subcultured (1%) to MOPS (L). Cells at stationary phase were subcultured (2%) into MOPS (L) again, and OD_{600} was measured with or without 0.2 uM.

4.2.2 Expression of HupC in different media

I amplified *hupC* (*lmo2429*) from the EGD-e chromosome and cloned it into pET28a(+). The 6H-HupC was expressed in *E. coli* BL21 and purified by Ni-NTA agarose. Mice were immunized with purified 6His-HupC to generate α-HupC sera (Figure 22).

I grew EGD-e and its mutants in different media and used an α-HupC western blot to evaluate the expression of HupC. By doing immunoblots, the deletion of HupC and the complementation of *hupC* in ΔHupC strain were confirmed. There

was no band detected in the culture of ΔHupC, but the band showed up in the complemented strain. Several media were tested in the experiments, including BHI, BHI containing 1 mM 2, 2'-bipyridyl, KRM and MOPS (L). 6H-HupC is a soluble protein found in the cytoplasm of BL21, but according to the immunoblots, after separating the listerial cell membrane and cytoplasm, HupC was found in the membrane fraction, which indicated that HupC forms a complex with HupG, the membrane permease of the Hup ABC transporter, in *vivo*. The expression level of HupC in iron deficient medium, such as KRM and MOPS (L) was almost the same as in BHI. There was about 2 fold over expression observed when 1 mM bipyridyl was added in BHI. The expression of HupC in a Δfur mutant, which could be taken as the maximum expression level of HupC, is about 3 fold higher than that of wild type (Figure 23, 24).

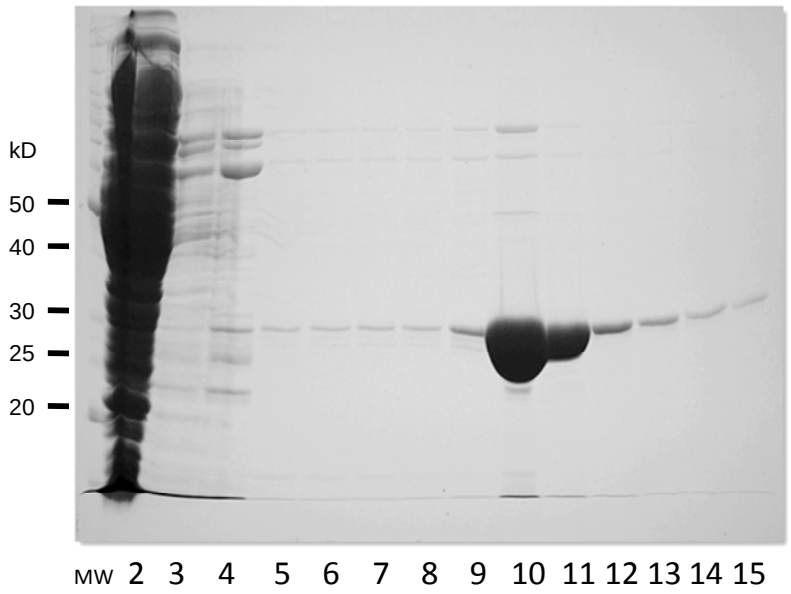

Figure 22 Purification of 6H-HupC

hupC was cloned into pET28a (+) and the 6H-HupC was expressed in BL21. Lane 10-15: 6H-HupC was eluted from Ni-NTA column by 250 mM imidazole.

The reason for the low expression level of HupC in iron-deficient medium probably is due to the promoter of *hup* operon. Although the the *hup* operon is Fur regulated, the natural *hup* promoter is a weak promoter that cannot support transcription of the genes in this operon at a high level. On the other hand, since *hupC* is the last gene in hup operon, therefore the farthest from the promoter region, it may be transcribed less than the first two genes, hupD and hupG. I also tried to make his-tagged HupG, but after transformation into BL21, no expression was observed. HupG is a transmembrane protein; it may be toxic to the host strain. I changed the host strain from BL21 to CD43, which is more

suitable for over-expression of membrane proteins, but HupG still was not expressed. I also tried to add the his-tag to the C-terminus of HupG instead of the N-terminus, and to fuse HupG with MalE, however, all these approaches did not help the expression of HupG. Therefore, untill now, there is no α-HupG available for immunoblots.

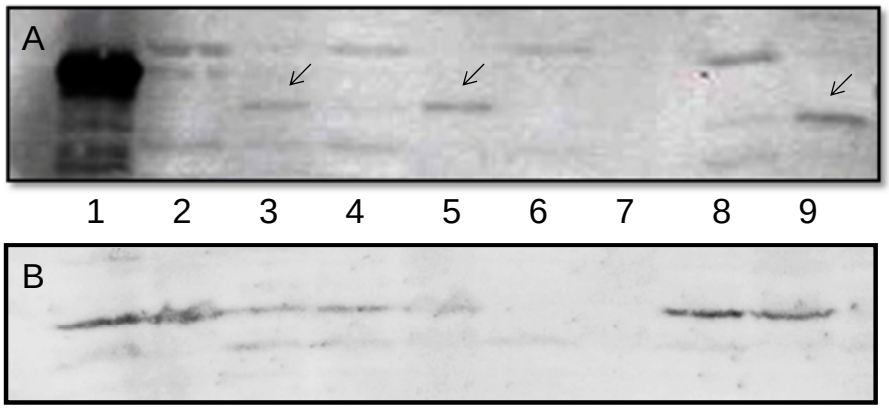

Figure 23 α-HupC immunoblots I

(A) EGD-e WT, ΔHupC and complemented ΔHupC cell lysates analyzed by an anti-HupC immunoblot. Bacteria were grown in BHI overnight, subcultured (1%) in BHI or BHI with 0.4 mM BP. After centrifugation, cell pellets were resuspended in water to equivalent cell densities and cytoplasmic and membrane fractions were separated. Lane 1, purified 6H-HupC; lanes 2,3, cytoplasmic and membrane fractions of EGD-e WT grown in BHI; lane 4,5, cytoplasmic and membrane fractions of EGD-e WT grown in BHI+BP; lane 6,7, cytoplasmic and membrane fractions of ΔHupC grown in BHI+BP; lane 8,9, cytoplasmic and membrane fractions of complemented ΔHupC grown in BHI+BP. The bands for HupC are marked by arrows. (B) ΔFur, EGD-e WT, ΔHupC and complemented ΔHupC were grown in BHI overnight, then subcultured (1%) in BHI with 1 mM BP or subcultured in MOPS(L) twice, and the cytoplasmic membrane fractions were subjected to SDS-PAGE and transferred to nitrocellulose for an α-HupC imminoblot. Lane 1, 2: membrane fractions of ΔFur in BHI and MOPS(L); lane 3, 4, 5: membrane fractions of EGD-e WT in BHI, BHI with 1mM BP and MOPS(L); lane 6, 7: membrane fractions of ΔHupC in BHI with 1 mM BP and MOPS(L); lane 8, 9: membrane fractions of complemented ΔHupC in BHI with 1 mM BP and MOPS(L).

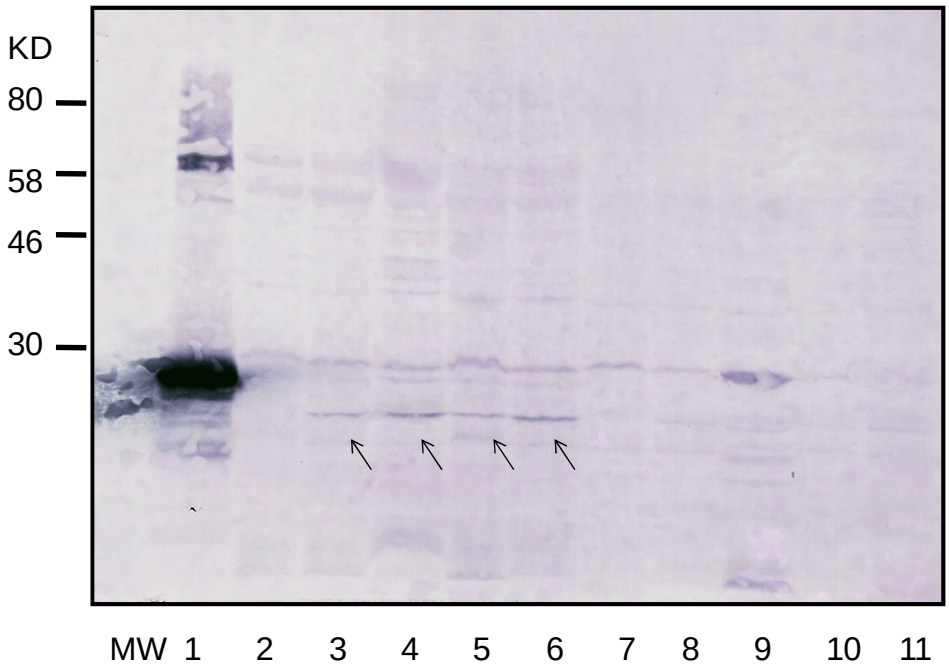

Figure 24 -HupC immunoblots II

Cells of EGD-e WT, Δfur and ΔHupC were grown in BHI overnight and subcultured twice in MOPS(L) and KRM. Cells were lyzed by French press at 14,000 psi and the cytoplsma and membrane fractions were separated by centrifugation at 14,000 rpm for 1 hour. Membrane fraction of each strain was extracted by 1% SDS at 25°C for 30 min. the volume of each sample was adjusted to contain 2×10^{10} cells membranes/ml and 30 ul of each sample was subjected to SDS-PAGE and then transferred to nitrocellulose membrane for α-HupC immunolblot. Lane 1 is purified 6H-HupC; Lanes 2-6: membrane fractions ΔHupC in MOPS(L), Δfur in MOPS(L), EGD-e WT in BHI, EGD-e WT in KRM and EGD-e WT in MOPS(L); lanes 7-11: cytoplasm fractions of samples in the same order as lanes 2 to lane 6. The bands for HupC are marked by arrows.

4.3 Nutrition tests of ΔHupC, ΔHupG and their complemented strains.

4.3.1 Growth of mutants when hemin was the only iron source

2, 2'-bipyridyl (BP) can form complexes with many transition metals including iron. It has been used in media to chelate iron and render it unavailable to bacteria. Previous studies show that the complex of $[Fe(BP)_3]^{2+}$ cannot be utilized by *L. monocytogenes* as an iron source (118), so BP can be added to iron replete medium, like BHI, to chelate free iron.

In BP treated BHI, the growth of EGD-e wild type, Δ*hupC*, Δ*hupG*, complemented Δ*hupC* and complemented Δ*hupG* were all inhibited due to the low concentration of free iron in the medium. After adding 0.2 uM hemin to the culture, the growth of WT, complemented ΔhupC and complemented Δ*hupG* started to accelerate and reached a higher cell density compared with the controls without hemin. The addition of hemin slightly enhanced the growth of Δ*hupC* and Δ*hupG*. Especially for Δ*hupG*, it grew at almost the same rate with or without hemin. These growth curves showed that the deletion of *hupC* and *hupG* in the *hup* operon impaired the uptake of hemin, and hemin uptake was recovered when these genes were complemented. The growth patterns of all strains tested in the experiments were the same when hemin was dissolved either

in fresh made NaOH solution or in DMSO (Figure 25, 26).

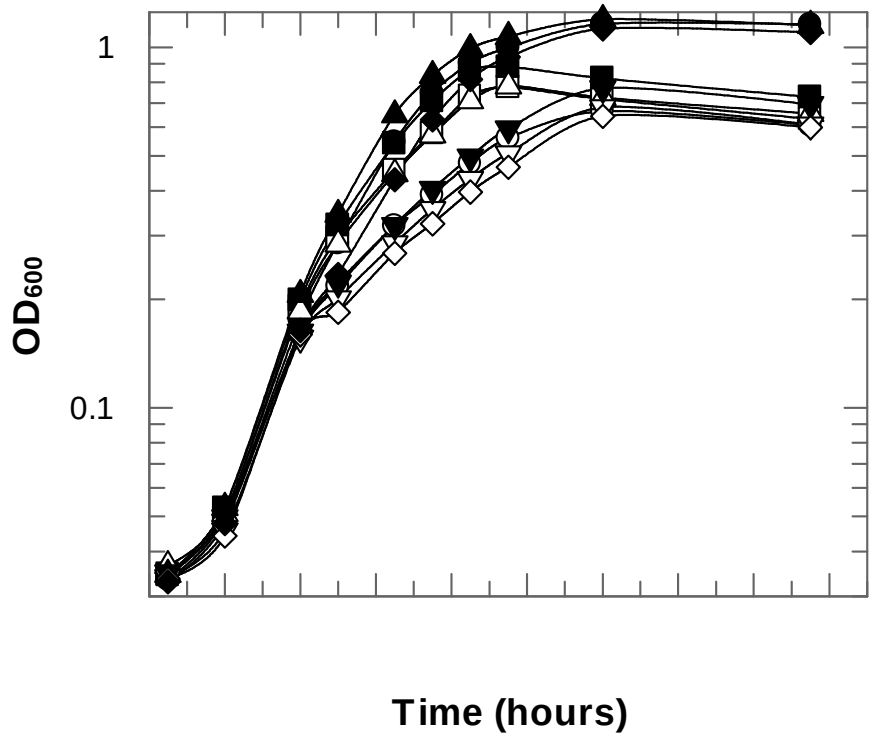

Figure 25 Growth of mutants in BHI with 2, 2'-bipyridyl I

Cells were grown in BHI overnight, then 2.5×10^7 cells were subcultured into BHI containing 0.4 mM 2, 2'-bipyridyl. After 2 hours, hemin dissolved in 0.1M NaOH was added to a final concentration of 0.2 uM. For each curve, a closed symbol means 0.2 uM hemin was added, open symbol means no hemin was added. Symbols for each strain in this figure: EGD-e WT (○), ΔhupC (□), complemented ΔhupC (△), ΔhupG (▽), complemented hupG (◇).

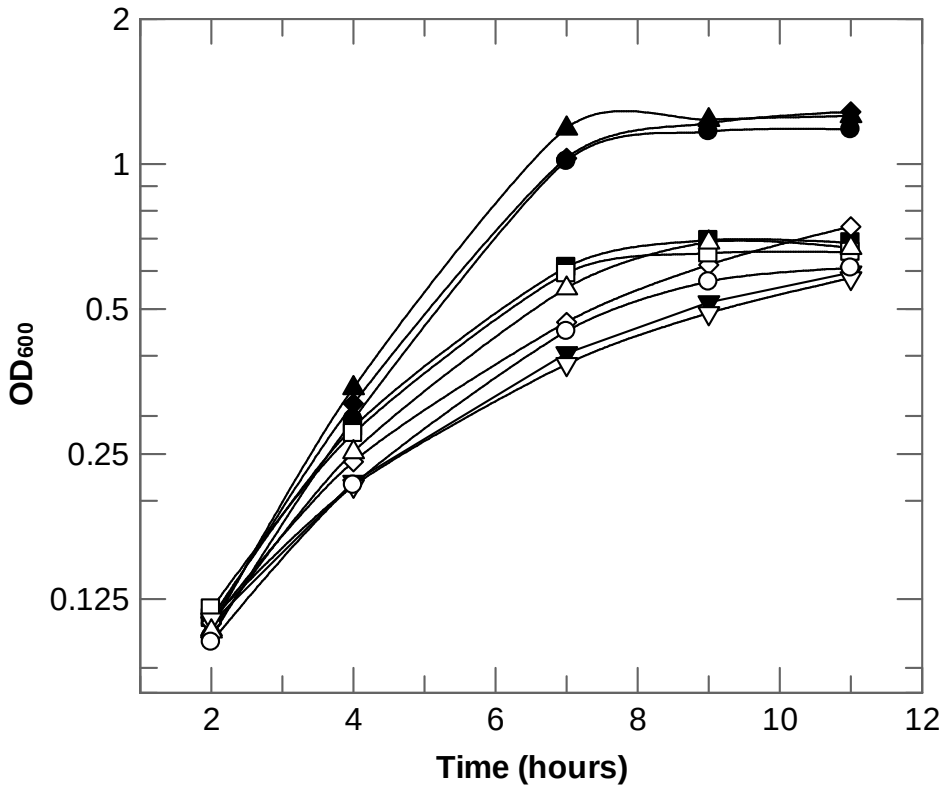

Figure 26 Growth of mutants in BHI with 2, 2'-bipyridyl II

Cells were grown in BHI overnight, then 2.5×10^7 cells were subcultured into BHI containing 1 mM 2, 2'-bipyridyl. After 2 hours, hemin dissolved in 40% DMSO was added to a final concentration of 0.2 uM. For each curve, closed symbols means 0.2 uM hemin was added, open symbol means no hemin was added. Symbol for each strain in this figure: EGD-e WT (○), ΔHupC (□), complemented ΔhupC (△), ΔHupG (▽), complemented HupG (◇).

4.3.2 Nutrition tests

Siderophore nutrition test are qualitative method to evaluate the uptake of iron

by bacteria. If the bacteria in the agar medium are able to use the iron complex applied on the paper disc, then after incubation, the bacteria will grow around and disc, forming a round growth halo. Although no data is available to show the diffusion pattern of nutrients (siderophores, hemin, hemoglobin) in the solid agar, we can assume that the concentration of nutrient decrease quickly along the diameter of the paper disc. If the bacterial cells have a high affinity and uptake rate, a dense, big halo will be seen around the disc. Low affinity and slow uptake rate usually result in a small and faint halo. However, sometimes a big, faint halo may show up even when the ability of cell to use the nutrient is poor. This happens probably because there is more time for the nutrient to diffuse further on the plate before it is used up by the cells close to the disc. For the same reason, sometimes a small, but very dense halo also means that the strain in the plate has a good ability to utilize the nutrient applied on the disc.

In my nutrition tests (Figure 27), ferrichrome was a positive control to show that all the strains in BHI top agar were growing in an identical fashion. All the strains showed a big, dense halo around the disc with ferrichrome. For wild-type, there were strong and big halos around hemoglobin and 50 uM hemin, and still a small, weak halo even if the concentration of hemin was as low as 0.5 uM. As expected, the two mutants, Δ*hupC* and Δ*hupG*, exhibited very different results from the wild type. Δ*hupC* showed a very small and faint halo around hemoglobin, no halo aroud 0.5 uM heme, a very small and weak halo around 5 uM hemin. No halos were observed around hemoglobin, 05 uM hemin and 5uM

hemin on the plate of Δ*hupG*. Both Δ*hupC* and Δ*hupG* have a small halo around 50 uM hemin indicating these two mutants still have can uptake hemin with a lower affinity. It was noteworthy that the halos around 50 uM hemin and 15 uM hemoglobin on the Δ*hupC* plate are bigger than those of Δ*hupG*, which means the deletion of the transmembrane permease of the Hup ABC transporter, impaired the uptake of hemin and hemoglobin more (Table 7). It is possible that the ATPase in different ABC transporters can substitute each other, so the deletion of HupC, the ATPase in Hup transporter affects hemin uptake to a lesser extent. The complementation of Δ*hupC* and Δ*hupG* restored both the uptake hemin and hemoglobin, but Δ*hupC* seemed to be better complemented. The complemented *hupG* was not the wild type gene; the residue A119 in the wild type *hupC* was substituded by cysteine, which could be a possible reason for this.

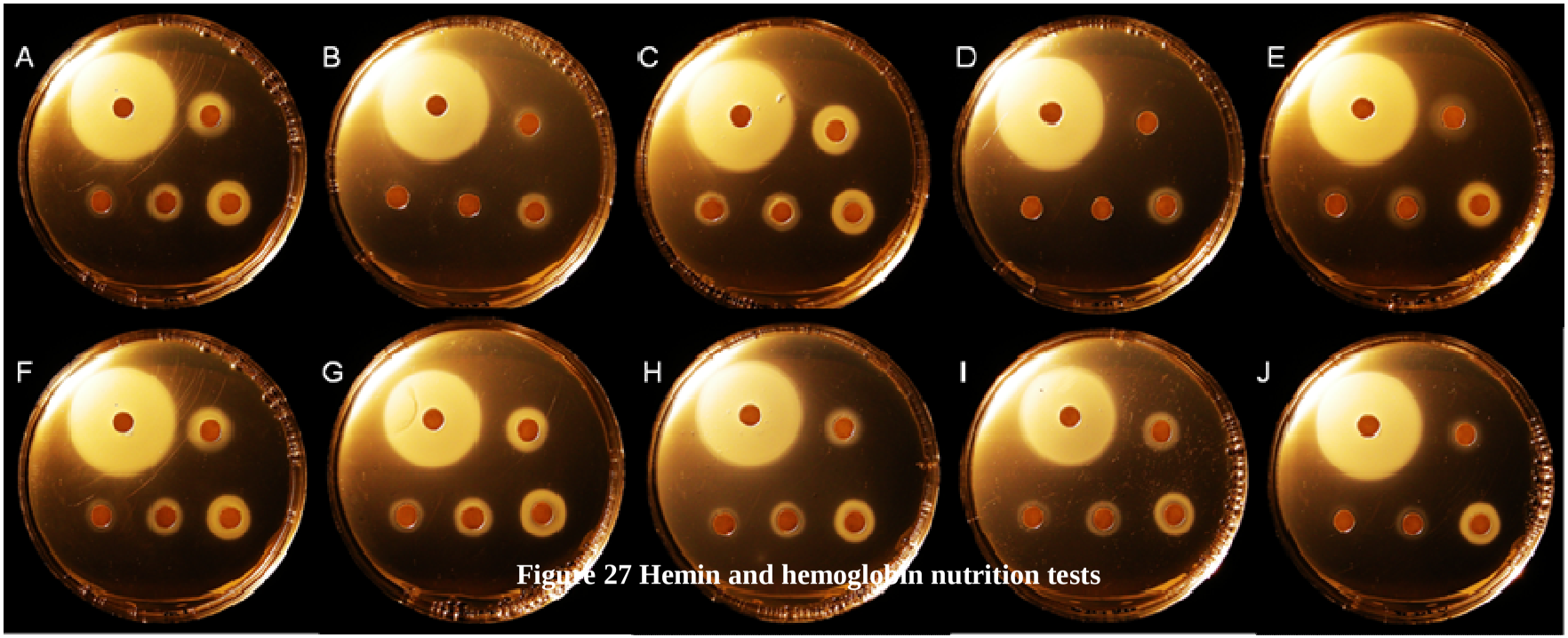

Figure 27 Hemin and hemoglobin nutrition tests

Five paper discs with 10ul of different iron compounds on them were placed on each plate in the same order: top left, 50uM ferrichrome; top right, 15uM hemoglobin; bottom left to bottom right, 0.5uM, 5uM and 50uM hemin respectively. Hemin was dissolved in 40% DMSO, hemoglobin was dissolved in TBS and ferrichrome was dissolved in distilled water. A and F, EGD-e WT; B, ΔHupC; C, complemented ΔhupC; D, ΔhupG; E, complemented ΔhupG; G, ΔStrA; H, ΔSrtB; I, ΔSrtAB; J, Δlmo2185.

	***Ferrichrome* (50 uM)**		***Hemoglobin* (1 mg/ml)**		***Hemin* (50 uM)**		***Hemin* (5 uM)**		***Hemin* (0.5 uM)**	
EGD-e WT	17.5	D	7	D	7	D	6	M	5	W
Δ*hupC*	17	D	4.5	W	5	W	4	W	-	-
Δ*hupC:pPL2hupC*$^{+}$	17	D	7	D	7	D	6	M	5	W
Δ*hupG*	17	D	-	-	6	W	-	-	-	-
Δ*hupG:pPL2hupC*$^{+}$	17.5	D	7.5	M	7	D	6	M	6	W
Δ*SrtA*	16	D	6.5	D	7	D	6	D	5	W
Δ*SrtB*	17	D	6.5	M	6.5	D	5	M	4	W
Δ*SrtAB*	16	D	6	M	6	D	5	M	4.5	W
Δ*lmo2185(SvpA)*	17	D	5	W	6.5	D	5	W	4	W

Table 7 Summary of hemin and hemoglobin nutrition tests

The diameters and appearance of growth haloes of each strain in Figure 4.8 are summarized. Number represents the diameter of the halos (mm, from the center of the disc to the eage of the halo). Letters represents the appearance of the halo: “D”, dense; “M”, medium; “W”, weak. “-“means no halo was observed.

The sortase-dependent, putative heme/hemoglobin transport systems are found in many Gram-positive bacteria. In these systems, cell wall anchored proteins may participate in the binding and uptake of heme on the surface of the cell. One well known example is the Isd system in *S. aureus*.

Previous studies in our lab did not show that sortases and surface proteins anchored by them had an impact on the hemin/hemoglobin uptake in *L. monocytogenes*. I also did nutrition tests on four sortase-related mutants in *L. monocytogenes*, ΔSrtA, ΔSrtB, ΔSrtAB, and Δlmo2185, which was formerly called "ΔSvpA". The first three mutants were kindly provided by Dr. Pascal Cossart. The deletion of *lmo2185* was made by Dr. Sally Newton.

According to the nutrition tests, the deletion of sortase A did not show any effects on the uptake of hemin or hemoglobin. When sortase B or both sortase A and B were deleted, the uptake of hemoglobin occurred, but seemed weaker. For the double deletion, ΔSrtAB, the uptake of hemin also looked decreased. When it came to the deletion of gene *lmo2185*, which encodes a surface protein anchored by sortase B, it was quite obvious that the uptake of hemoglobin was impaired. These data suggested that the sortase B and the protein that anchored by it were probably needed for the utilization of hemoglobin as iron source in *L. monocytogenes*.

To further evaluate the uptake of hemoglobin by these mutants, I did nutrition tests varying the concentration of hemoglobin from 0.15 uM to 15 uM on the plates. The results showed that removal of sortase B reduced the uptake of

hemoglobin, and the deletion of lmo2185 had the most significant effect on hemoglobin uptake. Deletion of sortase A did not show any effect (Figure 28). When grown in BHI containing 1mM BP, the growth curves of EGD-e and Δ*lmo2185* were very similar if no hemin was added to the medium. When 0.15 uM hemin was added, the growth of both were stimulated but the growth of WT was faster (Figure 29 B).

The protein encoded by *lmo2185* is a surface protein, which was formally called "SvpA" (Surface virulence protein A). It has an N-terminal signal pepide, and a C-terminal sorting sequence for sortase B, and was anchored on the cell wall and secreted out of the cell. The Fur-regulated "SvpA-sortase B" locus had been studied in our lab before. BLASTP showed that the protein encoded by *lmo2185* contains NEAT domain, which is found in cell surface proteins in Gram-positive bacteria to scavage heme from host hemoproteins. This protein has 29% identity to IsdC in *S. aureus*. In my *Listeria* cell envelope fractionation experiments, this protein was mainly found in the cell supernatant fraction (118), and strongly over expressed in iron deficient media, even when hemin, hemoglobin or ferrichrome was added (Figure 29 C). Based on the data described here, I propose a hypothesis that this protein encoded by *lmo2185* is a surface heme receptor, that has affinity for both hemoglobin and heme. However, nutrition test and growth curve data are not enough to make a conclusion about the function of this protein. The role of this protein in heme/hemoglobin uptake needs further investigation.

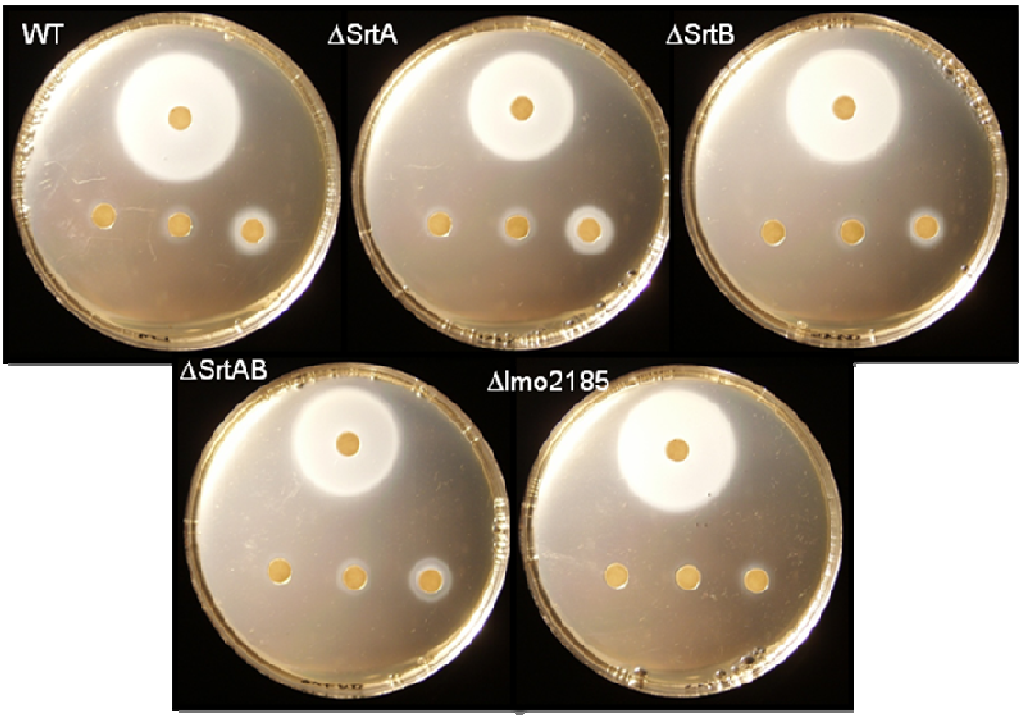

Figure 28 Hemoglobin nutrition tests of ΔSrtA, ΔSrtB, ΔSrtAB and Δ*lmo2185*

Four paper dics were placed on each plate in the same order: disc containing 50 uM ferrichrome was on the top. Bottom from left to right were 0.15 uM, 1.5 uM and 15 uM hemoglobin.

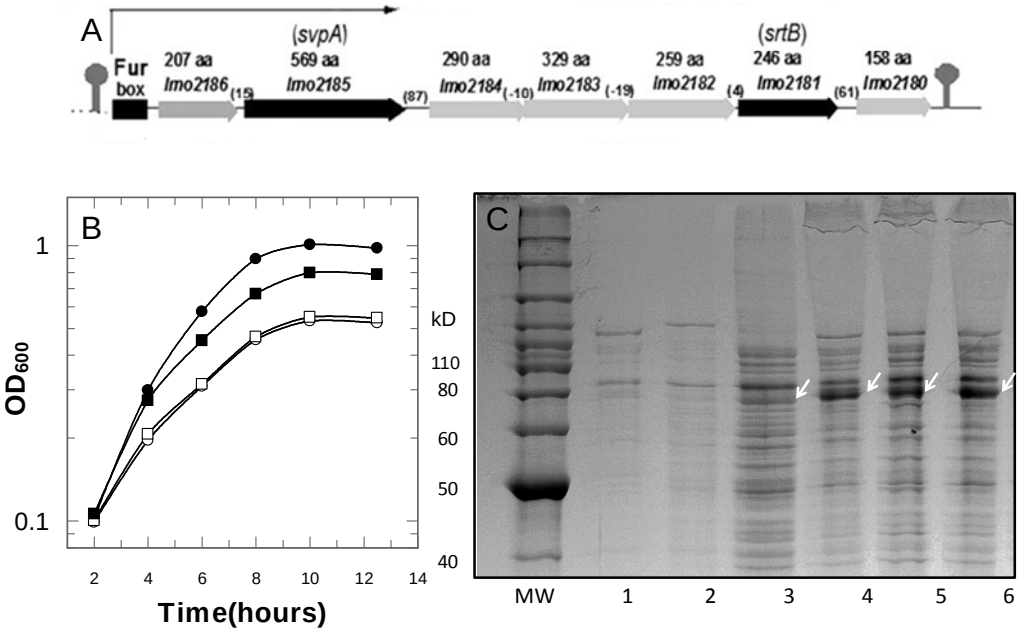

Figure 29 The *lmo2185*-SrtB locus and overexpression of the protein encoded by *lmo2185* in iron deficient medium

(A) Schematic representation of the *Lmo2185-srtB* locus of *L. monocytogenes*. (B) Growth curves of EGD-e wild type and Δlmo2185 in BHI with 1 mM BP. ○, WT without hemin; ●, WT with 0.2 uM hemin; □, Δlmo2185 without hemin; ■, Δlmo2185 with 0.2 uM hemin. (C) the protein encoded by lmo2185 was overexpressed in KRM with BP. Lane 1, peptidoglycan (PG) fraction of cells grown in BHI; lane 2, PG fraction of cells grown in KRM (before digestion by amidase); lane 3, PG fraction of cells grew in KRM (after digestion by amidase); lane 4, PG fraction of cells grew in KRM containing 0.4 uM BP and 2.5 uM hemoglobin; lane 5, PG fraction of cells grown in KRM containing 0.4 uM BP and 5 uM hemin; lane 6, PG fraction of cells grew in KRM containing 0.4 uM BP and 20 uM ferrichrome.

All the deletion mutants used in nutrition tests and transport experiments are spontaneous streptomycin-resistant mutants selected from BHI plates containing 100 ug/ml streptomycin. To ensure that these streptomycin-resistant mutations do not affect iron uptake, I did nutrition tests to compare Δ*hupC*, Δ*hupG* with Δ*hupC* (Sm^r), Δ*hupG* (Sm^r). These experiments confirmed that these streptomycin-resistant mutants are exactly same as their parent strains in the tests (Figure 30).

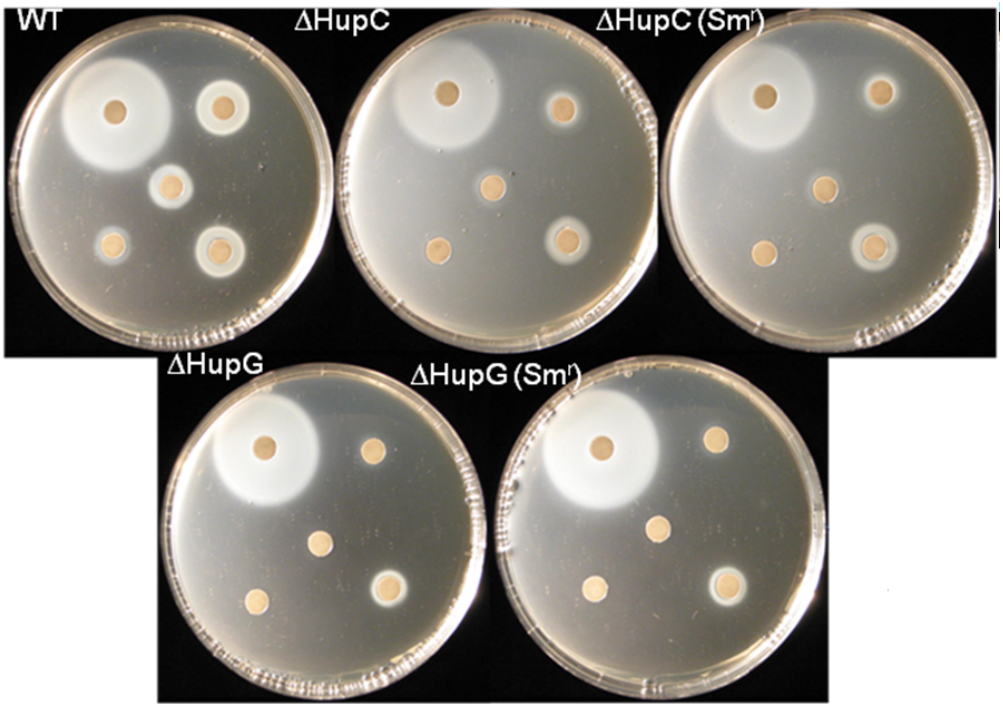

Figure 30 Nutrition tests of streptomycin-resistant mutants and their parent strains

Five paper discs were placed on each plate in the same order: top left, 50 uM ferrichrome; top right, 15 uM hemoglobin; bottom left, 0.5 uM hemin; central, 5 uM hemin; bottom right, 50 uM hemin.

4.4 [^{59}Fe]-hemin binding and uptake in *L. monocytogenes*

4.4.1 Synthesis of [^{59}Fe]-hemin

To quantitatively measure the hemin binding and uptake of *L. monocytogenes* wild type and its mutants, I synthesized ^{59}Fe labeled hemin by inserting ^{59}Fe into the tetrapyrrole macrocycle ring of protoporphyrin IX. The insertion and coordination of Fe and other metals, such as Mg and Co in porphyrin rings has been well studied due to their great biochemical interests. The formation of iron-porphyrin complexes is fast under enzymatic catalysis in *vivo*, but very slow under non enzymatic, aqueous condition (125). Many factors affect the insertion of a metal ion in porphyrin, including what kind of metal ion, side chains of the porphyrin and solvents used in the reaction (52).

Some metal ions exhibit different reaction rates in different solvents. It is important to choose a solvent system in which both protoporphyrin IX and the iron compound have good solubility. In the beginning, I synthesized [^{59}Fe]-hemin using dimethylformamide (DMF) as the solvent (2, 184). Briefly, protoporphyrin IX and $^{59}FeCl_3$ (M: M=5:1) were dissolved in DMF and heated at 150°C for 1 hour. The solution was cooled to room temperature and dried by rotary evporation. The solid was redissolved in CH_2Cl_2, and spotted on a

preparative TLC plate, and developed by the mixture of 2, 6-lutidine and water (5:3, V: V). After developing, the band of hemin was cut from the plate and hemin was extracted from silica gel by CH_2Cl_2/water (1:1, V: V); the final product of hemin was dried after the silica gel was filtered out. There are two major problems for this protocol: first, only a small percentage ^{59}Fe was inserted to protoporphyrin IX, which can been see from the auto radiograph of the TLC. Second, the extraction of hemin from silica gel using CH_2Cl_2 and water was inefficient. A significant amount of hemin still remained in the gel causing a low product yield.

The low percentage of insertion was due to the Fe^{3+} in $^{59}FeCl_3$. Protoporphyrin IX prefers ferrous iron to form a complex, rather than ferric iron. The reaction rate for the insertion of ferrous iron is much higher than the rate of ferric iron. When $FeCl_3$ was substituted by $FeCl_2$ or $FeSO_4$, the yield of hemin was much higher with the same protocol. However, as a commercial radioisotope, ^{59}Fe is only available in $^{59}FeCl_3$ form. Therefore, the synthesis protocol must be modified regarding the radioactive iron in ferric state to improve the yield.

In order to do that, I switched to another protocol, in which ascorbic acid (Vitamin C) was used as the reductant (58): protoporphyrin IX dimethyl ester in pyridine was added to glacial acetic acid at 50°C under nitrogen atmosphere. $^{59}FeCl_3$ in 17 mM ascorbic acid was added. After 1.5 hour, cold $FeCl_2$ in methanol and acetic acid was added and reacted for another 2 hours. After that,

chloroform was added to the solution and acetic acid and pyridine were washed away by water. Unreacted protoporphyrin IX dimethyl ester was removed by HCl washing. The organic phase was dried and crude product was dispersed in tetrahydrofuran (THF) and stirred with 3 N NaOH overnight. [^{59}Fe]-hemin was precipitated from the NaOH solution by adding 10 N HCl and collected by centrifugation. After changing to this protocol, the insertion of ^{59}Fe in protoporphyrin was improved, but the specific activity was only about 1 cpm/pmol, which seriously limited our ablity to do binding and uptake experiments. The reason was that a large portion of ^{59}Fe was still left unreacted in the reaction. Ascorbic acid is an antioxidant. In mitochondria, it is the reducing agent for ferrochelatase to insert ferrous iron into protoporphyrin in the last step of heme biosynthesis pathway. In this protocol, it was used as the agent to reduce $^{59}Fe^{3+}$ to $^{59}F^{2+}$, but it seemed like the reduction was not efficient. The purification steps in this protocol were time-consuming but the recovery of hemin was much higher than the silica gel extraction in the first protocol.

To enhance the specific activity of [^{59}Fe]-hemin, I finally used the method mentioned in chapter 2. Instead of using ascorbic acid, thioglycolic acid was the reductant in the reaction. Thioglycolic acid proved to be a more powerful reductant than ascorbic acid by the results of the synthesis. When a small amount of thioglycolic acid was added to $^{59}FeCl_3$ solution, the color of the solution turned blue immediately. Most of $^{59}Fe^{3+}$ was reduced to ferrous state and incorporated into porphyrin (Figure 31). The specific activity of

[^{59}Fe]-hemin by this method was about 100 to 140 cpm/pmole, which was high enough to support binding and uptake experiments with hemin concentrations at the nano molar level. The purification steps were quick, straightforward and efficient.

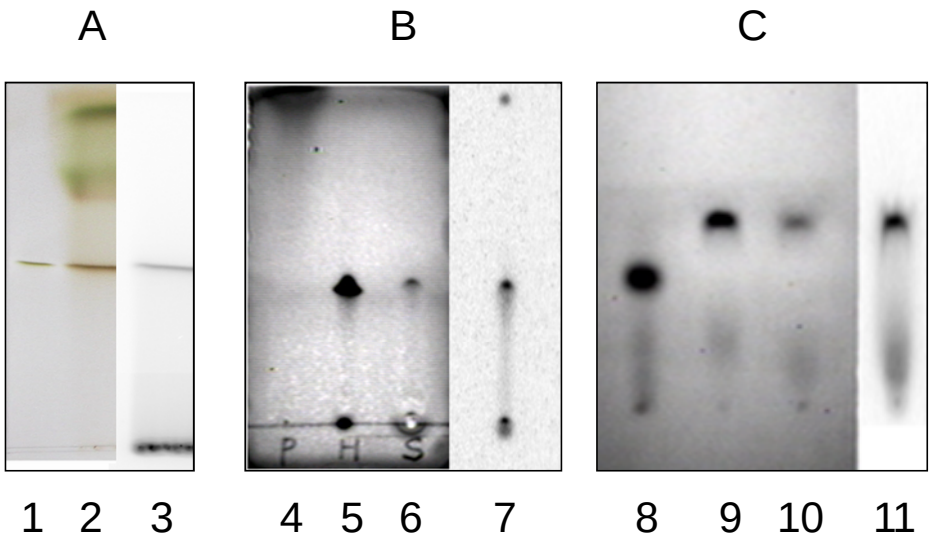

Figure 31 [^{59}Fe]-hemin TLC

(A) Synthesis of [^{59}Fe]-hemin in DMF without reductant, Lane 1, standard hemin; lane 2, [^{59}Fe]-hemin; lane 3, auto radiograph of lane 2. (B) Synthesis of [^{59}Fe]-hemin using ascorbic acid, Lane 4, protoporphyrin IX; lane 5, standard hemin; lane 6, [^{59}Fe]-hemin; lane 7, auto radiograph of lane 6. (C) Synthesis of [^{59}Fe]-hemin using thioglycolic acid, Lane 8, protoporphyrin IX; lane 9, standard hemin; lane 10, [^{59}Fe]-hemin; lane 11, auto radiograph of lane 10. The black spot on the top of lane 7 was spotted after running of the TLC to indicate where the radioactive hemin was. It could be seen from these pictures that the insertion rate of ^{59}Fe was improved by the use of thioglycolic acid.

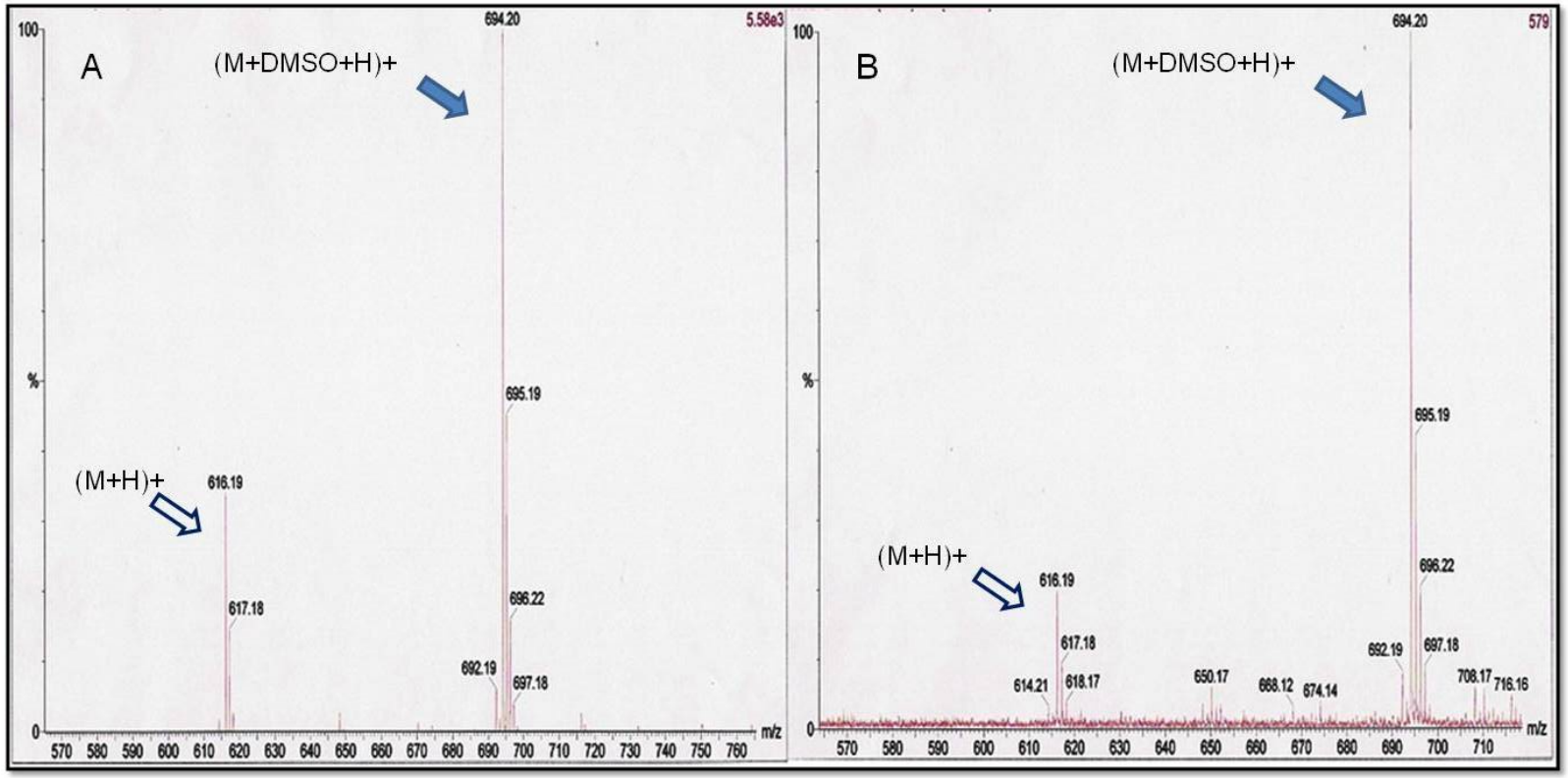

Figure 32 ESI mass spectrometry of standard hemin and synthesized hemin (non-radioactive)

(A) Standard hemin; (B) Synthesized hemin; Hemin was dissolved in 40% DMSO. In both graphs, two major molecular ion peaks were indentified: $(hemin+H)^+$, m/z=616.19 (open arrow); $(hemin+DMSO+H)^+$, m/z=694.20 (closed arrow).

4.4.2 Optimization of experimental conditions of [^{59}Fe]-hemin binding and uptake

The physical and chemical properties of hemin are different from other iron complexes, like ferric enterobactin and ferrichrome, because of its unique structure. The experimental conditions of siderophore binding and uptake cannot be simply transplanted to the experiments for hemin. Regarding the solvents for heme, I already discussed it at the beginning of this chapter. Another special property of hemin is its strong surface binding activity. Hemin is a hydrophobic, low polarity molecule with big planar, aromatic ring. It is strongly absorbed to surfaces or to polymers. In early experiments, we found that hemin strongly bound to nitrocellulose fiters, which were used for siderophore binding experiments in our lab. The binding of hemin to the filter gave a high background and distorted the results. We tested different filters, including nitrocellulose, glass membrane, polycarbonate, cellulose acetate plus and Duropore. Among these filters, hemin bound to cellulose acetate and Duropore less than the other three, after washing with 0.9% LiCl. Since hemin is hydrophobic, the adhesion of hemin to the filter could be largely contributed by hydrophobic interactions with the polymer lattice of the filter. Instead of using 0.9% LiCl, we tried to use buffer containing detergent to wash the filter. Tween-20, triton X-100 and SDS were tested and it turned out that 0.05% Tween-20 reduced the binding the most. Based on these results, we chose

Duropore filters to collect cells and 0.05% Tween in 50mM Tris as the washing buffer (Figure 33).

Another important concern is “iron depletion”. If we want to use Michaelis–Menten kinetic model to describe the transport of hemin, the concentration of hemin (substrate) must be high enough to make sure that all transporters (enzyme) are saturated throughout the transport period. In the uptake experiments, to avoid iron depletion in low-hemin-concentration reactions, we increased the reaction volume from 10 ml to 25 ml, and used 30 min instead of 1 hour as the time for uptake. In the experiments, the counts (CPM) of the cells on the filter are kept less than 10% of the total possible counts of the reaction.

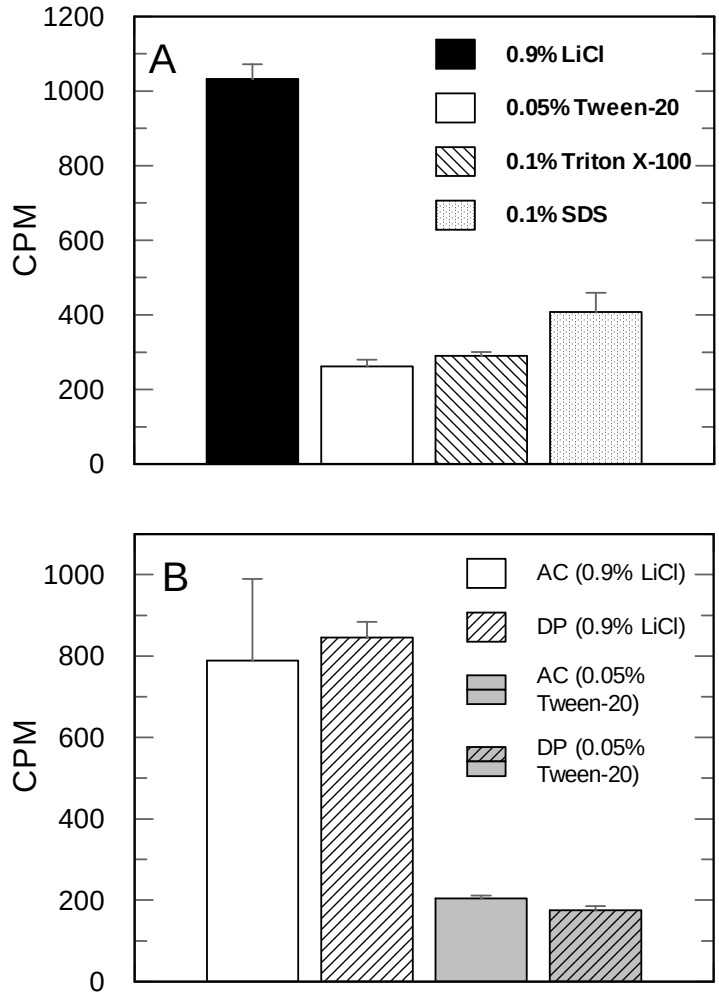

Figure 33 Effects of detergents in washing buffer

(A) 25 ml of 50 nM [^{59}Fe]-hemin solution was filtered on cellulose acetate (AC) filter and washed with 50 mM Tris (pH 9.0) containing different detergents. (B) The binding to cellulose acetate and Durophore filters, of 25 ml 50 nM [^{59}Fe]-hemin with different washing buffer was compared.

4.4.3 [^{59}Fe]-hemin binding

I tested the [^{59}Fe]-hemin binding of EGD-e wild type, ΔSrtA, ΔSrtB and ΔSrtAB. The mutant Δ*hup*, a full deletion of the *hup* operon that was made by Mr. Qiaobin Xiao was also included as a control. [^{59}Fe]-hemin was incubated with cells in MOPS (L) medium for 1 min on ice. EGD-e wild type has high affinity for hemin: the K_d is about 21 nM and capacity is 111 pmol/10^9cells/min. The deletion of whole *hup* operon had effects on binding of hemin. The capacity of Δ*hup* was about 40 pmol/10^9cells, and the K_d is 12 nM. The deletion of sortase A seemed had no effects either, but it was potentially noteworthy that the affinity (K_d) of ΔSrtA was higher than wild type. The data revealed that sortase B is crucial for hemin binding in *L. monocytogenes*. Once sortase B was deleted, as in ΔSrtB and ΔSrtAB, both capacity and affinity of hemin binding dropped significantly. Capacity decreased about 80% (Figure 34) (Table 8). I also tested the hemin binding of Δ*lmo2185* (ΔSvpA), the result was similar the sortase B mutant: the capacity was much less than that of wild type.

The [^{59}Fe]-hemin binding experiments provided important information: first of all, *L. monocytogenes* still can fully bind hemin even when all three genes in hup region were deleted, which means another hemin binding component(s) must exist in the cells membrane or cell wall. It is hard to explain why ΔHupC and ΔHupG seriously impaired the uptake in nutrition test if the cells still can

bind with hemin when all three genes are gone. One explanation is that the putative secondary hemin transport system has high capacity and affinity to bind hemin, but has much lower affinity and rate to transport hemin across the cytoplasmic membrane compared to the Hup transporter, or probably, the hemin binding by lmo2185 is not related to hemin uptake.

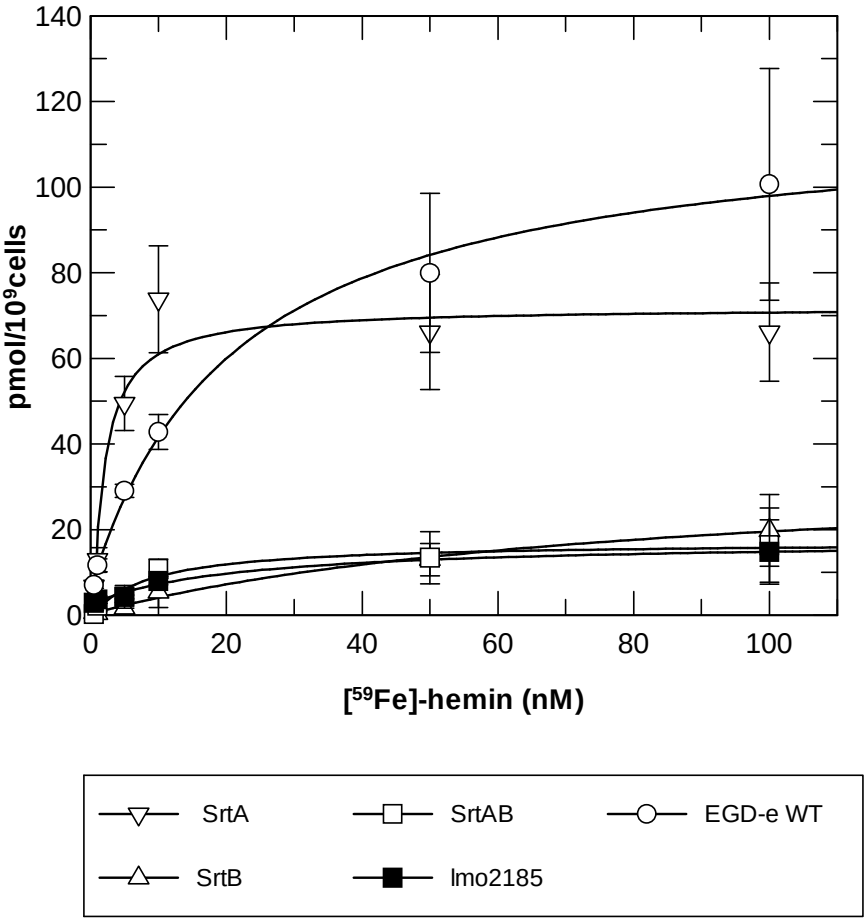

Figure 34 [^{59}Fe]-hemin binding

Second, sortase B and the protein anchored by it are absolutely needed for hemin binding. Considering the nutrition tests of ΔSrtB and Δl*mo2185* (ΔSrtB

and Δlmo2185 still transport hemin), it looks like there is probably an isd-like hemin/hemoglobin binding system in *L.monocytogenes*. It is unlikely that the Hup transporter is a part of this system since the distance between hup and sortase B locus is very far. The SrtB-SvpA locus actually has an ABC transporter gene cluster inside itself consisting with *lmo2184*, *lmo2183* and *lmo2182*. But according to previous study, the deletion of *lmo2183* did not impact either the uptake of hemin or hemoglobin. The [^{59}Fe]-hemin binding data suggested the function of the proteins encoded by *lmo2182*, *lmo2183*, *lmo2184* and *lmo2185* require further study.

	Capacity (pmol/10^9cells)	Std. Error	K_d (nM)	Std. Error
EGD-e WT	111.26	5.84	21.5	4.67
ΔSrtA	94.14	30.12	1.32	1.19
ΔSrtB	34.76	7.37	80.50	36.01
ΔSrtAB	17.57	2.08	8.49	4.50
Δlmo2185	14.37	1.98	25.18	13.2

Table 8 Summary of [^{59}Fe]-hemin binding

4.4.4 [^{59}Fe]-hemin uptake

L. monocytogenes EGD-e wild type transported [^{59}Fe]-hemin with a V_{max} of 480 pmol/10^9cells /min and a K_m of 1.44 uM. Comparing with the FeEnt transport in *E.coli* and hydroxamate siderophores transport in *L. monocytogenes*, the V_{max} was quite high but the affinity was relatively low (micromolar level). The deletion of the whole *hup* operon reduced the V_{max} about 27% (V_{max} of Δ*hup* was 359 pmol/109cells/min) and increased the K_m to 1.88 uM (Figure 35).

The fact that EGD-e still has over 70% uptake remaining after the deletion of *hup* indicated that there was a secondary system (or maybe more) exists in *L. monocytogenes*, which can take over the uptake of hemin when *hup* is absent. The uptake rate ratio, $V_{wt}/V_{\Delta hup}$ decreased from 3.5 to 1.5 when the concentration of hemin increased. The reason for this could be that Hup transporter has a higher affinity for hemin and works at low concentrations of hemin. When the hemin concentration goes up, the secondary transport system, whose affinity for hemin is lower, starts to turn on. The secondary system has lower affinity than Hup but transports hemin at higher velocity, possible because more copies of this transporter are expressed in the cells than the Hup transporter.

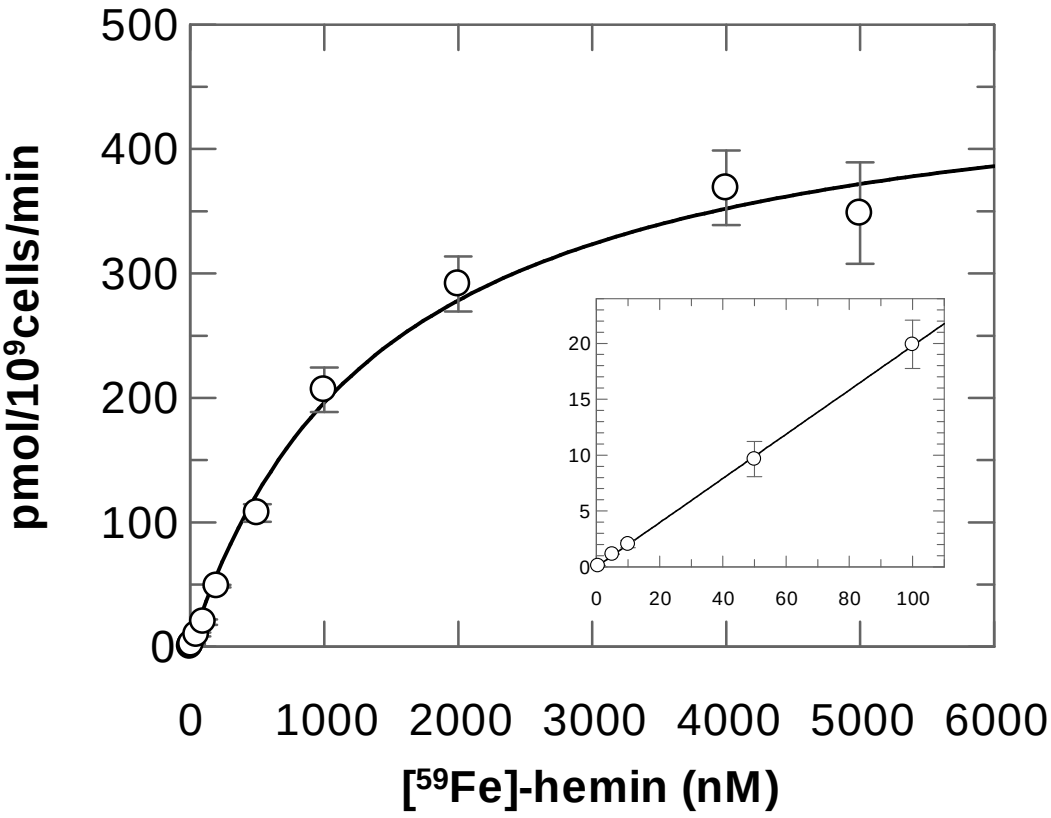

Figure 35 [^{59}Fe]-hemin uptake of EGD-e wild type

V_{max} and K_m were calculated by GraFit 6 using "Enzyme kinetics" method. The insert shows the uptake at lower hemin concentrationS (from 0.5 nM to 100 nM).

One noteworthy thing in the chemistry of hemin uptake in *L. monocytogenes* EGD-e is that the K_m (1.44 uM) is about 300 fold higher than K_d (4.68 nM). It could be explained that the binding and transport of hemin are two separate processes that happen on the cell wall and cytoplasmic membrane respectively: hemin is first bound by a high affinity protein complex, that is probably sortase-dependent, in the cell wall, then deliver it to the downstream transporters,

like Hup or the unknow secondary transporter, but the process of transport is much slower than hemin binding.

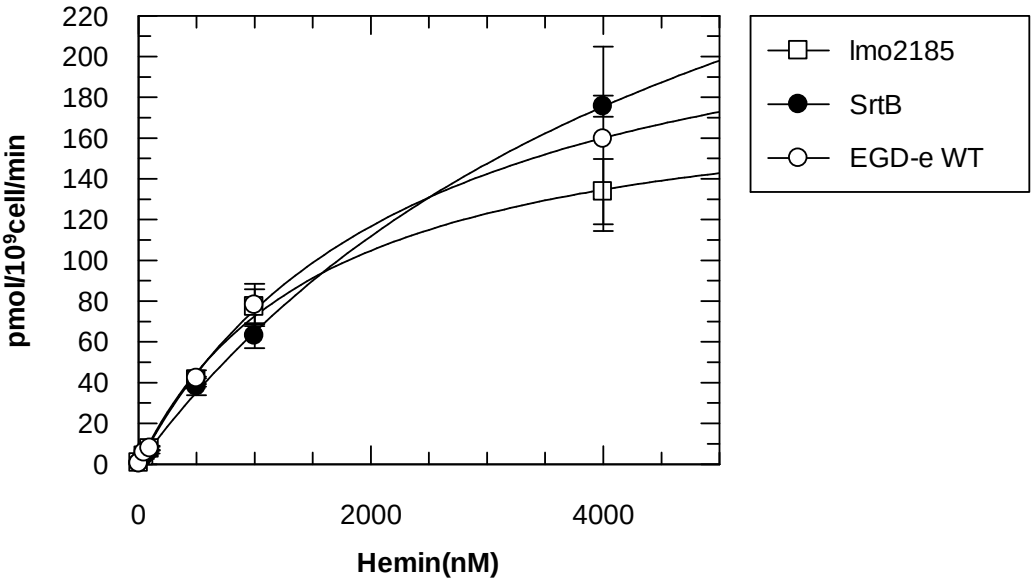

	K_m (nM)	Std. Error	V_{max} (pmol/10^9cells/min)	Std.Error
EGD-e WT	2361.9	169.3	254.4	8.8
ΔSrtB	5285.7	473.2	407.3	22.7
Δ*lmo2185*	1597.0	205.4	188.4	10.5

Figure 36 [^{59}Fe]-hemin uptake of ΔSrtB and Δlmo2185

I also checked the [^{59}Fe]-hemin uptake by ΔSrtB and Δ*lmo2185* (Figure 36). Compared with EGD-e wild type, sortase B and the surface protein encoded by *lmo2185* did not show significant effects on hemin uptake, but it was quite clear that the deletion of sortase B increased the K_m of the transport. It is still an

interesting question what the function of *lmo2185* is. Binding experiments showed that it was needed for *Listeria* to bind hemin.

One question for the hemin uptake in *L. monocytogenes* is if there were other hemin transport systems turned on when Hup system was deleted. To answer this question, I grew EGD-e wild type and ΔHup strain in BHI containing 2, 2'-bipyridyl and subjected the cytoplasm and membrane fractions of each strain to SDS-PAGE gel. The SDS-PAGE results for the wild type and ΔHup showed there were no new proteins present and no overexpressed proteins (data not shown).

4.5 Fluorescence labeling of HupG in *vivo*

Besides using radioactive labeled hemin, I also tried to use site-directed fluorescence-labeling approach to investigate the hemin of Hup transporter. If we could make single cysteine mutants on an approperate position on HupG and label it with a fluorophore, then we may be able to study the transport of hemin though the transmembrane permease by fluorescence quenching. In our lab, Cao, et al had used this method to study the FeEnt transport by FepA (31).

The crystal structure of HupG is not available. To choose the candidate residues for site directed mutagenesis on HupG, we used the crystal structure of BtuC, the permease of vitamin B_{12} ABC transporter as the structure model. HupG has 37% sequence indentity to BtuC. They share most similarities for the arrangement of the transmembrane α-helix boundless. Five residues on HupG

were chosen to make Cys mutants, they were A45, S54, A119, S194 and S308. According to the sequence alignment and the structure of BtuC, the homologies of these residues in BtuC were all located on the top of the protein, which were most likely to be labeled by fluors (Figure 37).

Cysteine mutants were made on pUC18/lmo2430 and cloned into pPL2 with hup promoter, then conjugated with Δ*hupG*. The expression (complementation) of HupG(Cys) was tested by nutrition tests. Among five mutants, A45C did not complement Δ*hupG*, but the other four did (Figure 38).

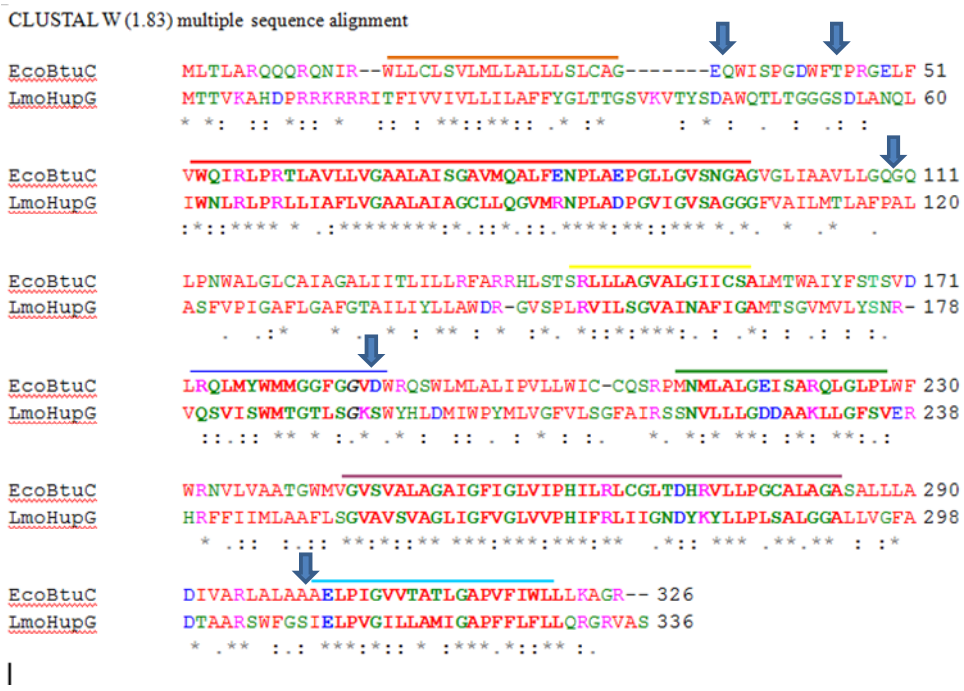

Figure 37 Cysteine mutants in HupG

The sequence of HupG and *E.coli* BtuC were aligned by CLUSTAL W (1.83). Regions having the most homology were labeled by colored bars. The residues for mutagenesis on HupG were indicated by blue arrows. In the figure below the alignment file, the positions of the five candidate residues on HupG were showed based on the crystal structure of BtuC (the residure number is the number in HupG). The colored regions on BtuC corresponded to the regions that labeled by the bars in same color in the alignment file.

The labeling procedure was adapted from the FM labeling of FepA *in vivo*. At the beginning, *L. monocytogenes* cells were boiled for 5 min in SDS sample buffer after labeling and subjected to SDS-PAGE, the gel was scanned by fluorescence scanner. Quite a few proteins were labeled but no difference of the labeling patter nbetween WT, Δ*hupG* and the cysteine mutants. To enhance the labeling, I increased the concentration of FM from 1 uM to 5uM; I used bead beater to break the cells before boiling in sample buffer and increased the number of cells loaded on the gel to see more proteins bands. In some experiments, after labeling, the membrane fraction of the cells was separated from cytoplasm and cell walls, and examined alone. After these modifications of the experimental procedure, more labeled proteins were observed but the labeling pattern of the cysteine mutants were still as same as those of WT and ΔHupG (Figure 39).

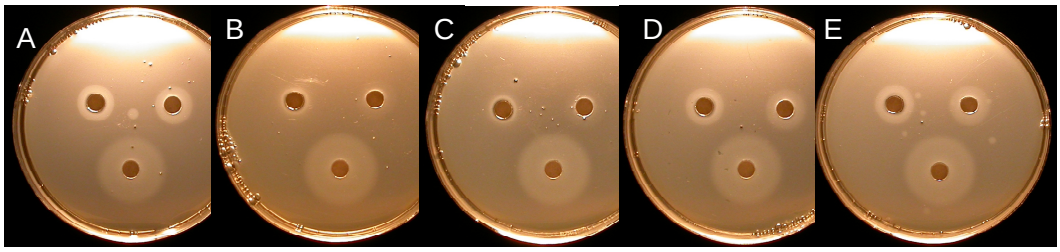

Figure 38 Nutrition tests of complemented ΔHupG(Cys)

Three paper discs were placed on each plate in the same order: top left: 15 uM hemoglobin; top right: 50 uM hemin; bottom, 50 uM ferrichrome. (A) EGD-e wild type, (B) ΔHupG, (C) A45C, (D) A119C, (E) S54C.

To get more details about the labeling, I also did the FM labeling of the membrane fractions *in vitro*. After separating the membrane and cytoplasm, membrane proteins were extracted by 0.5% sarkosyl. The solution of membrane proteins was treated either with or without 1% SDS, and then labeled by 1uM FM at 37°C for 15 min. As expected, more proteins were labeled, but the labeling pattern of ΔHupG and its cysteine mutants was still the same (Fiqure 40).

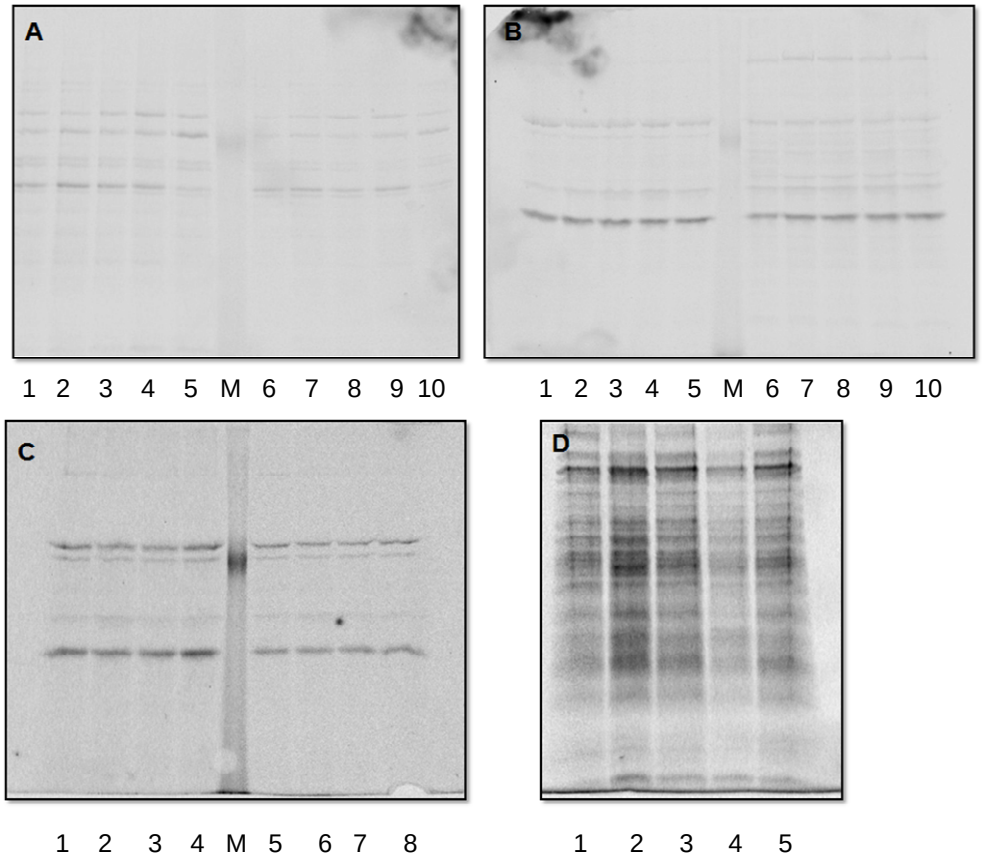

Figure 39 FM labeling of Cys-mutants in HupG

(A) Cells in lane 1-5 are labeled with 5uM FM, cells in lane 6-10 are labeled with 1uM FM. After labeling, cells were boiled in SDS sample buffer for 5 min and subjected to SDS-PAGE. Lane 1, 6: S54C; lane 2, 7: A119C; lane 3, 8: A45C; lane 4, 9:Δ*hupG*; lane 5, 10: EGD-e wild type. (B) Cells in lane 1-5 are labeled with 1uM FM. Cells in lane 6-10 are labeled with 5uM FM. After labeling, cells were broken by bead beater and boiled in SDS sample buffer for 5 min and subjected to SDS-PAGE. Lane 1, 6: S54C; lane 2, 7: A119C; lane 3, 8: A45C; lane 4, 9:ΔHupG; lane 5, 10: EGD-e wild type. (C) Labeling of S194C and S308C. Cells were labeling with 5uM FM. After labeling, cells were broken by bead beater and boiled in SDS sample buffer for 5 min and subjected to SDS-PAGE. Lane 1-4, 4×10^9cells was loaded; lanes 5-8, 2×109cells were loaded. Lane 1, 5: EGD-e wild type; lane 2, 6: ΔHupG; lane 3, 7: S194C; lane 4, 8: S308C. (D) Labeling of membrane fractions. After 5uM FM labeling, cells were broken by bead beater. Membrane fractions were separated by centrifugation and membrane proteins were exacted by 0.5% sarkosyl in TBS. Proteins of 4×10^9cells were loaded to each lane. Lane 1 to lane 5: EGD-e wild type, A119C, S54C, S194C and S308C, respectively.

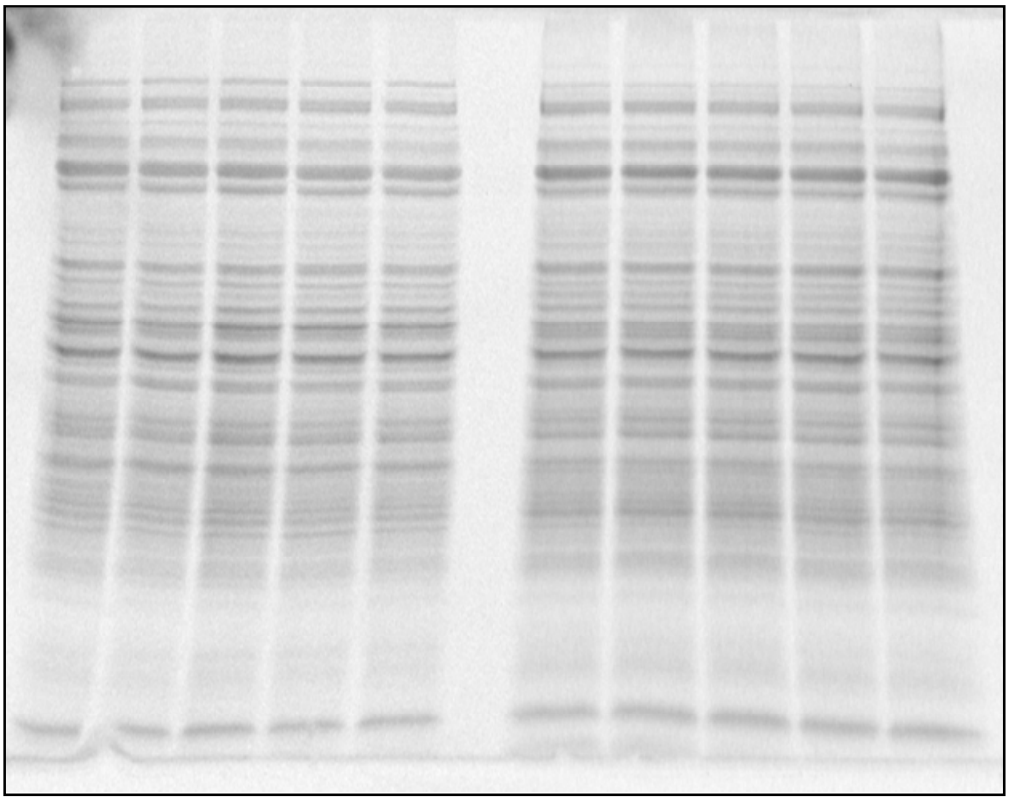

Figure 40 FM labeling of membrane fractions *in vitro* with or without SDS

Lane 1-5, membrane sample without adding 1% SDS; Lane 6-10, membrane samples adding 1% SDS. Lane1, 6: ΔHupG; lane 2, 7: A119C; lane 3, 8: S54C; lane 4, 9: S194C; lane 5, 10: S308C.

Overall, I got cysteine mutants on HupG and they were expressed, but the labeling of these mutants *in vivo* or *in vitro* was not successful. There was no problem for FM to pass though the multiplayer peptidoglycan to get membrane protein labeled, which could be confirmed by the labeling of the proteins in membrane fraction. So the reasons for the unsuccessful labeling could be that the cysteine residues were buried inside of the protein. It is also possible that

since HupD, HupG and HupC form an ABC transporter, the membrane anchored lipoprotein HupD may cover the top of HupG, which causes the cysteines cannot be labeled by FM.

4.6 Conclusions

1. Proteins encoded by *hup* operon do not reach a very high level in the media I tested. HupC associated with the cytoplasmic membrane in *vivo* showing the complex forming of Hup ABC transporter.

2. The deletion of HupC and HupG impair hemin and hemoglobin uptake and they are complemented by pPL2 system, which confirms that the ABC transporter encoded by *hup* operon is in charge of hemin uptake.

3. EGD-e wild type has an overall affinity for hemin at nanomolar level. Sortase B and the protein encoded by lmo2185, which was formerly called "SvpA", are involved in hemin binding in *L. monocytogenes*. Deletion of SrtB and lmo2185 significantly reduce the capacity and affinity of hemin binding. Sortase A has no effect on the binding.

4. EGD-e wild type transports hemin with an overall K_m at the micromolar level. Transport system(s) other than Hup exist(s) in *L.monocytogenes*, which can transport hemin with lower affinity but high rate.

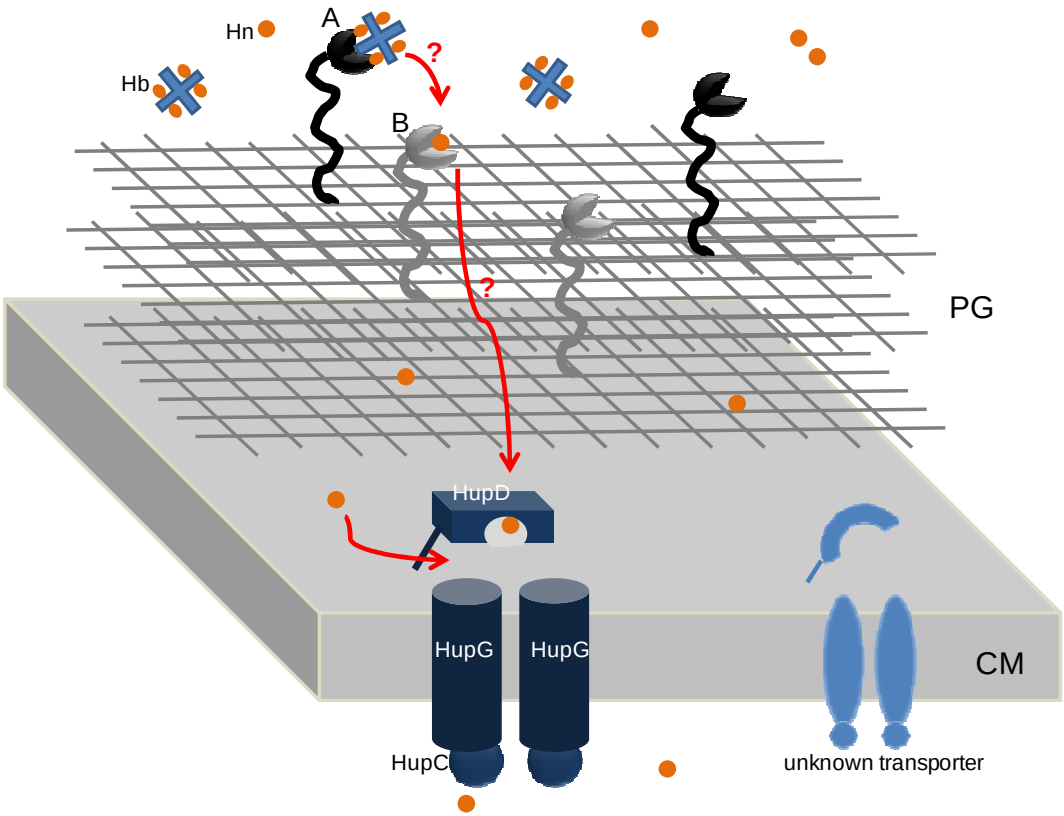

Figure 41 Schematic representation of the proposed hemin uptake pathway in the cell envolpe of *L. monocytogenes*

The existence of surface hemoglobin receptor (A) or hemin receptor (B) is still unknown, as well as the hemin pathway that labeled by "?".

Chapter 5 Study of the Function of TonB C-terminus

5.1 Overview of the TonB dependent outer membrane receptor FepA

FepA is an outer membrane siderophore receptor. It binds and transports ferric enterobactin (FeEnt) with high affinity. FepA is also the receptor for colicin B and bacteriophage H8 to enter *E.coli* cells (134, 161). Like FhuA and FecA, FepA also belongs to the "ligand-gated porin" (LGP) family. There are two domains in FepA (Figure 42). The C-terminal domain formed by 22 β-strands inserts itself in the outer membrane like a barrel. The N-terminal globular domain is inside the barrel and blocks the channel like a plug. On the top of the barrel domain, there are 11 loops, which are important for FepA to recognize and bind substrates. As other LGPs, FepA has a "TonB box" at the beginning of the N-terminal domain.

The function of FepA is TonB-dependent. Without TonB, FepA still binds but cannot transport FeEnt. A lot of work has been done to elucidate the mechanism of FepA in our lab and other labs as well (4, 31, 83, 86, 97, 102, 116, 140, 152); however there are still two interesting questions about FepA that need to be answered: First, what is the conformational change of N-terminal plug domain

causing the channel to open during the transport? Secondly, how does the inner membrane-anchored TonB facilitate FepA to transport ferric enterobactin across the outer membrane?

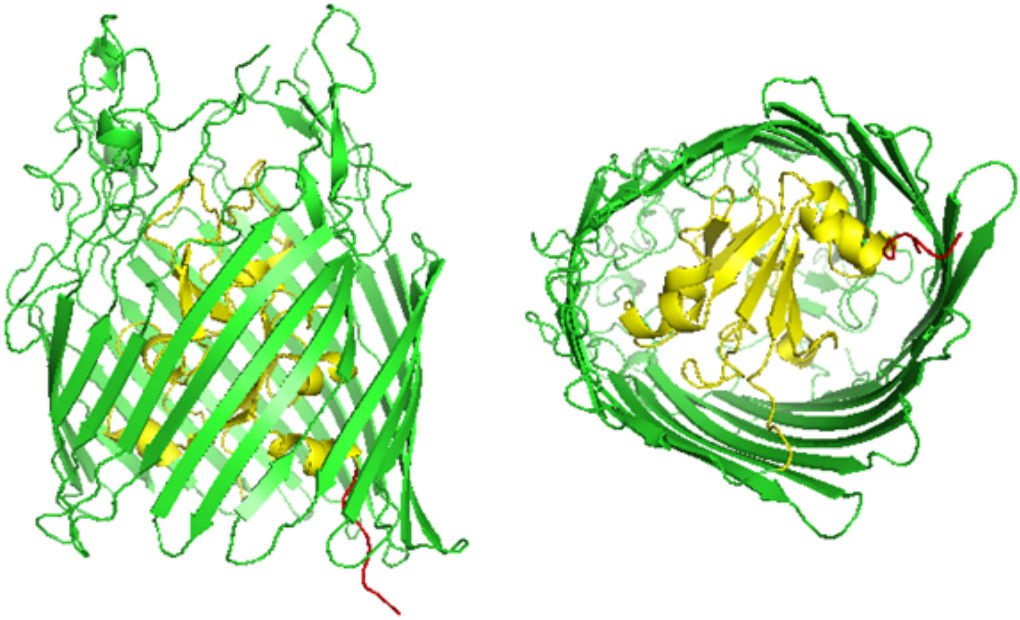

Figure 42 Structure of FepA

FepA contain two domains, the C-terminal β-barrel domain (green) and N-terminal globular domain (yellow). The “TonB box” (red) contacts the C-teminal domain of TonB during transport. Structures showed in this figure are side view (left) and the view from periplasmic side (right).

5.2 FeEnt inhibits the transport of FeTrn through FepA

In order to answer the first question, Li Ma, et al constructed a number of cysteine mutants in FepA by site-directed mutagenesis and investigated the

fluorescein-5-maleimide (FM) labeling patterns of these mutants in *vivo* (102). They found a mutant, G54C, on the surface of N domain that is normally buried within the β-barrel was labeled by FM from the periplasm during transport. The labeling of G54C provided evidence that the N domain comes out from the β-barrel, and a "ball-and-chain" mechanism was proposed. Before making this conclusion, one thing need be confirmed: that G54C was labeled by FM from the periplasmic side but not from the top side of FepA. To demonstrate that FM was not able to label G54C from top during FeEnt transport, we designed an inhibition experiment between ferric TRENCAM (FeTrn) and FeEnt.

TRENCAM (Trn), a synthetic analog of enterobactin, can be recognized and transported by FepA (Figure 43). The main structural difference between Trn and enterobactin is that the macrocyclic ester ring of enterobactin was substituted by a tertiary amine in Trn (172). The K_d of FeTrn binding to FepA is about 10^{-8} M and the size of Trn molecule is similar to that of FM.

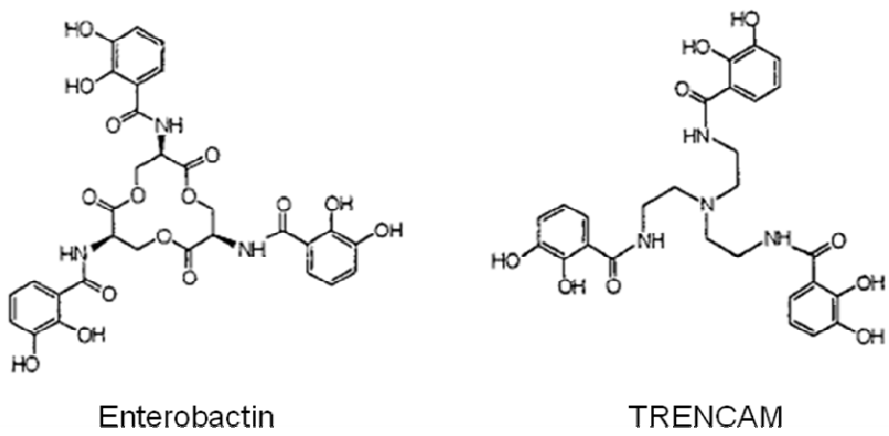

Figure 43 Enterobactin and TRENCAM

We tested the uptake of ^{59}FeTrn by *E. coli* BN1071 (wild type) and OKN3 (*fepA*$^{-}$). BN1071 transports ^{59}FeTrn at a V_{max} of 36 pmol/10^9cell/min, about half of the V_{max} of ^{59}FeEnt. The K_m is 3.6 nM, which is about 5-10 fold higher than that of ^{59}FeEnt. As expected, OKN3 transports ^{59}FeTrn much slower (V_{max}=12.3 pmol/10^9cell/min, K_m=56.9 nM) due to the missing of FepA in this strain (Figure 44). However, the uptake was not completely eliminated, which suggested that some other transporters other than FepA also can transport FeTrn at a lower rate.

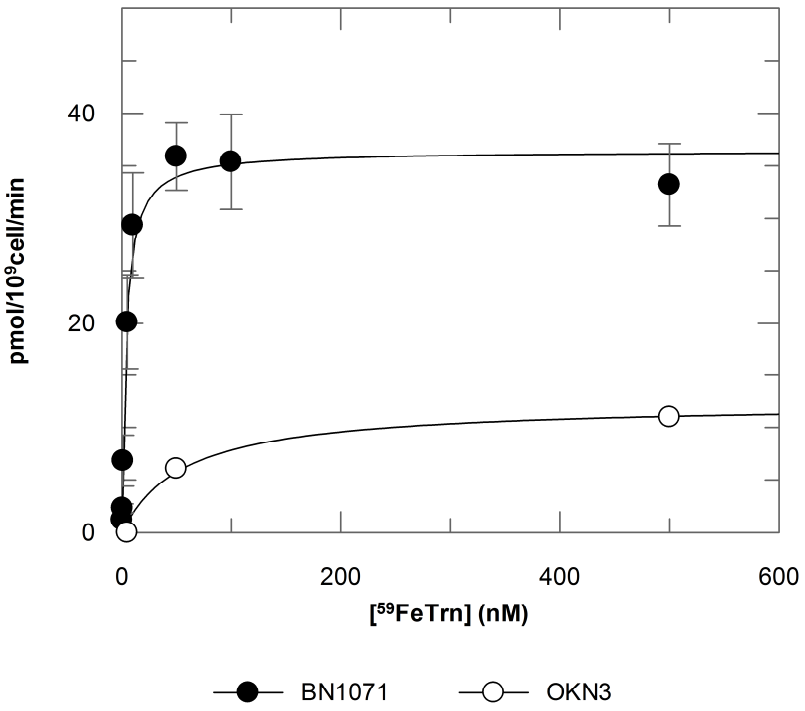

	K_m (nM)	Std. Error	V_{max} (pmol/10^9cell/min)	Std. Error
BN1071	3.63	0.68	36.41	1.34
OKN3	56.90	25.96	12.30	1.52

Figure 44 ^{59}FeTrn uptakes by BN1071 and OKN3

In the competitive inhibition experiments, the concentration of ^{59}FeTrn was kept at 100 nM high to ensure that FeTrn could be transported at the maxima rate. Different concentrations of FeEnt varying from 0.05 nM to 500 nM were added into the transport reaction and the transport rate of ^{59}FeTrn decreased while increasing the concentration of FeEnt. The IC_{50} for the inhibition of FeTrn uptake by FeEnt was 8.31 (±3.14) nM (Figure 45). This data showed that FeEnt has a great affinity to occupy the ferric siderophore binding sites on FepA. FeTrn has affinity to FepA about 10^{-8} M, but 8 nM FeEnt was already capable to strongly inhibited the uptake of FeTrn at a concentration of 100 nM level. This means when FeEnt was present during the transport, it efficiently blocked the access of other molecules to FepA even at nano molar levels. Considering the much lower affinity of fluorescein maleimide to FepA, it was very unlikely that fluorescein maleimide could surpass FeEnt and labeled G54C from the exterior. If G54C was labeled, it should be labeled by the fluor molecule from the periplasmic side, and this required the N-terminal plug domain to come out from the β-barrel, and allow this residue to be exposed. So these inhibition experiments supported the “ball-and-chain” theory of FeEnt transport by FepA.

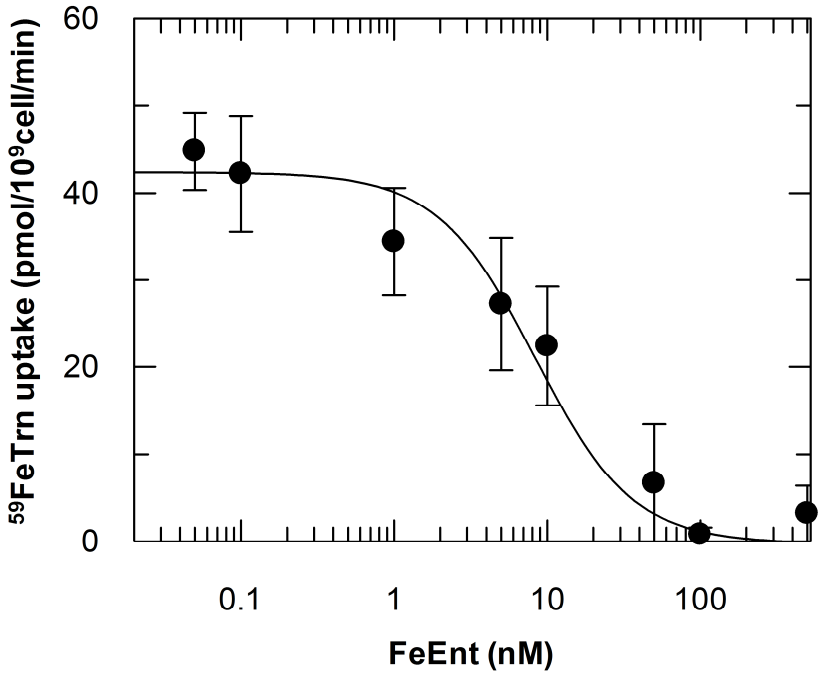

Figure 45 Inhibition of ^{59}FeTrn uptake by FeEnt

5.3 Generation of α-TonB polyclonal antibody

An α-TonB antibody is an important reagent for the study of the function of TonB. In our lab, Dr. Newton cloned the 6His-tagged TonB and I purified the 6His-tagged protein by using Ni-NTA affinity column. On SDS-PAGE gel, the purified 6H-TonB showed two major bands: One band with a size about 36 kD and another one with a size about 27 kD. According to the amino acid sequence of TonB, the small band is monomeric 6H-TonB. The 36 kD product was smaller than 6H-TonB dimer but close to the size of 6H-TonB monomer plus a TonB C-terminus (~7.8 kD). I cannot confirm what kind of aggregation of this product is, but interestingly, western blot showed that TonB in the cell lysates of BN1071 and OKN1/pT23 existed as this form (Figure 46).

The first α-TonB immunoblot showed that there were also several other antibodies in the rabbit sera due to the existence of contaminating proteins in the 6H-TonB sample that I injected to the rabbit. I did antibody adsorption by repeatly suspending BN1071 cells in the rabbit sera, and most of the contaminating antibodies were taken away by the cells. However, a major contaminant, α-OmpA was still remaining. To get rid of α-OmpA, I coupled purified OmpA to Sepharose 6B cellulose and let rabbit sera pass through the resin. Most of the α-OmpA stayed with OmpA in the column, which was verified by immunoblot (Figure 47).

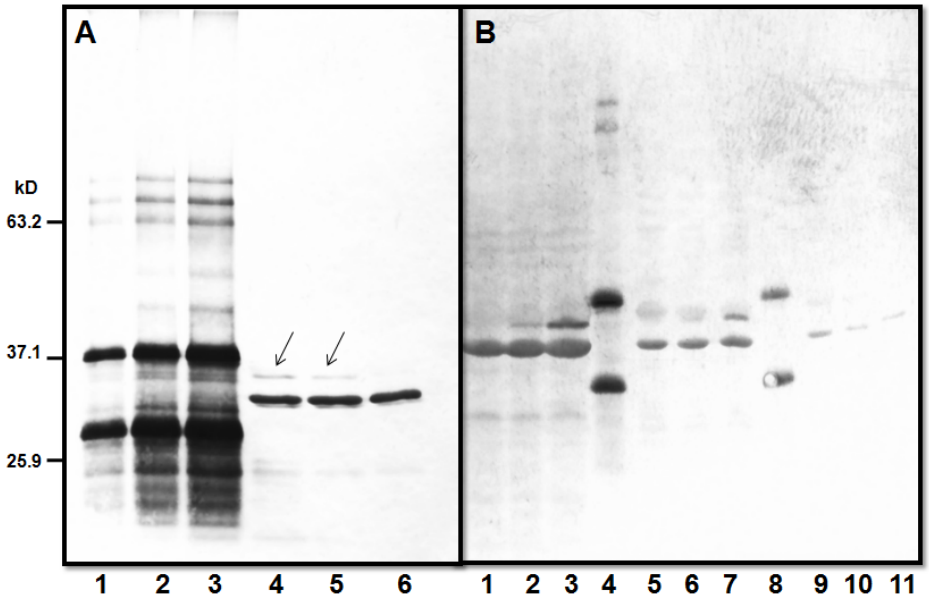

Figure 46 α-TonB immunoblots

(A) α-TonB blot before adsorption. Lane 1-3: 0.04, 0.2 and 1 ug purified 6H-TonB, respectively. Lane 4-6: 1×10^7 cells' lysates of OKN1/pT23, BN1071 and OKN1, respectively. The bands for TonB are pointed out by arrows. (B) α-TonB blot with different amount of cells before adsorption. Lane 1-3: 5×10^7 cells of OKN1, BN1071 and OKN1/pT23; lane 4: 0.8 ug 6H-TonB; lane5-7: 1×10^7 cells of OKN1, BN1071 and OKN1/pT23; lane 8: 0.2 ug 6H-TonB; lane 9-11: 0.2×10^7 cells of OKN1, BN1071 and OKN1/pT23.

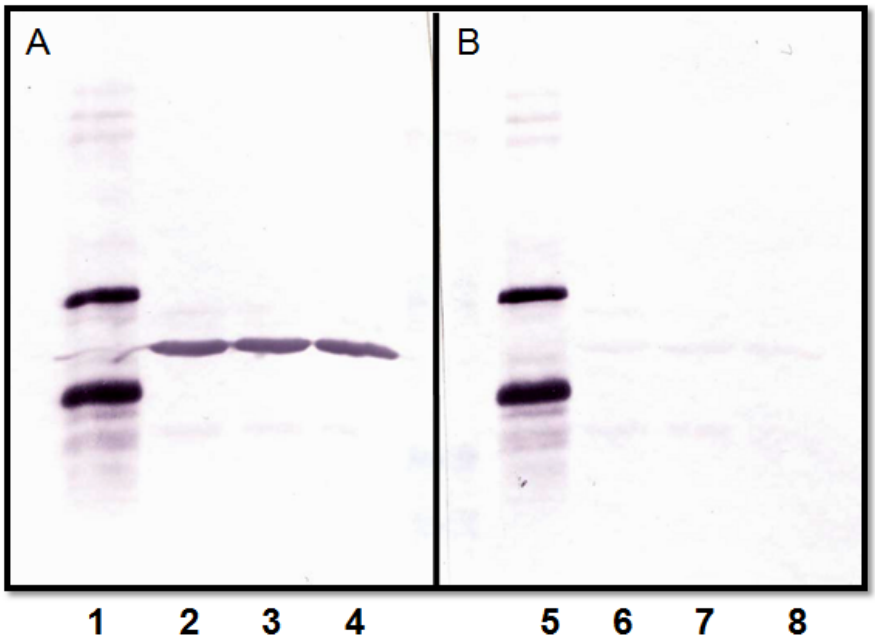

Figure 47 -TonB immunoblots before and after the adsorption of α-OmpA

(A) Before adsorption. Lane 1-4: purified 6H-TonB, OKN1/pT23, BN1071 and OKN1. (B) After adsorption. Lane 5-8: purified 6H-TonB, OKN1/pT23, BN1071 and OKN1.

5.4 Functional characterization of GFP-TonB hybrid proteins

So far, two mechanisms have been proposed to describe the function of TonB. In the shuttle mechanism, once charged with the energy from proton motive force, TonB leaves the inner membrane to the periplasmic side of the outer membrane and transfers energy to the outer membrane receptors. The discharged TonB shuttles back and associates with ExbB-ExbD complex in the inner

membrane again. Unlike the shuttle mechanism, the rotary mechanism proposes that, in *vivo*, TonB is dimerized and associates with a single copy of ExbB-ExbD complex. The N-terminus of TonB remains in the inner membrane during the whole transport cycle. Energy is transduced to the C-terminus of TonB by the spinning of rigid rod domain of the TonB dimer. The spinning C-terminus of TonB interacts with the receptors and transfers energy to them.

In our lab, Dr. Wallace Kaserer constructed GFP-TonB fusion proteins to investigate whether TonB disassociated with the inner membrane or not during the FeEnt transport (86). The TonB promoter, enhanced GFP gene and TonB gene were amplified by PCR and ligated into plasmid pHSG575 respectively to give the final construct of pGT. In the second construction, a small linker with a sequence of "EAAAK" was inserted between GFP and TonB to give the final construct of pGLT.

The expression of these two fusion proteins was tested by immunoblot using α-TonB antibody and the molecular weight of the fusion proteins were correct. To evaluate the function of GFP-TonB fusion proteins, we tested the binding and uptake of ^{59}FeEnt by the strains carrying these constructs and compared the results with BN1071, which expresses wild type TonB. Even fused with a protein with a similar size to itself, TonB is still functional and supports the binding and uptake of FeEnt. The K_d, capacity, V_{max} and K_m of OKN1/pGT and OKN/pGLT are comparable to those of BN1071 and OKN1/pTS23 (Figure 48). Since the GFP moieties in these fusion proteins stays in cytoplasm (fluorescent

data and protein localization data by Dr. Kaserer), this data indicates that TonB does not leave the inner membrane and transfer to outer membrane during FeEnt transport, which argues against the shuttle mechanism.

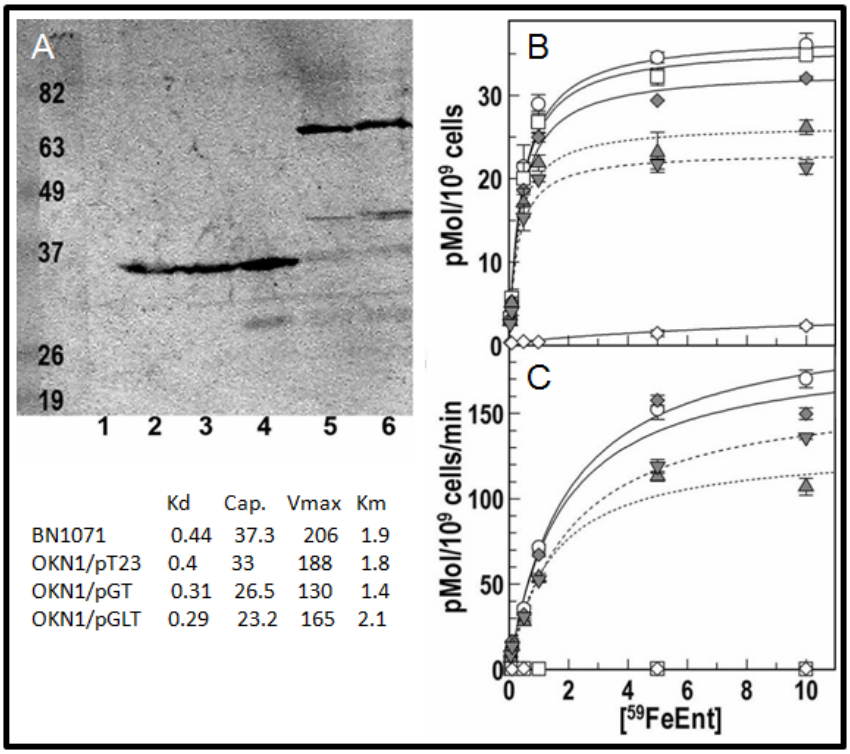

Figure 48 ^{59}FeEnt binding and transport of GFP-TonB fusion proteins

(A) α-TonB western blot showed that GFP and TonB were fused together. Lane 2-3: wild type TonB; lane 5-6: pGT and pGLT. (B) ^{59}FeEnt binding of BN1071 (○), OKN1 (□), OKN1/pT23 (♦), OKN3 (◊) and strains expressing GFP-TonB (▲) and GFP-L-TonB (▼). (C) ^{59}FeEnt transport of the same strains in panel B. The ^{59}FeEnt binding and transport parameters of BN1071, OKN1/pT23, OKN1/pGT and OKN1/pGLT were summarized in the table under panel A.

5.5 Study of the affinity between peptidoglycan and TonB C-terminus

5.5.1 TonB C-terminus has affinity for peptidoglycan

LysM motif was first found in the lysozyme of *Bacillus* phage (61). The function of LysM is to bind to bacteria cell wall (peptidoglycan). It was widely found in peptidoglycan hydrolases, phage lysins and virulence factor proteins (27). The crystal structure of LysM motif in *E. coli* lytic murein transglycosylase D (MltD) solved by NMR shows that LysM has a βααβ secondary structure (11).

TonB C-terminus has sequence homology to LysM motif. The last 69 amino acids in the C-terminus of TonB has 19% identity and 77% homology with the LysM domain in MltD. CLUSTALW and LSQMAN alignments between C-terminus of TonB (RCSB 1Ihr) and LysM (RCSB 1e0g) indicated two residues, D189 and E205 in the C-terminus of TonB were the potential sites for peptidoglycan binding. These two residues correspond to the D11 on lysM, which is one critical residue in the peptidoglycan binding sites (Figure 49).

```
CLUSTAL 2.0.11 multiple sequence alignment


TonB69C         RIEGQVKVKFDVTPDGRVDNVQILSAKPANMFEREVKNAMRRWRYEPGKPGSGIVVNILF 60
LysM            -----DSITYRVR-KG--DSLSSIAKRHG----VNIKDVMR-WNSDTANLQPGDKLTLFV 47
                     .:.: *  .*  *.:. :: : .     ::*:.** *. :..:  .*  :.::.

TonB69C         KINGTTEIQ 69
LysM            K-------- 48
                *
```

Figure 49 The structure of LysM motif in MltD and amino acid sequence alignment between TonB69C and LysM

The protein sequence of TonB69C and LysM were aligned by CLUSTAL 2.0.11. Putative PG binding sites were indicated by red arrows.

In Kaserer's paper (86), co-sedimentation experiments showed that the soluble MalE-TonB69C fusion protein associated with purified peptidoglycan and was found in the pellet sample after centrifugation, but MalE, and the periplasmic binding protein, FepB still stayed in the supernatant. These results suggested that MalE-TonB69C has specific affinity to peptidoglycan, while other proteins do not.

5.5.2 Site-direct mutagenesis on MalE-TonB69C

Site-direct mutagenesis could be a desirable method for us to characterize the binding property of TonB C-terminus to peptidoglycan. First, we can select

appropriate residues on TonB69C and change them to cysteines, and then we can label the mutated TonB69C by fluors and measure the affinity of TonB C-teminus to peptidoglycan by extrinsic fluorescence quenching. By using site-directed mutagenesis, we can also perform alanine scaning on TonB69C to survey the binding site(s).

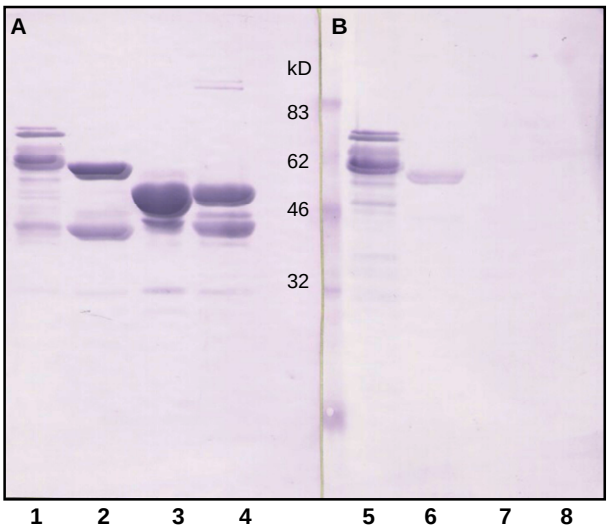

Figure 50 Immunoblots of MalE-TonB fusion proteins

(A) α-MalE blot. Lane 1-4: pSTonB, pSTonB104C, pSTonB69C, pMalP2. (B) α-TonB blot. Lane 1-4: pSTonB, pSTonB104C, pSTonB69C, pMalP2. α-TonB could not recognize MalE-TonB69C, which may because TonB was truncated too much.

Dr. Daniel Scott cloned the whole TonB gene or part of it C-terminal 69 residues of TonB into the plasmid pMALp2 and constructed pSTonB (MalE and TonB), pSTonB104C (MalE and C-terminal 104 residues of TonB) and pSTonB69C (MalE and C-terminal 69 residues of TonB) (86). I purified these fusion proteins and tested them by α-MalE and α-TonB immuno blots (Figure 49). Based on pSTonB69C, I made three single-cysteine mutants on TonB69: S222C, S195C and N227C (Figure 51). Serine is a good candidate for cysteine substitution since it has similar side chain as cysteine. Furthermore, serine and cysteine have similar dihedral angles in polypeptide; Therefore, changing a residue from serine to cysteine should not disrupt protein secondary structure. If the mutant sites are too close to the binding pocket, the fluor labeling could affect the binding interaction. S222, S195 and N227 have suitable distance to the putative binding sites, which is another reason that they were chosen. For the two putative binding sites, E205 and D189, I made E205A and double mutant E205A/D189A. I also tried to make single-alanine mutant, D189A, but I did not obtain this mutant finally.

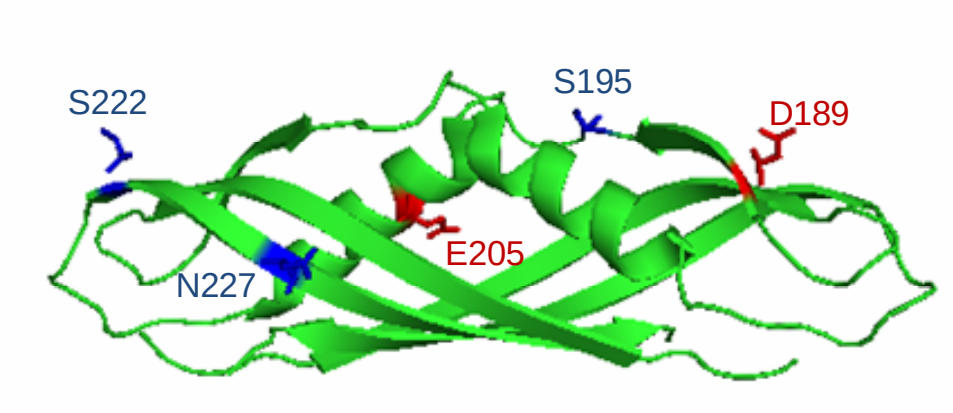

Figure 51 Residues selected for site-directed mutagenesis on TonB C-terminus

Five residues were mutated: S222, S195 and N227 (blue, in stick format) were changed to cysteines; E205 and D189 (red, in stick format) were changed to alanines.

5.5.3 Fluorescence quenching of MalE-TonB69C(S222C)-FM by peptidoglycan

MalE-TonB69C(S222C) was purified and labeled by FM (Figure 52 and 53). The molar ratio of [FM]/[protein] was at least 5:1 to allow fully labeling of the cysteine residues. After labeling, the mixture was loaded to amylose resin, excess FM was washed away and MalE-TonB69C(S222C)-FM was eluted by maltose. The fluorescent scaning image of the gel showed that the labeling was very efficient and high yield. The purified peptidoglycan (PG) sample was also subjected to SDS-PAGE to make sure that there were no contaminated proteins

in the sample (Figure 53 C). When adding increased amount of PG into the protein solution, the fluorescence indensity of FM decreased and the measured K_d was about 0.75 (±0.1) ug/ml (Figure 54). The level of the quenching of S222C-FM was not very high (about 15% quenching after subtracting the buffer background). It is possible that the location of S222 is too far from the peptidoglycan binding site, so the binding only causes a slight effect at that position: the chemical environment of FM was not changed significantly. Therefore, more cysteine mutants in different position of TonB C-terminus need to be tested in the future.

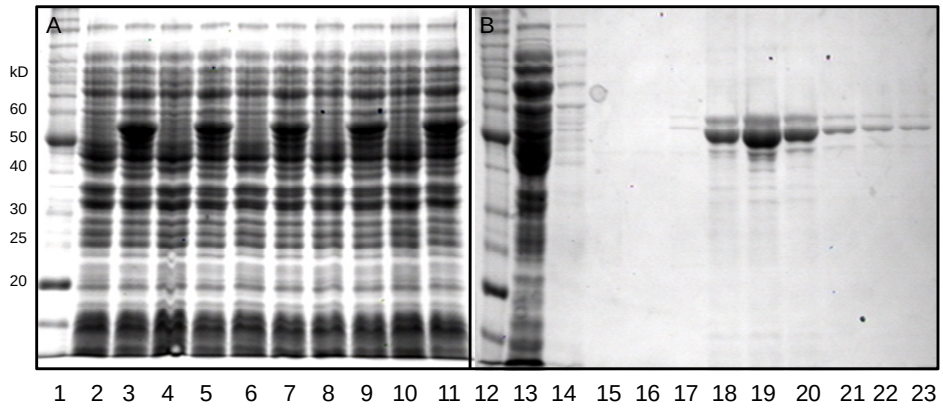

Figure 52 Expression and purification of MalE-TonB69C (S222C)

(A) Five constructs of MalE-TonB69C (S222C) were induced by IPTG and the cell lysates were analyzed by SDS-PAGE. Lane 2, 4, 6, 8, 10: cell lysates without adding IPTG; lane 3, 5, 7, 9, 11: cell lysates with 0.5 mM IPTG. (B) MalE-TonB69C (S222C) was purified with amylose resin. Lane 17-23 showed the fusion protein eluted by 10 mM Maltose.

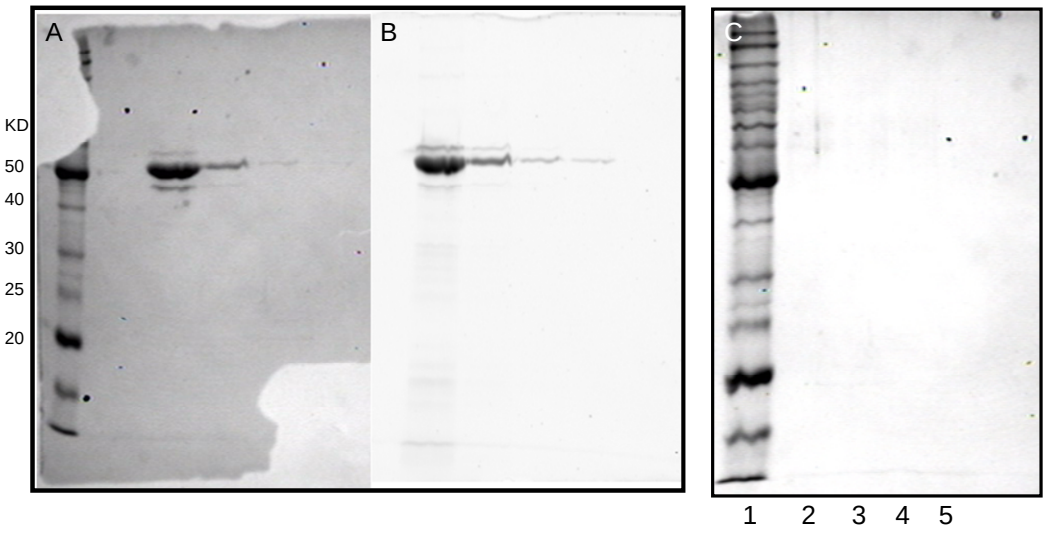

Figure 53 FM labeling of MalE-TonB69C (S222C) in *vitro*

(A) After labeling, MalE-TonB69C (S222C)-FM was repurified by amylose column. (B) The same SDS-PAGE gel in panel A was scanned by fluorescent scanner and the image showed that the protein was labeled. (C) Purified PG sample was subjected to SDS-PAGE with increasing amount (from lane 2 to 5). No contaminating proteins were observed in each sample.

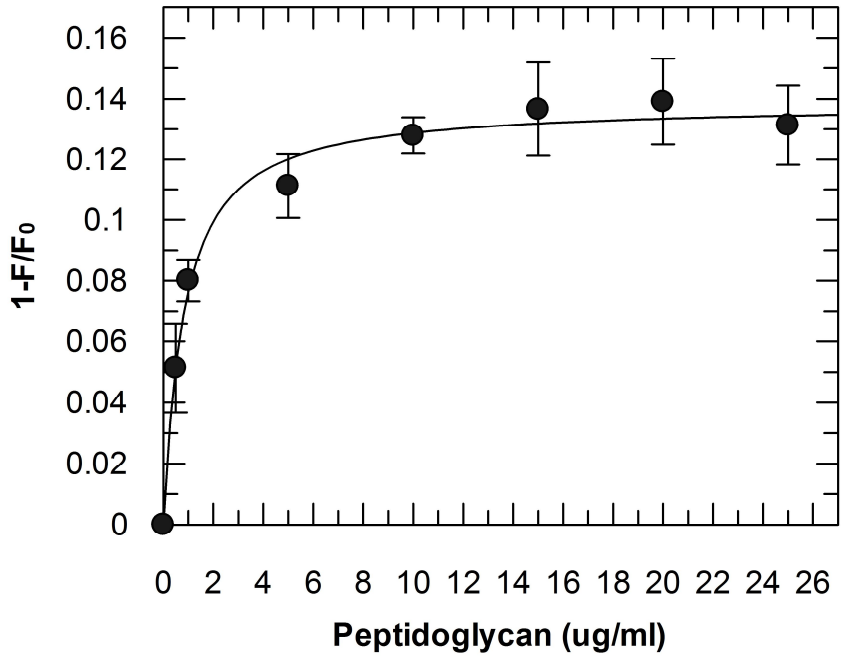

Figure 54 Extrinsic fluorescence quenching of MalE-TonB69C(S222C)-FM

5.5.4 Co-sedimentation of TonB69C with peptidoglycan

Peptidoglycan is a polymer of sugars and amino acids, not soluble in water, and it is pelleted from water by centrifugation. If the TonB C-terminus binds to it, then after high speed centrifugation, the water-soluble TonB C-terminus should be found in the pellet of peptidoglycan. Mr. Qiaobin Xiao and Dr. Klebba established a protocol to co-sediment MalE-TonB69C with peptidoglycan from buffer and I used this protocol to test my mutants. Based on pSTonB69C, I made MalE-TonB69C (E205A) and MalE-TonB69C (E205A/D189A). These two

mutant fusion proteins were purified and mixed with peptidoglycan, which was carefully dispersed in Tris-HCl buffer by sonication. After centrifugation, both the supernatant sample and pellet sample were subjected to SDS-PAGE and stained by Coomassie blue. Unlike what was expected, after changing E205 and both E205 and D189 to alanine, MalE-TonB69C still bound with peptidoglycan: when the amount of peptidoglycan was increased, the amount of the fusion protein also increased in the pellet. Meanwhile, the amount of the fusion protein in the supernatant decreased (Figure 55 and 56).

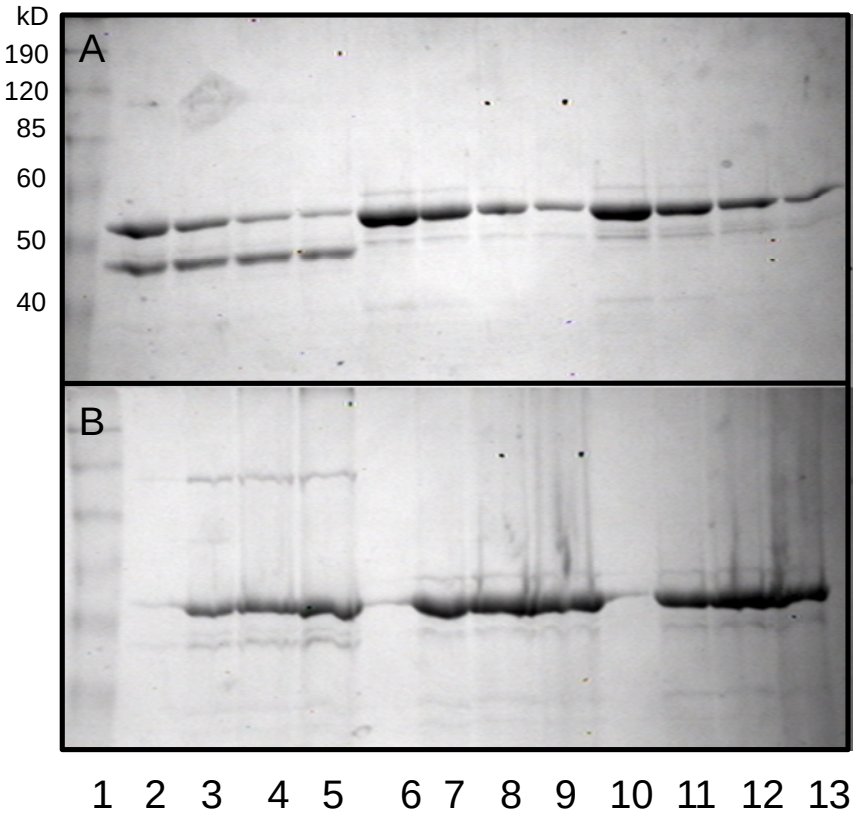

Figure 55 Affinity of MalE-TonB69C (E205A) for peptidoglycan

MaLE, MalE-TonB69C and MalE-TonB69C (E205A) were mixed with increasing amount of PG. After centrifugation, supernatants (A) and pellets (B) were subjected to SDS-PAGE. Lane 2-5: MalE (the lower band) with 0, 5, 20, 40 ul of PG; lane 6-9: MalE-TonB69C with 0, 5, 20, 40 ul of PG; lane 10-13: MalE-TonB69C (E205A) with 0, 5, 20, 40 ul of PG.

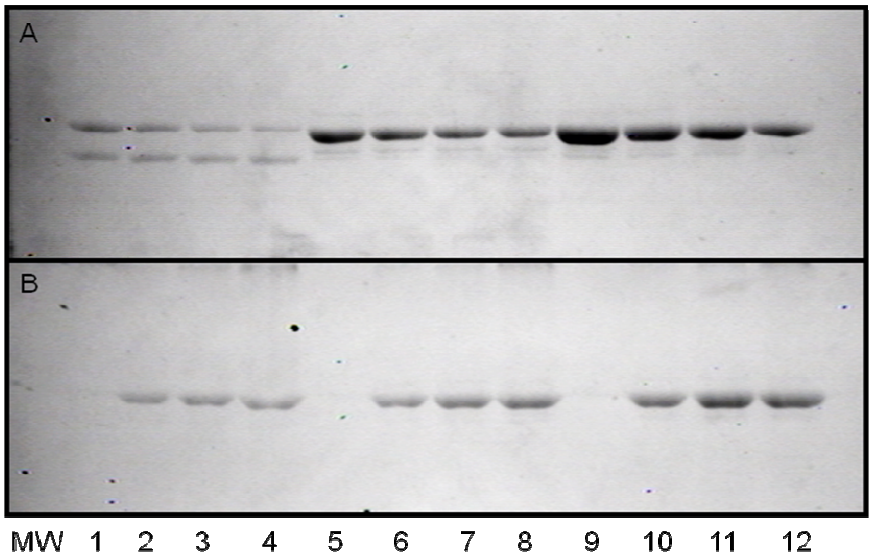

Figure 56 Affinity of MalE-TonB69C (E205A/D189A) for peptidoglycan

MaLE, MalE-TonB69C and MalE-TonB69C (E205A/D189A) were mixed with increasing amount of PG. After centrifugation, supernatants (A) and pellets (B) were subjected to SDS-PAGE. Lane 2-5: MalE (the lower band) with 0, 5, 20, 40 ul of PG; lane 6-9: MalE-TonB69C with 0, 5, 20, 40 ul of PG; lane 10-13: MalE-TonB69C (E205A/D189A) with 0, 5, 20, 40 ul of PG.

Instead of using a MalE-TonB fusion protein, it was desirable to use TonB C-terminus alone to evaluate the binding between TonB and PG. In pSTonB69C, there is a factor-Xa cutting site between MalE and TonB69C. The cutting site in MalE-TonB69C was somehow buried inside after protein folding, so 0.05% SDS was needed to slightly denature the protein to let the cutting site be accessible to factor-Xa. I tried to use factor-Xa to digest the fusion protein, but TonB69C

cannot be fully cut even when 0.05% SDS was applied. I cloned the fusion protein again with three cutting site in between MalE and TonB69C, but the digestion was not improved. So I employed an alternate approach to get TonB C-terminus. I cloned TonB69C into pET21a (+) with NdeI and XhoI sites and purified 6H-TonB69C (Figure 57). Co-sedimentation experiments showed that 6H-TonB69C also has affinity to PG (Figure 58). It will be also desirable to construct cysteine mutants on 6H-TonB69C to measure the binding by fluorescence quenching.

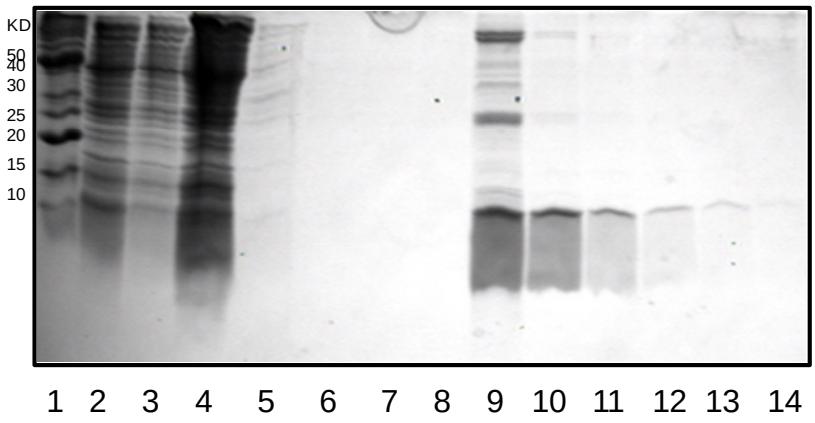

Figure 57 Purification of 6H-TonB69C

6H-TonB was induced by IPTG and purified by Ni-NTA column. Fractions were collected and analyze by 10-17% gradient SDS-PAGE. Lane 2: cell lysate; lane 3-8: imidazole gradient wash; lane 9-14: 6H-TonB69C was eluted from the column by 250 mM imidazole.

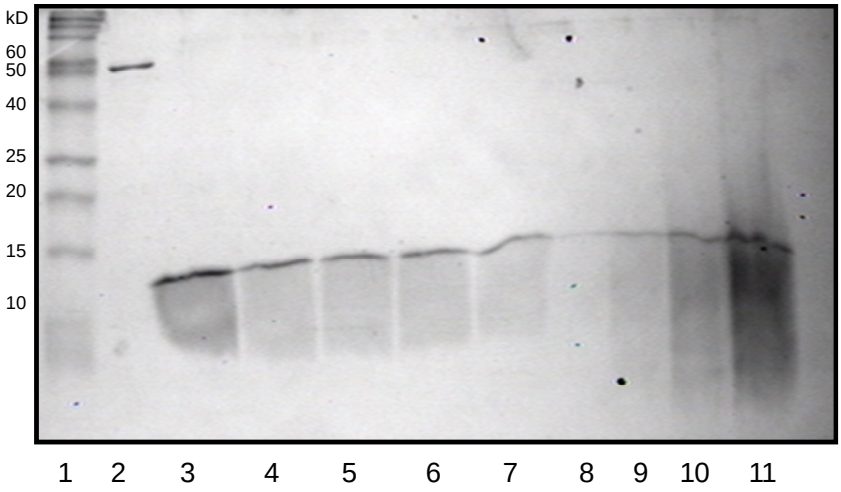

Figure 58 Affinity of 6H-TonB for peptidoglycan

The experimental procedure was as same as that described previously. The amount of 6H-TonB69C decreased in the supernatants when increasing the amount of PG (lane 3-7) while the amount of 6H-TonB69C in the pellets increased (lane 8-11).

5.6 Conclusions

1. The binding of FeEnt to FepA efficiently excludes the accessibility of FM to the N-terminal domain of FepA.

2. When GFP is fused to the N-terminus of TonB, the fusion proteins still facilitates the binding and transport of FeEnt by FepA.

3. The C-terminus of TonB has affinity to peptidoglycan and changing residue E205 and residue D189 to alanine does not eliminate the binding.

Reference

1. **Abergel, R. J., M. C. Clifton, J. C. Pizarro, J. A. Warner, D. K. Shuh, R. K. Strong, and K. N. Raymond.** 2008. The siderocalin/enterobactin interaction: a link between mammalian immunity and bacterial iron transport. J Am Chem Soc **130:**11524-34.

2. **Adler, A. D., F. R. Longo, F. Kampas, and J. Kim.** 1970. On Preparation of Metalloporphyrins. Journal of Inorganic & Nuclear Chemistry **32:**2443-&.

3. **Althaus, E. W., C. E. Outten, K. E. Olson, H. Cao, and T. V. O'Halloran.** 1999. The ferric uptake regulation (Fur) repressor is a zinc metalloprotein. Biochemistry **38:**6559-69.

4. **Annamalai, R., B. Jin, Z. Cao, S. M. Newton, and P. E. Klebba.** 2004. Recognition of ferric catecholates by FepA. J Bacteriol **186:**3578-89.

5. **Arnaud, M., A. Chastanet, and M. Debarbouille.** 2004. New vector for efficient allelic replacement in naturally nontransformable, low-GC-content, gram-positive bacteria. Appl Environ Microbiol **70:**6887-91.

6. **Arnoux, P., R. Haser, N. Izadi, A. Lecroisey, M. Delepierre, C. Wandersman, and M. Czjzek.** 1999. The crystal structure of HasA, a hemophore secreted by Serratia marcescens. Nat Struct Biol **6:**516-20.

7. **Axen, R., J. Porath, and S. Ernback.** 1967. Chemical coupling of peptides and proteins to polysaccharides by means of cyanogen halides. Nature **214:**1302-4.

8. **Babusiak, M., P. Man, R. Sutak, J. Petrak, and D. Vyoral.** 2005. Identification of heme binding protein complexes in murine erythroleukemic cells: study by a novel two-dimensional native separation -- liquid chromatography and electrophoresis. Proteomics **5:**340-50.

9. **Bae, T., and O. Schneewind.** 2003. The YSIRK-G/S motif of staphylococcal protein A and its role in efficiency of signal peptide processing. J Bacteriol **185:**2910-9.

10. **Baichoo, N., and J. D. Helmann.** 2002. Recognition of DNA by Fur: a reinterpretation of the Fur box consensus sequence. J Bacteriol **184:**5826-32.

11. **Bateman, A., and M. Bycroft.** 2000. The structure of a LysM domain from E. coli membrane-bound lytic murein transglycosylase D (MltD). J Mol Biol **299:**1113-9.

12. **Bates, C. S., G. E. Montanez, C. R. Woods, R. M. Vincent, and Z. Eichenbaum.** 2003. Identification and characterization of a Streptococcus pyogenes operon involved in binding of hemoproteins and acquisition of iron. Infect Immun **71:**1042-55.

13. **Bearden, S. W., T. M. Staggs, and R. D. Perry.** 1998. An ABC transporter system of Yersinia pestis allows utilization of chelated iron by Escherichia coli SAB11. J Bacteriol **180:**1135-47.

14. **Behari, J., and P. Youngman.** 1998. Regulation of hly expression in Listeria monocytogenes by carbon sources and pH occurs through separate mechanisms mediated by PrfA. Infect Immun **66:**3635-42.

15. **Bergmann, B., D. Raffelsbauer, M. Kuhn, M. Goetz, S. Hom, and W. Goebel.** 2002. InlA- but not InlB-mediated internalization of Listeria monocytogenes by non-phagocytic mammalian cells needs the support of other internalins. Mol Microbiol **43:**557-70.

16. **Bierne, H., C. Garandeau, M. G. Pucciarelli, C. Sabet, S. Newton, F. Garcia-del Portillo, P. Cossart, and A. Charbit.** 2004. Sortase B, a new class of sortase in Listeria monocytogenes. J Bacteriol **186:**1972-82.

17. **Bierne, H., S. K. Mazmanian, M. Trost, M. G. Pucciarelli, G. Liu, P. Dehoux, L. Jansch, F. Garcia-del Portillo, O. Schneewind, and P. Cossart.** 2002. Inactivation of the srtA gene in Listeria monocytogenes inhibits anchoring of surface proteins and affects virulence. Mol Microbiol **43:**869-81.

18. **Bigot, A., Charbit, A.** 2008. Genetic manipulations, p. 284. *In* D. Liu (ed.), Handbook of *Listeria monocytogenes*. CRC Press.

19. **Blake, M. S., K. H. Johnston, G. J. Russell-Jones, and E. C. Gotschlich.** 1984. A rapid, sensitive method for detection of alkaline phosphatase-conjugated anti-antibody on Western blots. Anal Biochem **136:**175-9.

20. **Blanvillain, S., D. Meyer, A. Boulanger, M. Lautier, C. Guynet, N. Denance, J. Vasse, E. Lauber, and M. Arlat.** 2007. Plant carbohydrate scavenging through tonb-dependent receptors: a feature shared by phytopathogenic and aquatic bacteria. PLoS ONE **2:**e224.

21. **Bracken, C. S., M. T. Baer, A. Abdur-Rashid, W. Helms, and I. Stojiljkovic.** 1999. Use of heme-protein complexes by the Yersinia enterocolitica HemR receptor: histidine residues are essential for receptor function. J Bacteriol **181:**6063-72.

22. **Braun, V.** 2005. Bacterial iron transport related to virulence. Contrib Microbiol **12:**210-33.

23. **Braun, V.** 2001. Iron uptake mechanisms and their regulation in pathogenic bacteria. Int J Med Microbiol **291:**67-79.

24. **Braun, V., and H. Killmann.** 1999. Bacterial solutions to the iron-supply problem. Trends Biochem Sci **24:**104-9.

25. **Brown, J. S., and D. W. Holden.** 2002. Iron acquisition by Gram-positive bacterial pathogens. Microbes Infect **4:**1149-56.

26. **Buchanan, S. K., B. S. Smith, L. Venkatramani, D. Xia, L. Esser, M. Palnitkar, R. Chakraborty, D. van der Helm, and J. Deisenhofer.** 1999. Crystal structure of the outer membrane active transporter FepA from Escherichia coli. Nat Struct Biol **6:**56-63.

27. **Buist, G., A. Steen, J. Kok, and O. P. Kuipers.** 2008. LysM, a widely distributed protein motif for binding to (peptido)glycans. Mol Microbiol **68:**838-47.

28. **Burkhard, K. A., and A. Wilks.** 2007. Characterization of the outer membrane receptor ShuA from the heme uptake system of Shigella dysenteriae. Substrate specificity and identification of the heme protein ligands. J Biol Chem **282:**15126-36.

29. **Burkhard, K. A., and A. Wilks.** 2008. Functional characterization of the Shigella dysenteriae heme ABC transporter. Biochemistry **47:**7977-9.

30. **Camilli, A., A. Portnoy, and P. Youngman.** 1990. Insertional mutagenesis of Listeria monocytogenes with a novel Tn917 derivative that allows direct cloning of DNA flanking transposon insertions. J Bacteriol **172:**3738-44.

31. **Cao, Z., P. Warfel, S. M. Newton, and P. E. Klebba.** 2003. Spectroscopic observations of ferric enterobactin transport. J Biol Chem **278:**1022-8.

32. **Carniel, E.** 2001. The Yersinia high-pathogenicity island: an iron-uptake island. Microbes Infect **3:**561-9.

33. **Cescau, S., H. Cwerman, S. Letoffe, P. Delepelaire, C. Wandersman, and F. Biville.** 2007. Heme acquisition by hemophores. Biometals **20:**603-13.

34. **Chakraborty, R., E. Storey, and D. van der Helm.** 2007. Molecular mechanism of ferricsiderophore passage through the outer membrane receptor proteins of Escherichia coli. Biometals **20:**263-74.

35. **Chakraborty, T., M. Leimeister-Wachter, E. Domann, M. Hartl, W. Goebel, T. Nichterlein, and S. Notermans.** 1992. Coordinate regulation of virulence genes in Listeria monocytogenes requires the product of the prfA gene. J Bacteriol **174:**568-74.

36. **Chang, C., A. Mooser, A. Pluckthun, and A. Wlodawer.** 2001. Crystal structure of the dimeric C-terminal domain of TonB reveals a novel fold. J Biol Chem **276:**27535-40.

37. **Collier, G. S., J. M. Pratt, C. R. De Wet, and C. F. Tshabalala.** 1979. Studies on haemin in dimethyl sulphoxide/water mixtures. Biochem J

179:281-9.

38. **Comfort, D., and R. T. Clubb.** 2004. A comparative genome analysis identifies distinct sorting pathways in gram-positive bacteria. Infect Immun **72:**2710-22.

39. **Conte, M. P., C. Longhi, M. Polidoro, G. Petrone, V. Buonfiglio, S. Di Santo, E. Papi, L. Seganti, P. Visca, and P. Valenti.** 1996. Iron availability affects entry of Listeria monocytogenes into the enterocytelike cell line Caco-2. Infect Immun **64:**3925-9.

40. **Cowart, R. E., and B. G. Foster.** 1985. Differential effects of iron on the growth of Listeria monocytogenes: minimum requirements and mechanism of acquisition. J Infect Dis **151:**721-30.

41. **Dabiri, G. A., J. M. Sanger, D. A. Portnoy, and F. S. Southwick.** 1990. Listeria monocytogenes moves rapidly through the host-cell cytoplasm by inducing directional actin assembly. Proc Natl Acad Sci U S A **87:**6068-72.

42. **Datsenko, K. A., and B. L. Wanner.** 2000. One-step inactivation of chromosomal genes in Escherichia coli K-12 using PCR products. Proc Natl Acad Sci U S A **97:**6640-5.

43. **Davidson, A. L., and J. Chen.** 2004. ATP-binding cassette transporters in bacteria. Annu Rev Biochem **73:**241-68.

44. **Dawson, R. J., K. Hollenstein, and K. P. Locher.** 2007. Uptake or extrusion: crystal structures of full ABC transporters suggest a common mechanism. Mol Microbiol **65:**250-7.

45. **Dawson, R. J., and K. P. Locher.** 2006. Structure of a bacterial multidrug ABC transporter. Nature **443:**180-5.

46. **Dawson, R. J., and K. P. Locher.** 2007. Structure of the multidrug ABC transporter Sav1866 from Staphylococcus aureus in complex with AMP-PNP. FEBS Lett **581:**935-8.

47. **di Guan, C., P. Li, P. D. Riggs, and H. Inouye.** 1988. Vectors that

facilitate the expression and purification of foreign peptides in Escherichia coli by fusion to maltose-binding protein. Gene **67:**21-30.

48. **Domann, E., J. Wehland, M. Rohde, S. Pistor, M. Hartl, W. Goebel, M. Leimeister-Wachter, M. Wuenscher, and T. Chakraborty.** 1992. A novel bacterial virulence gene in Listeria monocytogenes required for host cell microfilament interaction with homology to the proline-rich region of vinculin. EMBO J **11:**1981-90.

49. **Eakanunkul, S., G. S. Lukat-Rodgers, S. Sumithran, A. Ghosh, K. R. Rodgers, J. H. Dawson, and A. Wilks.** 2005. Characterization of the periplasmic heme-binding protein shut from the heme uptake system of Shigella dysenteriae. Biochemistry **44:**13179-91.

50. **Escolar, L., J. Perez-Martin, and V. de Lorenzo.** 1999. Opening the iron box: transcriptional metalloregulation by the Fur protein. J Bacteriol **181:**6223-9.

51. **Evans, J. S., B. A. Levine, I. P. Trayer, C. J. Dorman, and C. F. Higgins.** 1986. Sequence-imposed structural constraints in the TonB protein of E. coli. FEBS Lett **208:**211-6.

52. **Falk, J. E.** 1964. Porphyrins and Metalloporphyrins. American Elsevier Publishing Company, INC., New York.

53. **Farber, J. M., and P. I. Peterkin.** 1991. Listeria monocytogenes, a food-borne pathogen. Microbiol Rev **55:**476-511.

54. **Ferenci, T., and U. Klotz.** 1978. Affinity chromatographic isolation of the periplasmic maltose binding protein of Escherichia coli. FEBS Lett **94:**213-7.

55. **Ferguson, A. D., R. Chakraborty, B. S. Smith, L. Esser, D. van der Helm, and J. Deisenhofer.** 2002. Structural basis of gating by the outer membrane transporter FecA. Science **295:**1715-9.

56. **Ferguson, A. D., E. Hofmann, J. W. Coulton, K. Diederichs, and W. Welte.** 1998. Siderophore-mediated iron transport: crystal structure of FhuA with bound lipopolysaccharide. Science **282:**2215-20.

57. **Fisher, C. W., and S. E. Martin.** 1999. Effects of iron and selenium on the production of catalase, superoxide dismutase, and listeriolysin O in Listeria monocytogenes. J Food Prot **62:**1206-9.

58. **Follett, J. R., Y. A. Suzuki, and B. Lonnerdal.** 2002. High specific activity heme-Fe and its application for studying heme-Fe metabolism in Caco-2 cell monolayers. Am J Physiol Gastrointest Liver Physiol **283:**G1125-31.

59. **Friedman, M. E., and W. G. Roessler.** 1961. Growth of Listeria monocytogenes in defined media. J Bacteriol **82:**528-33.

60. **Garibaldi, J. A., and J. B. Neilands.** 1955. Isolation and Properties of Ferrichrome-A. Journal of the American Chemical Society **77:**2429-2430.

61. **Garvey, K. J., M. S. Saedi, and J. Ito.** 1986. Nucleotide sequence of Bacillus phage phi 29 genes 14 and 15: homology of gene 15 with other phage lysozymes. Nucleic Acids Res **14:**10001-8.

62. **Gat, O., G. Zaide, I. Inbar, H. Grosfeld, T. Chitlaru, H. Levy, and A. Shafferman.** 2008. Characterization of Bacillus anthracis iron-regulated surface determinant (Isd) proteins containing NEAT domains. Mol Microbiol **70:**983-99.

63. **Gedde, M. M., D. E. Higgins, L. G. Tilney, and D. A. Portnoy.** 2000. Role of listeriolysin O in cell-to-cell spread of Listeria monocytogenes. Infect Immun **68:**999-1003.

64. **Geoffroy, C., J. L. Gaillard, J. E. Alouf, and P. Berche.** 1987. Purification, characterization, and toxicity of the sulfhydryl-activated hemolysin listeriolysin O from Listeria monocytogenes. Infect Immun **55:**1641-6.

65. **Ghigo, J. M., S. Letoffe, and C. Wandersman.** 1997. A new type of hemophore-dependent heme acquisition system of Serratia marcescens reconstituted in Escherichia coli. J Bacteriol **179:**3572-9.

66. **Ghuysen, J. M., D. J. Tipper, and J. L. Strominger.** 1965. Structure of

the Cell Wall of Staphylococcus Aureus, Strain Copenhagen. Iv. The Teichoic Acid-Glycopeptide Complex. Biochemistry **4:**474-85.

67. **Glaser, P., L. Frangeul, C. Buchrieser, C. Rusniok, A. Amend, F. Baquero, P. Berche, H. Bloecker, P. Brandt, T. Chakraborty, A. Charbit, F. Chetouani, E. Couve, A. de Daruvar, P. Dehoux, E. Domann, G. Dominguez-Bernal, E. Duchaud, L. Durant, O. Dussurget, K. D. Entian, H. Fsihi, F. Garcia-del Portillo, P. Garrido, L. Gautier, W. Goebel, N. Gomez-Lopez, T. Hain, J. Hauf, D. Jackson, L. M. Jones, U. Kaerst, J. Kreft, M. Kuhn, F. Kunst, G. Kurapkat, E. Madueno, A. Maitournam, J. M. Vicente, E. Ng, H. Nedjari, G. Nordsiek, S. Novella, B. de Pablos, J. C. Perez-Diaz, R. Purcell, B. Remmel, M. Rose, T. Schlueter, N. Simoes, A. Tierrez, J. A. Vazquez-Boland, H. Voss, J. Wehland, and P. Cossart.** 2001. Comparative genomics of Listeria species. Science **294:**849-52.

68. **Glauner, B.** 1988. Separation and quantification of muropeptides with high-performance liquid chromatography. Anal Biochem **172:**451-64.

69. **Grigg, J. C., C. L. Vermeiren, D. E. Heinrichs, and M. E. Murphy.** 2007. Heme coordination by Staphylococcus aureus IsdE. J Biol Chem **282:**28815-22.

70. **Hamon, M., H. Bierne, and P. Cossart.** 2006. Listeria monocytogenes: a multifaceted model. Nat Rev Microbiol **4:**423-34.

71. **Hanahan, D.** 1983. Studies on transformation of Escherichia coli with plasmids. J Mol Biol **166:**557-80.

72. **Hanson, M. S., S. E. Pelzel, J. Latimer, U. Muller-Eberhard, and E. J. Hansen.** 1992. Identification of a genetic locus of Haemophilus influenzae type b necessary for the binding and utilization of heme bound to human hemopexin. Proc Natl Acad Sci U S A **89:**1973-7.

73. **Hantke, K.** 2001. Iron and metal regulation in bacteria. Curr Opin Microbiol **4:**172-7.

74. **Henderson, D. P., and S. M. Payne.** 1994. Characterization of the Vibrio cholerae outer membrane heme transport protein HutA: sequence of the gene, regulation of expression, and homology to the family of

TonB-dependent proteins. J Bacteriol **176:**3269-77.

75. **Higgins, C. F., and K. J. Linton.** 2004. The ATP switch model for ABC transporters. Nat Struct Mol Biol **11:**918-26.

76. **Ho, W. W., H. Li, S. Eakanunkul, Y. Tong, A. Wilks, M. Guo, and T. L. Poulos.** 2007. Holo- and apo-bound structures of bacterial periplasmic heme-binding proteins. J Biol Chem **282:**35796-802.

77. **Hoette, T. M., R. J. Abergel, J. Xu, R. K. Strong, and K. N. Raymond.** 2008. The role of electrostatics in siderophore recognition by the immunoprotein Siderocalin. J Am Chem Soc **130:**17584-92.

78. **Hollenstein, K., R. J. Dawson, and K. P. Locher.** 2007. Structure and mechanism of ABC transporter proteins. Curr Opin Struct Biol **17:**412-8.

79. **Hollenstein, K., D. C. Frei, and K. P. Locher.** 2007. Structure of an ABC transporter in complex with its binding protein. Nature **446:**213-6.

80. **Izadi, N., Y. Henry, J. Haladjian, M. E. Goldberg, C. Wandersman, M. Delepierre, and A. Lecroisey.** 1997. Purification and characterization of an extracellular heme-binding protein, HasA, involved in heme iron acquisition. Biochemistry **36:**7050-7.

81. **Jacquamet, L., D. Aberdam, A. Adrait, J. L. Hazemann, J. M. Latour, and I. Michaud-Soret.** 1998. X-ray absorption spectroscopy of a new zinc site in the fur protein from Escherichia coli. Biochemistry **37:**2564-71.

82. **Jeney, V., J. Balla, A. Yachie, Z. Varga, G. M. Vercellotti, J. W. Eaton, and G. Balla.** 2002. Pro-oxidant and cytotoxic effects of circulating heme. Blood **100:**879-87.

83. **Jiang, X., M. A. Payne, Z. Cao, S. B. Foster, J. B. Feix, S. M. Newton, and P. E. Klebba.** 1997. Ligand-specific opening of a gated-porin channel in the outer membrane of living bacteria. Science **276:**1261-4.

84. **Jin, B., S. M. Newton, Y. Shao, X. Jiang, A. Charbit, and P. E. Klebba.** 2006. Iron acquisition systems for ferric hydroxamates, haemin

and haemoglobin in Listeria monocytogenes. Mol Microbiol **59:**1185-98.

85. **Johansson, J., P. Mandin, A. Renzoni, C. Chiaruttini, M. Springer, and P. Cossart.** 2002. An RNA thermosensor controls expression of virulence genes in Listeria monocytogenes. Cell **110:**551-61.

86. **Kaserer, W. A., X. Jiang, Q. Xiao, D. C. Scott, M. Bauler, D. Copeland, S. M. Newton, and P. E. Klebba.** 2008. Insight from TonB hybrid proteins into the mechanism of iron transport through the outer membrane. J Bacteriol **190:**4001-16.

87. **Kenney, C. D., and C. N. Cornelissen.** 2002. Demonstration and characterization of a specific interaction between gonococcal transferrin binding protein A and TonB. J Bacteriol **184:**6138-45.

88. **Klebba, P. E., M. A. McIntosh, and J. B. Neilands.** 1982. Kinetics of biosynthesis of iron-regulated membrane proteins in Escherichia coli. J Bacteriol **149:**880-8.

89. **Kodding, J., F. Killig, P. Polzer, S. P. Howard, K. Diederichs, and W. Welte.** 2005. Crystal structure of a 92-residue C-terminal fragment of TonB from Escherichia coli reveals significant conformational changes compared to structures of smaller TonB fragments. J Biol Chem **280:**3022-8.

90. **Koppisch, A. T., C. C. Browder, A. L. Moe, J. T. Shelley, B. A. Kinkel, L. E. Hersman, S. Iyer, and C. E. Ruggiero.** 2005. Petrobactin is the primary siderophore synthesized by Bacillus anthracis str. Sterne under conditions of iron starvation. Biometals **18:**577-85.

91. **Lauer, P., M. Y. Chow, M. J. Loessner, D. A. Portnoy, and R. Calendar.** 2002. Construction, characterization, and use of two Listeria monocytogenes site-specific phage integration vectors. J Bacteriol **184:**4177-86.

92. **Lee, H. S., A. H. Abdelal, M. A. Clark, and J. L. Ingraham.** 1991. Molecular characterization of nosA, a Pseudomonas stutzeri gene encoding an outer membrane protein required to make copper-containing N2O reductase. J Bacteriol **173:**5406-13.

93. **Lee, W. C., M. L. Reniere, E. P. Skaar, and M. E. Murphy.** 2008. Ruffling of metalloporphyrins bound to IsdG and IsdI, two heme-degrading enzymes in Staphylococcus aureus. J Biol Chem **283:**30957-63.

94. **Letoffe, S., C. Deniau, N. Wolff, E. Dassa, P. Delepelaire, A. Lecroisey, and C. Wandersman.** 2001. Haemophore-mediated bacterial haem transport: evidence for a common or overlapping site for haem-free and haem-loaded haemophore on its specific outer membrane receptor. Mol Microbiol **41:**439-50.

95. **Letoffe, S., F. Nato, M. E. Goldberg, and C. Wandersman.** 1999. Interactions of HasA, a bacterial haemophore, with haemoglobin and with its outer membrane receptor HasR. Mol Microbiol **33:**546-55.

96. **Lim, J. H., M. S. Kim, H. E. Kim, T. Yano, Y. Oshima, K. Aggarwal, W. E. Goldman, N. Silverman, S. Kurata, and B. H. Oh.** 2006. Structural basis for preferential recognition of diaminopimelic acid-type peptidoglycan by a subset of peptidoglycan recognition proteins. J Biol Chem **281:**8286-95.

97. **Liu, J., J. M. Rutz, P. E. Klebba, and J. B. Feix.** 1994. A site-directed spin-labeling study of ligand-induced conformational change in the ferric enterobactin receptor, FepA. Biochemistry **33:**13274-83.

98. **Liu, M., and B. Lei.** 2005. Heme transfer from streptococcal cell surface protein Shp to HtsA of transporter HtsABC. Infect Immun **73:**5086-92.

99. **Lo, R. Y.** 2001. Genetic analysis of virulence factors of Mannheimia (Pasteurella) haemolytica A1. Vet Microbiol **83:**23-35.

100. **Locher, K. P., A. T. Lee, and D. C. Rees.** 2002. The E. coli BtuCD structure: a framework for ABC transporter architecture and mechanism. Science **296:**1091-8.

101. **Lowry, O. H., N. J. Rosebrough, A. L. Farr, and R. J. Randall.** 1951. Protein measurement with the Folin phenol reagent. J Biol Chem **193:**265-75.

102. **Ma, L., W. Kaserer, R. Annamalai, D. C. Scott, B. Jin, X. Jiang, Q. Xiao, H. Maymani, L. M. Massis, L. C. Ferreira, S. M. Newton, and P. E. Klebba.** 2007. Evidence of ball-and-chain transport of ferric enterobactin through FepA. J Biol Chem **282:**397-406.

103. **Maresso, A. W., T. J. Chapa, and O. Schneewind.** 2006. Surface protein IsdC and Sortase B are required for heme-iron scavenging of Bacillus anthracis. J Bacteriol **188:**8145-52.

104. **Marraffini, L. A., A. C. Dedent, and O. Schneewind.** 2006. Sortases and the art of anchoring proteins to the envelopes of gram-positive bacteria. Microbiol Mol Biol Rev **70:**192-221.

105. **Marraffini, L. A., and O. Schneewind.** 2005. Anchor structure of staphylococcal surface proteins. V. Anchor structure of the sortase B substrate IsdC. J Biol Chem **280:**16263-71.

106. **Mazmanian, S. K., E. P. Skaar, A. H. Gaspar, M. Humayun, P. Gornicki, J. Jelenska, A. Joachmiak, D. M. Missiakas, and O. Schneewind.** 2003. Passage of heme-iron across the envelope of Staphylococcus aureus. Science **299:**906-9.

107. **Mazmanian, S. K., H. Ton-That, K. Su, and O. Schneewind.** 2002. An iron-regulated sortase anchors a class of surface protein during Staphylococcus aureus pathogenesis. Proc Natl Acad Sci U S A **99:**2293-8.

108. **Miroux, B., and J. E. Walker.** 1996. Over-production of proteins in Escherichia coli: mutant hosts that allow synthesis of some membrane proteins and globular proteins at high levels. J Mol Biol **260:**289-98.

109. **Montanez, G. E., M. N. Neely, and Z. Eichenbaum.** 2005. The streptococcal iron uptake (Siu) transporter is required for iron uptake and virulence in a zebrafish infection model. Microbiology **151:**3749-57.

110. **Moore, C. M., and J. D. Helmann.** 2005. Metal ion homeostasis in Bacillus subtilis. Curr Opin Microbiol **8:**188-95.

111. **Navarre, W. W., and O. Schneewind.** 1999. Surface proteins of

gram-positive bacteria and mechanisms of their targeting to the cell wall envelope. Microbiol Mol Biol Rev **63:**174-229.

112. **Neidhardt, F. C., P. L. Bloch, and D. F. Smith.** 1974. Culture medium for enterobacteria. J Bacteriol **119:**736-47.

113. **Neilands, J. B.** 1981. Microbial iron compounds. Annu Rev Biochem **50:**715-31.

114. **Neilands, J. B.** 1995. Siderophores: structure and function of microbial iron transport compounds. J Biol Chem **270:**26723-6.

115. **Neugebauer, H., C. Herrmann, W. Kammer, G. Schwarz, A. Nordheim, and V. Braun.** 2005. ExbBD-dependent transport of maltodextrins through the novel MalA protein across the outer membrane of Caulobacter crescentus. J Bacteriol **187:**8300-11.

116. **Newton, S. M., J. S. Allen, Z. Cao, Z. Qi, X. Jiang, C. Sprencel, J. D. Igo, S. B. Foster, M. A. Payne, and P. E. Klebba.** 1997. Double mutagenesis of a positive charge cluster in the ligand-binding site of the ferric enterobactin receptor, FepA. Proc Natl Acad Sci U S A **94:**4560-5.

117. **Newton, S. M., J. D. Igo, D. C. Scott, and P. E. Klebba.** 1999. Effect of loop deletions on the binding and transport of ferric enterobactin by FepA. Mol Microbiol **32:**1153-65.

118. **Newton, S. M., P. E. Klebba, C. Raynaud, Y. Shao, X. Jiang, I. Dubail, C. Archer, C. Frehel, and A. Charbit.** 2005. The svpA-srtB locus of Listeria monocytogenes: fur-mediated iron regulation and effect on virulence. Mol Microbiol **55:**927-40.

119. **Occhino, D. A., E. E. Wyckoff, D. P. Henderson, T. J. Wrona, and S. M. Payne.** 1998. Vibrio cholerae iron transport: haem transport genes are linked to one of two sets of tonB, exbB, exbD genes. Mol Microbiol **29:**1493-507.

120. **Ochsner, U. A., Z. Johnson, and M. L. Vasil.** 2000. Genetics and regulation of two distinct haem-uptake systems, phu and has, in Pseudomonas aeruginosa. Microbiology **146 (Pt 1):**185-98.

121. **Ollinger, J., K. B. Song, H. Antelmann, M. Hecker, and J. D. Helmann.** 2006. Role of the Fur regulon in iron transport in Bacillus subtilis. J Bacteriol **188:**3664-73.

122. **Pallen, M. J., A. C. Lam, M. Antonio, and K. Dunbar.** 2001. An embarrassment of sortases - a richness of substrates? Trends Microbiol **9:**97-102.

123. **Pawelek, P. D., N. Croteau, C. Ng-Thow-Hing, C. M. Khursigara, N. Moiseeva, M. Allaire, and J. W. Coulton.** 2006. Structure of TonB in complex with FhuA, E. coli outer membrane receptor. Science **312:**1399-402.

124. **Perry, A. M., H. Ton-That, S. K. Mazmanian, and O. Schneewind.** 2002. Anchoring of surface proteins to the cell wall of Staphylococcus aureus. III. Lipid II is an in vivo peptidoglycan substrate for sortase-catalyzed surface protein anchoring. J Biol Chem **277:**16241-8.

125. **Phillips, J. N.** 1963. Comprehensive Biochemistry, vol. 9. Elsevier, Amsterdam.

126. **Pinkett, H. W., A. T. Lee, P. Lum, K. P. Locher, and D. C. Rees.** 2007. An inward-facing conformation of a putative metal-chelate-type ABC transporter. Science **315:**373-7.

127. **Pohl, E., R. K. Holmes, and W. G. Hol.** 1999. Crystal structure of the iron-dependent regulator (IdeR) from Mycobacterium tuberculosis shows both metal binding sites fully occupied. J Mol Biol **285:**1145-56.

128. **Ponka, P.** 1997. Tissue-specific regulation of iron metabolism and heme synthesis: distinct control mechanisms in erythroid cells. Blood **89:**1-25.

129. **Portnoy, D. A., T. Chakraborty, W. Goebel, and P. Cossart.** 1992. Molecular determinants of Listeria monocytogenes pathogenesis. Infect Immun **60:**1263-7.

130. **Postle, K., and R. F. Good.** 1983. DNA sequence of the Escherichia coli tonB gene. Proc Natl Acad Sci U S A **80:**5235-9.

131. **Postle, K., and R. J. Kadner.** 2003. Touch and go: tying TonB to transport. Mol Microbiol **49:**869-82.

132. **Poyart, C., and P. Trieu-Cuot.** 1997. A broad-host-range mobilizable shuttle vector for the construction of transcriptional fusions to beta-galactosidase in gram-positive bacteria. FEMS Microbiol Lett **156:**193-8.

133. **Premaratne, R. J., W. J. Lin, and E. A. Johnson.** 1991. Development of an improved chemically defined minimal medium for Listeria monocytogenes. Appl Environ Microbiol **57:**3046-8.

134. **Rabsch, W., L. Ma, G. Wiley, F. Z. Najar, W. Kaserer, D. W. Schuerch, J. E. Klebba, B. A. Roe, J. A. Laverde Gomez, M. Schallmey, S. M. Newton, and P. E. Klebba.** 2007. FepA- and TonB-dependent bacteriophage H8: receptor binding and genomic sequence. J Bacteriol **189:**5658-74.

135. **Ran, Y., H. Zhu, M. Liu, M. Fabian, J. S. Olson, R. t. Aranda, G. N. Phillips, Jr., D. M. Dooley, and B. Lei.** 2007. Bis-methionine ligation to heme iron in the streptococcal cell surface protein Shp facilitates rapid hemin transfer to HtsA of the HtsABC transporter. J Biol Chem **282:**31380-8.

136. **Raymond, K. N., E. A. Dertz, and S. S. Kim.** 2003. Enterobactin: an archetype for microbial iron transport. Proc Natl Acad Sci U S A **100:**3584-8.

137. **Reniere, M. L., V. J. Torres, and E. P. Skaar.** 2007. Intracellular metalloporphyrin metabolism in Staphylococcus aureus. Biometals **20:**333-45.

138. **Rodionov, D. A., P. Hebbeln, M. S. Gelfand, and T. Eitinger.** 2006. Comparative and functional genomic analysis of prokaryotic nickel and cobalt uptake transporters: evidence for a novel group of ATP-binding cassette transporters. J Bacteriol **188:**317-27.

139. **Rodionov, D. A., A. G. Vitreschak, A. A. Mironov, and M. S. Gelfand.** 2002. Comparative genomics of thiamin biosynthesis in procaryotes. New genes and regulatory mechanisms. J Biol Chem **277:**48949-59.

140. **Rutz, J. M., J. Liu, J. A. Lyons, J. Goranson, S. K. Armstrong, M. A. McIntosh, J. B. Feix, and P. E. Klebba.** 1992. Formation of a gated channel by a ligand-specific transport protein in the bacterial outer membrane. Science **258:**471-5.

141. **Ruzin, A., A. Severin, F. Ritacco, K. Tabei, G. Singh, P. A. Bradford, M. M. Siegel, S. J. Projan, and D. M. Shlaes.** 2002. Further evidence that a cell wall precursor [C(55)-MurNAc-(peptide)-GlcNAc] serves as an acceptor in a sorting reaction. J Bacteriol **184:**2141-7.

142. **Ryoo, B. Y., Na, II, S. H. Yang, J. S. Koh, C. H. Kim, and J. C. Lee.** 2006. Synchronous multiple primary lung cancers with different response to gefitinib. Lung Cancer **53:**245-8.

143. **Ryter, S. W., and R. M. Tyrrell.** 2000. The heme synthesis and degradation pathways: role in oxidant sensitivity. Heme oxygenase has both pro- and antioxidant properties. Free Radic Biol Med **28:**289-309.

144. **Schauer, K., B. Gouget, M. Carriere, A. Labigne, and H. de Reuse.** 2007. Novel nickel transport mechanism across the bacterial outer membrane energized by the TonB/ExbB/ExbD machinery. Mol Microbiol **63:**1054-68.

145. **Schauer, K., D. A. Rodionov, and H. de Reuse.** 2008. New substrates for TonB-dependent transport: do we only see the 'tip of the iceberg'? Trends Biochem Sci **33:**330-8.

146. **Schleifer, K. H., and O. Kandler.** 1972. Peptidoglycan types of bacterial cell walls and their taxonomic implications. Bacteriol Rev **36:**407-77.

147. **Schmitt, M. P., and E. S. Drazek.** 2001. Construction and consequences of directed mutations affecting the hemin receptor in pathogenic Corynebacterium species. J Bacteriol **183:**1476-81.

148. **Schneewind, O., D. Mihaylova-Petkov, and P. Model.** 1993. Cell wall sorting signals in surface proteins of gram-positive bacteria. EMBO J **12:**4803-11.

149. **Schneider, E., and S. Hunke.** 1998. ATP-binding-cassette (ABC) transport systems: functional and structural aspects of the ATP-hydrolyzing subunits/domains. FEMS Microbiol Rev **22:**1-20.

150. **Schneider, R., and K. Hantke.** 1993. Iron-hydroxamate uptake systems in Bacillus subtilis: identification of a lipoprotein as part of a binding protein-dependent transport system. Mol Microbiol **8:**111-21.

151. **Schuerch, D. W., E. M. Wilson-Kubalek, and R. K. Tweten.** 2005. Molecular basis of listeriolysin O pH dependence. Proc Natl Acad Sci U S A **102:**12537-42.

152. **Scott, D. C., S. M. Newton, and P. E. Klebba.** 2002. Surface loop motion in FepA. J Bacteriol **184:**4906-11.

153. **Sean Peacock, R., A. M. Weljie, S. Peter Howard, F. D. Price, and H. J. Vogel.** 2005. The solution structure of the C-terminal domain of TonB and interaction studies with TonB box peptides. J Mol Biol **345:**1185-97.

154. **Sharp, K. H., S. Schneider, A. Cockayne, and M. Paoli.** 2007. Crystal structure of the heme-IsdC complex, the central conduit of the Isd iron/heme uptake system in Staphylococcus aureus. J Biol Chem **282:**10625-31.

155. **Shultis, D. D., M. D. Purdy, C. N. Banchs, and M. C. Wiener.** 2006. Outer membrane active transport: structure of the BtuB:TonB complex. Science **312:**1396-9.

156. **Siburt C. J. P., R. P. L., Weaver K. D., Noto J. M., Mietzner T. M., Cornelissen C. N., Fitzgerald M. C. and Crumbliss A.L.** 2009. Hijacking transferrin bound iron: protein–receptor interactions involved in iron transport in N. gonorrhoeae. Metallomics **1:**249.

157. **Silver, J., and B. Lukas.** 1983. Mossbauer Studies on Protoporphyrin-Ix Iron(Ii) Solutions. Inorganica Chimica Acta-Bioinorganic Chemistry **80:**107-113.

158. **Sinclair, P. R., Gorman, N., and Jacobs, J.M.** 1999. Current Protocols in Toxicology 8.3.1-8.3.7. John Wiley & Sons, Inc.

159. **Skaar, E. P., M. Humayun, T. Bae, K. L. DeBord, and O. Schneewind.** 2004. Iron-source preference of Staphylococcus aureus infections. Science **305:**1626-8.

160. **Skoble, J., D. A. Portnoy, and M. D. Welch.** 2000. Three regions within ActA promote Arp2/3 complex-mediated actin nucleation and Listeria monocytogenes motility. J Cell Biol **150:**527-38.

161. **Smallwood, C. R., A. G. Marco, Q. Xiao, V. Trinh, S. M. Newton, and P. E. Klebba.** 2009. Fluoresceination of FepA during colicin B killing: effects of temperature, toxin and TonB. Mol Microbiol **72:**1171-80.

162. **Smith, G. A., and D. A. Portnoy.** 1997. How the Listeria monocytogenes ActA protein converts actin polymerization into a motile force. Trends Microbiol **5:**272-6.

163. **Smith, K., and P. Youngman.** 1992. Use of a new integrational vector to investigate compartment-specific expression of the Bacillus subtilis spoIIM gene. Biochimie **74:**705-11.

164. **Sook, B. R., D. R. Block, S. Sumithran, G. E. Montanez, K. R. Rodgers, J. H. Dawson, Z. Eichenbaum, and D. W. Dixon.** 2008. Characterization of SiaA, a streptococcal heme-binding protein associated with a heme ABC transport system. Biochemistry **47:**2678-88.

165. **Stojiljkovic, I., and K. Hantke.** 1992. Hemin uptake system of Yersinia enterocolitica: similarities with other TonB-dependent systems in gram-negative bacteria. EMBO J **11:**4359-67.

166. **Stojiljkovic, I., J. Larson, V. Hwa, S. Anic, and M. So.** 1996. HmbR outer membrane receptors of pathogenic Neisseria spp.: iron-regulated, hemoglobin-binding proteins with a high level of primary structure conservation. J Bacteriol **178:**4670-8.

167. **Stork, M., M. Di Lorenzo, S. Mourino, C. R. Osorio, M. L. Lemos, and J. H. Crosa.** 2004. Two tonB systems function in iron transport in Vibrio anguillarum, but only one is essential for virulence. Infect Immun **72:**7326-9.

168. **Strominger, J. L., and J. M. Ghuysen.** 1967. Mechanisms of enzymatic bacteriaolysis. Cell walls of bacteri are solubilized by action of either specific carbohydrases or specific peptidases. Science **156:**213-21.

169. **Suits, M. D., N. Jaffer, and Z. Jia.** 2006. Structure of the Escherichia coli O157:H7 heme oxygenase ChuS in complex with heme and enzymatic inactivation by mutation of the heme coordinating residue His-193. J Biol Chem **281:**36776-82.

170. **Szmelcman, S., J. M. Clement, M. Jehanno, O. Schwartz, L. Montagnier, and M. Hofnung.** 1990. Export and one-step purification from Escherichia coli of a MalE-CD4 hybrid protein that neutralizes HIV in vitro. J Acquir Immune Defic Syndr **3:**859-72.

171. **Thompson, J. M., H. A. Jones, and R. D. Perry.** 1999. Molecular characterization of the hemin uptake locus (hmu) from Yersinia pestis and analysis of hmu mutants for hemin and hemoprotein utilization. Infect Immun **67:**3879-92.

172. **Thulasiraman, P., S. M. Newton, J. Xu, K. N. Raymond, C. Mai, A. Hall, M. A. Montague, and P. E. Klebba.** 1998. Selectivity of ferric enterobactin binding and cooperativity of transport in gram-negative bacteria. J Bacteriol **180:**6689-96.

173. **Tilney, L. G., and D. A. Portnoy.** 1989. Actin filaments and the growth, movement, and spread of the intracellular bacterial parasite, Listeria monocytogenes. J Cell Biol **109:**1597-608.

174. **Tipper, D. J., and J. L. Strominger.** 1968. Biosynthesis of the peptidoglycan of bacterial cell walls. XII. Inhibition of cross-linking by penicillins and cephalosporins: studies in Staphylococcus aureus in vivo. J Biol Chem **243:**3169-79.

175. **Ton-That, H., G. Liu, S. K. Mazmanian, K. F. Faull, and O. Schneewind.** 1999. Purification and characterization of sortase, the transpeptidase that cleaves surface proteins of Staphylococcus aureus at the LPXTG motif. Proc Natl Acad Sci U S A **96:**12424-9.

176. **Tong, Y., and M. Guo.** 2009. Bacterial heme-transport proteins and their heme-coordination modes. Arch Biochem Biophys **481:**1-15.

177. **Tong, Y., and M. Guo.** 2007. Cloning and characterization of a novel periplasmic heme-transport protein from the human pathogen Pseudomonas aeruginosa. J Biol Inorg Chem **12:**735-50.

178. **Towbin, H., T. Staehelin, and J. Gordon.** 1979. Electrophoretic transfer of proteins from polyacrylamide gels to nitrocellulose sheets: procedure and some applications. Proc Natl Acad Sci U S A **76:**4350-4.

179. **Trieu-Cuot, P., C. Carlier, C. Poyart-Salmeron, and P. Courvalin.** 1991. An integrative vector exploiting the transposition properties of Tn1545 for insertional mutagenesis and cloning of genes from gram-positive bacteria. Gene **106:**21-7.

180. **Tsai, H. N., and D. A. Hodgson.** 2003. Development of a synthetic minimal medium for Listeria monocytogenes. Appl Environ Microbiol **69:**6943-5.

181. **Ursinus, A., F. van den Ent, S. Brechtel, M. de Pedro, J. V. Holtje, J. Lowe, and W. Vollmer.** 2004. Murein (peptidoglycan) binding property of the essential cell division protein FtsN from Escherichia coli. J Bacteriol **186:**6728-37.

182. **Vazquez-Boland, J. A., G. Dominguez-Bernal, B. Gonzalez-Zorn, J. Kreft, and W. Goebel.** 2001. Pathogenicity islands and virulence evolution in Listeria. Microbes Infect **3:**571-84.

183. **Vercellotti, G. M., G. Balla, J. Balla, K. Nath, J. W. Eaton, and H. S. Jacob.** 1994. Heme and the vasculature: an oxidative hazard that induces antioxidant defenses in the endothelium. Artif Cells Blood Substit Immobil Biotechnol **22:**207-13.

184. **Walker, F. A., Balke, V. L., McDermott, G. A.** 1982. Models of the cytochromes b. 2. Effect of unsymmetrical phenyl substitution on pyrrole proton shifts of a series of low-spin (tetraphenylporphinato)iron(III) bis(N-methylimidazole) complexes. J. Am. Chem. Soc. **104:**1569-1574.

185. **Wandersman, C., and P. Delepelaire.** 2004. Bacterial iron sources: from siderophores to hemophores. Annu Rev Microbiol **58:**611-47.

186. **Ward, P. P., and O. M. Conneely.** 2004. Lactoferrin: role in iron homeostasis and host defense against microbial infection. Biometals **17:**203-8.

187. **Waterhouse, A. M., J. B. Procter, D. M. Martin, M. Clamp, and G. J. Barton.** 2009. Jalview Version 2--a multiple sequence alignment editor and analysis workbench. Bioinformatics **25:**1189-91.

188. **Wayne, R., K. Frick, and J. B. Neilands.** 1976. Siderophore protection against colicins M, B, V, and Ia in Escherichia coli. J Bacteriol **126:**7-12.

189. **Wejman, J. C., D. Hovsepian, J. S. Wall, J. F. Hainfeld, and J. Greer.** 1984. Structure of haptoglobin and the haptoglobin-hemoglobin complex by electron microscopy. J Mol Biol **174:**319-41.

190. **Welshimer, H. J.** 1963. Vitamin Requirements of Listeria Monocytogenes. J Bacteriol **85:**1156-9.

191. **Wilson, M. K., R. J. Abergel, K. N. Raymond, J. E. Arceneaux, and B. R. Byers.** 2006. Siderophores of Bacillus anthracis, Bacillus cereus, and Bacillus thuringiensis. Biochem Biophys Res Commun **348:**320-5.

192. **Wu, R., E. P. Skaar, R. Zhang, G. Joachimiak, P. Gornicki, O. Schneewind, and A. Joachimiak.** 2005. Staphylococcus aureus IsdG and IsdI, heme-degrading enzymes with structural similarity to monooxygenases. J Biol Chem **280:**2840-6.

193. **Yeowell, H. N., and J. R. White.** 1982. Iron requirement in the bactericidal mechanism of streptonigrin. Antimicrob Agents Chemother **22:**961-8.

194. **Zawadzka, A. M., R. J. Abergel, R. Nichiporuk, U. N. Andersen, and K. N. Raymond.** 2009. Siderophore-mediated iron acquisition systems in Bacillus cereus: Identification of receptors for anthrax virulence-associated petrobactin. Biochemistry **48:**3645-57.

195. **Zgurskaya, H. I., and H. Nikaido.** 2002. Mechanistic parallels in bacterial and human multidrug efflux transporters. Curr Protein Pept Sci **3:**531-40.

196. **Zunszain, P. A., J. Ghuman, T. Komatsu, E. Tsuchida, and S. Curry.** 2003. Crystal structural analysis of human serum albumin complexed with hemin and fatty acid. BMC Struct Biol **3:**6.